THESIS FOR THE DEGREE OF LICENTIATE OF ENGINEERING

in

Thermo and Fluid Dynamics

Homogeneous Lean Combustion in Downsized Spark-Ignited Engines

KRISTOFFER CLASÉN

Division of Combustion and Propulsion Systems

Department of Mechanics and Maritime Sciences

CHALMERS UNIVERSITY OF TECHNOLOGY

Gothenburg, Sweden 2020

Homogeneous Lean Combustion in Downsized Spark-Ignited Engines
KRISTOFFER CLASÉN

Thesis for the degree of Licentiate of Engineering 2020:11
ISSN 1652-8565

Division of Combustion and Propulsion Systems
Department of Mechanics and Maritime Sciences
Chalmers University of Technology
SE-412 96 Gothenburg
Sweden
Telephone +46 (0)31 772 1419

Chalmers Reproservice
Gothenburg, Sweden 2020

Homogeneous Lean Combustion in Downsized Spark-Ignited Engines

KRISTOFFER CLASÉN

Division of Combustion and Propulsion Systems
Department of Mechanics and Maritime Sciences
CHALMERS UNIVERSITY OF TECHNOLOGY

Abstract

Greenhouse-gases and noxious emissions from internal combustion engines propelling personal transportation vehicles is an imminent issue in the society and therefore it is vital to find means of improving efficiency and reducing emissions. It is expected that despite rapid electrification there will still be a substantial share of vehicles produced and sold, propelled solely or partly by combustion engines, in the next decades. This thesis investigates the use of homogeneous lean combustion in modern downsized gasoline engines to meet the demand for decreased impact of greenhouse- and noxious gases from the next generation personal transportation vehicles. Lean combustion offers substantial efficiency improvements to the current already-well-developed combustion systems. Historically, it has been proven difficult to achieve robust lean combustion with high efficiency and low emissions of nitrogen oxides, but modern downsized engines naturally provide more suitable conditions to burn lean mixtures making lean combustion more promising than ever before.

The purpose of the work presented in this thesis was to investigate lean combustion in a downsized engine. Additionally, the research has been targeted at investigating lean combustion at higher engine loads, an area characteristic to downsized engines and unexplored by the research community. To investigate high load lean combustion, one of the world's first downsized lean boosted engines which sustains high load lean operation has been developed, assessed and demonstrated. The research has proven the valuable combination of turbocharging and lean combustion which improved engine efficiency by up to 12%. Additionally, the investigations led to the discovery of the lean load limit which determines the highest load an engine can operate very lean. The working principals of the load limit could be determined and described to understand high load lean limitations and how it can be improved for future expansion of lean combustion.

Keywords: engine, efficiency, emissions, lean, combustion

List of publications

This thesis is based on the work contained in the following publications:

Paper I Clasen, K., Koopmans, L., and Dahl, D., "Homogeneous Lean Combustion in a 2lt Gasoline Direct Injected Engine with an Enhanced Turbo Charging System," SAE Technical Paper 2018-01-1670, 2018, doi:10.4271/2018-01-1670.

Paper II Clasen, K. and Koopmans, L., "Investigation of Homogeneous Lean SI Combustion in High Load Operating Conditions," SAE Technical Paper 2020-01-0959, 2020, doi:10.4271/2020-01-0959.

Acknowledgements

Unsurprisingly, I have been supported by a lot of people to reach this far in my pursuit for a PhD. I would like to thank Dr. Anders Johansson for opening the door for me to the Division of Combustion and Propulsion Systems at Chalmers. Today I would be elsewhere without your invitation to the division. I would also like to thank Professor Ingemar Denbratt for kindly offering me this PhD position which involved me in the European Upgrade-project. Ingemar's tireless support, patience and skills to navigate and negotiate throughout the Upgrade-project was crucial to end the project with high spirit and approved deliveries by the European commission.

I would like to shed some light upon Volvo Cars, despite that their management decided to opt out from the Upgrade-project halfway to the finish-line. The engineers and PhDs working at Volvo Cars whom have been supporting me in this project have been invaluable, especially in managing the whimsical multi-cylinder engine with prototype software that ought to origin from some sort of witchcraft. Dr. Daniel Dahl, Dr. Stefan Bohatsch, Anton Ajne, Mark O'Malley, Fredrik Wemmert, Lars Davidson, Magnus Örngrip, Peter Kroon, Martin Johansson, Robert Mattans, Peter Svensson, Peter Sandberg are only the ones I have been disturbing the most but I wish to thank all employees at Volvo that kindly have been providing their support.

My colleagues at the division naturally deserves to be acknowledged for always being kind friends who creates the outstanding working environment with high spirits and laughter all week long. So far, none has given up the hope on me despite me being exceptionally grumpy, probably worse than the grumpy cat, in the many stressful periods. A bunch of astonishing guys that deserve a special thank are the "laboratory engineers" in the engine lab at the division, whom keeps the difficult and challenging experimental activities running in the lab. Dr. Tim Benham, Anders Bragée, Robert Buadu, Dr. Alf-Hugo Magnusson, Anders Mattsson, Patrik Wåhlin, for an experimentalist such as myself, their support has been invaluable. I'd also like to thank Joop Somhorst for his support in various technical details such as filtration and for encouraging conversations.

Professor Lucien Koopmans, my supervisor, has had the difficult task of guiding me to this point. Being difficult to admit, I appreciate him pushing me towards various targets, when I tend to get stuck in the details and the always tempting engine lab. For his patience, guidance and belief in my capabilities he deserves my outmost gratitude.

I am forever grateful to my fiancée, Josefin, who has supported me in both good and bad times. She has been understanding in periods when I have spent more hours at work rather than home. She gives me the reason and motivation I often need to proceed and succeed.

The work included in this thesis was performed within a project called Upgrade, "High efficient Particulate free gasoline Engines", which was funded by the European Union Horizon 2020 Research and Innovation program's call for Green Vehicles, grant agreement no. 724036.

Table of contents

1 Introduction

Ever since the beginning of the industrial revolution, the ability of artificial transportation of people and goods has had a central role in the human society. Today, we are heavily dependent on the functioning of those high-technology supply chains that transports goods and people over vast distances in short time. Transportation enables us to live where we wish and to buy what we need and want, without the need for us to live and work at the location where our supplies are sourced. It is possible to focus on various kinds of production, from food to industrial manufacturing, to locations where the process is suitable, and transport the outcome to other places for consumption. It is also possible for people to travel, for example from short distances between home and work, to long distances across the globe, for example meetings or holidays.

However, the ability to conduct transportation in large scales comes at a cost in terms of energy. Only a minority of transport can be realized by natural resources such as wind and animal propulsion, hence artificial propulsion has taken its place ever since the introduction of the high-pressure steam engine in the early 1800's. A substantial share of the transportation sector is reliant upon the use of the internal combustion engine as a source of propulsion power, such as approximately 1.4 billion cars and 200 million trucks. The internal combustion engine is small relative to its power output, easy and cheap to make and relatively efficient. Engine fuels, liquid or gaseous hydrocarbon, have a high energy density, which enables large energy storage at low cost of weight which in turn enables long range capabilities. Most combustion engines use fuels which originate from fossil crude oil or gas, which when combusted contributes to CO_2 accumulation in the atmosphere. Internal combustion engines also contribute to local pollutions by emitting noxious compounds such as nitrogen oxides, hydrocarbons, carbon monoxide and particulates due to poor combustion systems and lack of sufficient emission aftertreatment, which cause harm to the local environment and cause premature deaths.

In 2016, it was estimated that transportation accounted for 27% of all CO_2 emissions emitted within Europe, where cars alone hold a share of 41% of transportation, making cars contributing to a total of 11% of the European total CO_2 emissions [1]. The car provides individuals with the possibility to transport themselves freely, comfortably and quickly, and the car has been widely embraced by the society. Infrastructure and city planning are nowadays shaped by the existence of cars, which, for some people have become a necessity to accommodate to the daily life. The car however is not merely a purely useful tool of transportation but is also subject to prestige, luxury, desire and competition amongst manufacturers of market share. Cars have been growing bigger, performance becomes higher and the numbers of cars have increased [2]. Despite remarkable efforts to reduce emissions from cars over the last 20 years, the car sector remains the only one that has not decreased its total CO_2 emissions in Europe [1].

The evolution of personal transportation is in 2020 facing challenges to ensure that the urgent demand for decreased emissions of CO_2 and noxious compounds are met. Despite progressive electrification, it is still expected that internal combustion engines will provide a significant share of propulsion, either solely or in combination with

electrification, in the coming decades [3]. Therefore, developing the internal combustion engine with for example advanced combustion concepts is vital to find adequate means of improving engine efficiency to ensure availability of clean, efficient and affordable propulsion for future vehicles. Air diluted spark ignition combustion, known as lean combustion or lean burn, is a well-known advanced combustion concept that can accomplish a significant efficiency increase. Lean combustion has, however, not yet seen its breakthrough since robustness and adequate fuel efficiency versus emissions trade-off has not been accomplished. There are two main types of lean spark-ignited combustion; stratified charge and homogeneous charge. Stratified charge denotes a stratification of the air and fuel mixture inside the combustion chamber. Stratified lean combustion has previously been introduced to the market but with limited success due to difficulties in suppressing NO_x and soot emissions [4, 5]. On the other hand, when a homogeneous charge is sufficiently diluted with air the NO_x emissions can be decreased to very low levels. A homogeneous lean charge is also less prone of forming particles when combusted. In recent years more attention has been paid to the homogeneous lean combustion mode. The increase in interest of alternative combustion strategies such as lean combustion originates from ambitious targets to reduce vehicle fleet average CO_2 emissions, such as the proposed reduction of at least 37.5% in the European Union from 2021 to 2030 [6]. Additionally, developments in lean exhaust aftertreatment systems creates new opportunities of realizing lean combustion with clean tailpipe emissions. The main drawbacks with a highly diluted homogeneous charge are that it becomes more difficult to ignite and combust, which limits the maximum applicable quantity of air-dilution. Especially, combustion difficulties are obtained at low load engine operation, where air motion is less intense, and density and temperatures are lower in the combustion chamber. These drawbacks present obstacles to implementation and challenges to the research community.

Another strategy to reduce fuel consumption that has been adopted amongst car manufacturers is engine downsizing. During regular driving, most of the engine operation time is spent producing only low torque at low speeds, seldomly exceeding 10% of its rated power capacity, which leaves most of the engine capability unutilized. By decreasing engine displacement, the engine must work harder relative to its size to produce the same power output as a larger engine. IC-engines work more effectively on higher specific loads, and by downsizing, the point of maximum engine efficiency therefore comes closer to the point of maximum time-density of driving. Downsized engines are commonly equipped with turbochargers to achieve the same torque and power outputs as larger engines. An advantage is that a smaller engine becomes a more frequent utilizer of the turbocharger which, if properly designed, can contribute to the engine efficiency. The turbocharger is mainly introduced to compensate for the power loss of the downsized engine compared to the larger one by increasing its volumetric efficiency. It is common that the specific engine load of the downsized engine is doubled compared to a naturally aspirated engine, which results in problems with heat, pressure and auto-ignition. Therefore, downsized engines are usually forced to adapt non-ideal conditions such as ignition retard or fuel-enrichment, to mitigate heat and auto-ignition when operating on high loads which penalizes the fuel efficiency and emission footprint.

1.1 Objectives

The research described in this thesis aims at investigating the potential synergetic combination of downsized spark-ignited engines and homogeneous lean combustion. Homogeneous lean combustion is generally benefitted from higher engine loads which increases charge temperature and turbulence making the lean charge easier to ignite and combust. Homogeneous lean combustion in turn is known to decrease combustion temperature and mitigation of auto-ignition, which is beneficial to downsized engines operating on elevated loads.

The objectives were the following:

- Achieve high load homogeneous lean combustion by turbocharging in a downsized engine, reaching 16 bar BMEP.
- Determine potential boundaries which limits applicable engine load.
- Achieve low engine out NO_x emissions, sub 1g/kWh.

2 Background

This chapter serves to introduce the reader to homogeneous lean combustion.

2.1 Historic perspective

The research field of lean combustion in spark-ignited engines has a long history, dating back as far as the beginning of the 20th century. In 1908, professor Bertrand Hopkins realized the importance of leaning out the air and fuel mixture, creating what was then called a weak mixture [7]. This ought to be one of the earliest publications available in the topic. Hopkins pointed out two main causes of the lean combustion superiority; Firstly, the ideal thermal efficiency was improved by weaker mixtures since weaker mixtures increased the specific heat capacity of the working gases. In other words, it meant that by an increased share of air in the mixture, the combustion cycle came closer to resemble the ideal air cycle where the highest theoretical thermal efficiency can be obtained of an internal combustion engine. Secondly, Hopkins highlighted that combustion of weaker mixtures also resulted in less heat losses to the cylinder walls. Hopkins proved his suggestion by experimental investigations in a 40 Bhp Crossley-engine running on coal-gas, equipped with a then state-of-the-art optical indicator to obtain cylinder pressure diagrams.

Another example of early pioneering work is the investigations made by Sir Harry Ricardo. In 1920, Ricardo conducted research on how to reduce thermal loading on the combustion chamber components by utilizing lean combustion and supercharging [8]. Ricardo identified problems with ignition of the lean charge however, and therefore implemented the use of a stratified charge to reduce the global mixture strength. Stratification works by increasing ignitability and flame speed of the initial flame development by introducing a richer portion of air-fuel mixture near the spark plug. By doing so, very lean global air-fuel mixtures can theoretically be combusted with maintained stability and robustness.

Despite some promising studies and the evident theoretical advantages, lean combustion did not seem to attract engine manufacturers, perhaps due to the practical issues. The hydrocarbon fuels used in SI-engines proved difficult to ignite using lean mixtures, partly due to undeveloped carburetor techniques. Progression to reduce engine auto-ignition resulted in progressively less volatile fuel which in turn proved even more disadvantageous for ignitability. It also became clear that lean combustion was sensitive to variations in operating conditions, and other issues such as maldistribution in multi-cylinder engine manifolds, which further implicated the use of lean combustion. Instead, most engines operated on rich mixtures to account for manifold maldistributions, poor ignitability and poor evaporative capability of carburetors. Apart from worse fuel economy, operating stoichiometric, or rich, would inevitably result in significant carbon monoxide and hydrocarbon emissions. These were some issues noted by Bolt and Holkeboer who were amongst the researchers that showed further interest in lean combustion in the sixties. In 1962, they conducted a study on the influence of compression ratio upon lean combustion and lean combustion limitations, and

commented in their discussion, that “future engines will undoubtedly run lean on part load” [9]. In 1967, Bolt and Harrington further investigated the influence of mixture motion on the lean limit and combustion of lean charges in a combustion bomb, driven by the indication from the current research that variations in the flow were the principal cause of cycle to cycle variations [10].

In the sixties, the effects of vehicle emissions started to become a concern which led to legislative actions such as the introduction of the Clean Air Act in the USA by 1970 [11]. In 1968, Lee and Wimmer emphasized the need for reduced noxious emissions such as hydrocarbons (HC), carbon monoxide (CO) and nitrogen oxides (NO_x), and therefore studied the combination of various fuels and lean combustion to reduce those emissions with promising results [12]. Similarly, in 1971 Tanuma et al. turned to lean combustion to reduce pollutant emissions and studied means of improving the lean limit such as turbulence, spark energy and combustion chamber geometry [13]. Consequently, due to the oil crisis of 1973, and the consecutive effects on the global market drastically increasing the cost of oil, resulted in increased demands for more fuel-efficient vehicles. In the seventies, several automakers introduced lean combustion in production engines. One technology emerged that is called pre-chamber stratification. It is a mean of mechanical stratification by rich fuel injection in the pre-chamber. Pre-chambers were incorporated by Honda in their so called CVCC (compound vortex controlled combustion) engine, Toyota the TGP system (turbulent generating pot) [14, 15]. Other manufacturers such as Chrysler developed an electronically controlled homogeneous lean combustion system called ELB (electronic lean burn), and Ford developed a direct injected stratified engine called PROCO [16]. Despite progress and market introduction of the lean burn engine, lean combustion did not reach a breakthrough and remained mostly marginalized. In reality, harsh engine running, poor acceleration capabilities, remaining problems with fuel distribution in the engine and occasional misfires were strongly discouraging arguments, as pointed out by Germane et al. in their review of lean combustion in -83 [17]. They also concluded that the pre-chamber technology failed due to cost, knock tendencies and sensitivity to residuals. Yet, Germane et al. also praised the concept of lean combustion as a promising technology.

In parallel, progress was made in developing catalytic converters as an alternative mean of reducing noxious emissions. From 1975, most new vehicles in USA were equipped with two-way catalysts that could oxidize carbon monoxide and hydrocarbons to comply with the regulations posed by EPA [11, 18]. Later, the three-way catalyst was developed which could also reduce nitrogen oxides. In 1976, Volvo Cars introduced the exhaust gas oxygen sensor (Lambda sensor) controlled catalytic converter system and by 1988 approximately 70% of newly produced Volvos were equipped with the system, as an example of the emerge of the after-treatment technology [19, 20]. What the introduction of the catalytic converter meant was that it was possible to realize clean emissions with an engine operating stoichiometric. Hence, stable and robust operation could be achieved derived from stoichiometric combustion in spark-ignited engines with compliant emissions, without the need for sometimes inconvenient alternative combustion processes such as air dilution. Since the emerge of the three-way catalyst, it has become standard equipment on the vast majority of spark-ignited engines and that still holds true today.

In the nineties, the lean combustion received new attention by reawaken interest in stratified combustion to once again trying to achieve improved fuel efficiency of spark-ignited engines. New more modern combustion systems with four valve cylinder heads and electronic injection enabled better control, hence improved prospects of utilizing lean combustion. One concept investigated was barrel stratification, which was introduced by intake port injection in one of the two intake ports, together with tumble-flow, creating a vertical separation of the rich and lean charge tumble-vortex halves which resulted in a stratified charge more easily ignitable than a homogeneous one [21, 22]. With the emerge of direct injection technology, further opportunities arose to implement in-cylinder stratified lean combustion. One such system was developed by Mitsubishi, where they used a reverse tumble flow and a wall guided injection system [23]. A similar system was developed by Toyota that incorporated swirl flow [24]. Additionally, AVL imposed a tumble-based wall guided direct injection system but concluded that the stratified lean operation was limited to low loads due to smoke and NO_x emissions [25]. The wall-guided systems have also proven troublesome due to wall-wetting of the piston surface, creating higher levels of soot and most manufacturers focus on spray guided systems today [26].

Yet again, difficulties in managing emissions and increasingly stringent emission legislation proved troublesome for lean combustion to be utilized. Around 2008, a lean NO_x aftertreatment technology was commercialized to cope with Tier 2 and Euro 5 regulations [27]. The system is known as the lean NO_x storage catalyst and offered new possibilities in utilizing lean combustion since combustion deficiencies resulting in NO_x could be managed by after-treatment. The system was implemented in the BMW 120i from 2007 which utilized a combination of stratified lean combustion at low load and homogeneous lean at intermediate loads [28]. Similarly, Mercedes developed and launched direct injected spray-guided stratified engines from 2006 and later introduced their so called BlueDIRECT. This system was based upon precision direct injection which enabled spray guided stratification. Stratified lean combustion was utilized together with a lean NO_x storage catalyst, a combustion system implemented in several of Mercedes engines from 2012 [29, 30]. Some Japanese carmakers did also persist in production of lean combustion engines who appeared to remain on the market between early nineties until approximately 2005. Honda was one of such, with the VTEC engine which in different versions was adapted to lean combustion, one of them called the VTEC-E which ran on port injected stratified lean combustion with swirl [22]. In practice, the bulk flow and turbulence make it difficult to position the richer portion at the desired location. Another issue is that the richer portion, when burnt, tends to produce higher combustion temperature locally which increases the formation of NO_x [31]. Additionally, if the stratified air-fuel mixing is poor and wall wetting occurs, it is likely that significant soot formation occurs [32, 33].

The drawback of lean NO_x adsorbers is that they frequently must be regenerated to reduce and purge the stored NO_x molecules, which in turn causes a fuel penalty that diminishes the gains from lean combustion. Simultaneously, the emission legislation is consistently becoming more restrictive, making it more difficult to combine lean combustion with complying tailpipe emission. Over the last five years, there has been

little activity reported from industry of production of lean combustion spark-ignited engines. Despite a long time of evolution with consistent progress in understanding the phenomena behind lean combustion challenges, improved technology and emerging after-treatment for NO_x reduction, lean combustion has not yet seen a significant breakthrough on the market. It appears that interest for lean combustion is periodically awoken when demands for further improvements in fuel efficiency is imposed. Despite development in engine technology the challenge remains to obtain the desired fuel efficiency gains from lean combustion in combination with low tailpipe emissions.

2.2 Lean combustion

Lean combustion is realized by the addition of excess air, air dilution, to spark-ignited stoichiometric combustion, which creates an over-stoichiometric mixture. Lean spark-ignited combustion is therefore striving towards achieving similar thermodynamic properties as is found in diesel engines. Spark-ignited engines are more commonly known as gasoline engines, which more specifically is categorized as a reciprocating 4-stroke spark-ignited internal combustion engine and the reader is referred to the literature such as Combustion Engine Fundamentals by Heywood for more details about the fundamental working principals of this engine type [34].

2.2.1 Advantages

With the historical perspective of the lean combustion research field in mind, it is safe to state that the working principles and the benefits that can be derived from air-diluted combustion is very well known. As discovered over 100 years ago, it is known that when the share of air is increased in the fuel air mixture, the share of two-atom molecules increases which increases the ratio of specific heats γ. This has a direct effect on the ideal thermal efficiency, given by the classical equation:

$$\eta_t = 1 - \frac{1}{CR^{\gamma-1}} \tag{1}$$

Thus, the higher the share of air, the higher the efficiency until the ideal air-cycle is reached.

When diluting with air, the flame temperature is lowered. Simultaneously, the increased total mass inside the combustion chamber lowers the average gas temperature. This results in a lower thermal gradient between combustion chamber walls and the flame and combustion products, resulting in lower heat losses of the combustion process. This is one of the most significant contributors to efficiency improvements caused by lean combustion that can be measured, in relation to stoichiometric combustion. It is an important factor since heat losses to combustion chamber walls is one of the largest single sources of losses in an IC-engine.

At stoichiometric combustion, the flame temperature and burnt gas temperatures reach such temperatures that dissociation of some combustion product molecules occurs, which prevents complete combustion. Since the flame temperature and combustion products temperatures decrease with lean combustion, dissociation of combustion products decreases. Additionally, due to the excess air providing excess oxygen molecules, higher

degree of oxidation of the fuel can be realized in practice compared to stoichiometric combustion, also contributing to higher combustion efficiency.

Since higher air mass flows are required to obtain lean combustion, less throttling is necessary and pumping losses are therefore reduced. This is an important aspect of part load, since pumping losses can be substantial at low engine loads. Pumping losses are evidently more significant for larger displacement engines and less of smaller, i.e. downsized, engines. Despite that pumping losses do not pose the greatest obstacle against higher efficiency; engines are spending most of their time operating at lower loads and small improvements in terms om pumping losses gives high yields in real life fuel efficiency. Ideally, a lean burn engine should operate at wide open throttle at the lowest torque levels to reach the highest efficiency. On the contrary, at higher loads, pumping losses remains unchanged or increase when moving away from stoichiometry. If high air mass flows are required, restrictions in the air management system might become significant. Additionally, if a turbocharger is utilized to create additional feeding of air, it is to be expected that increased exhaust back-pressures will be obtained in most cases to create the required boost pressure. Higher exhaust pressure in relation to boost pressure results in higher pumping work.

In Figure 1, an example of energy distribution is presented. The pie-charts illustrates the relative share of energy amongst different entities. Both stoichiometric and lean combustion is illustrated, and common of them both is that the work output in watts is the same. The measured change in heat loss represents the reduction of lost heat to cylinder walls, combustion loss change represents both increased oxidation and decreased dissociation, and changes in exhaust loss represents both effects of increased ideal thermal efficiency and lower exhaust temperatures. Lean exhaust enthalpy will remain similar to stoichiometric exhaust enthalpy, since the mass flow increases.

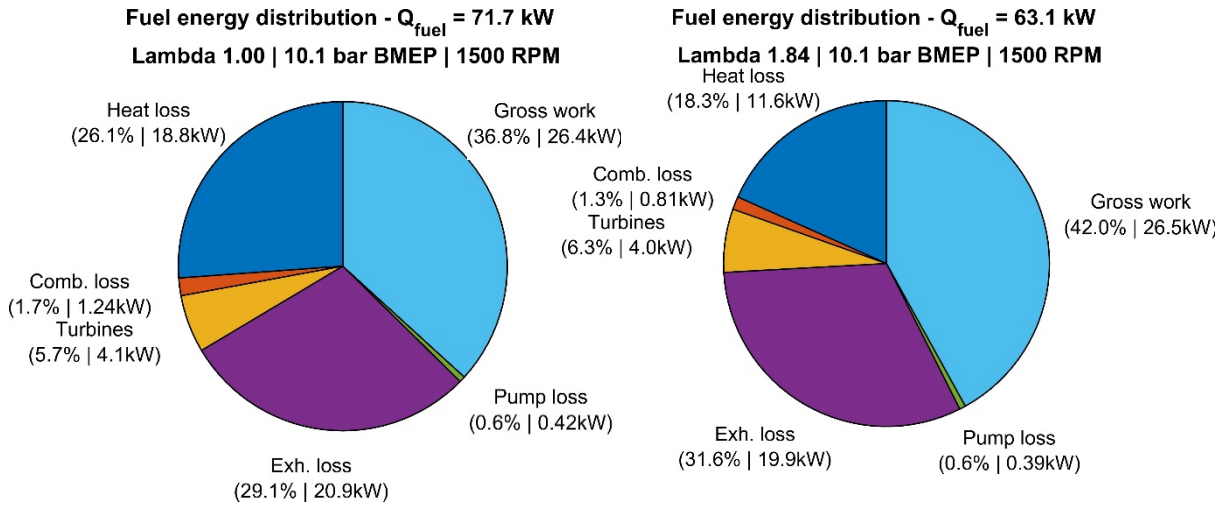

Figure 1. Distribution provided fuel of energy. Left: Stoichiometric combustion. Right: Lean combustion. Data obtained from measurement campaign 1. Energy balance is computed using a methodology suggested by Berntsson et al. [35].

Lean combustion also introduces secondary advantages. Since the combustion process is pre-mixed and controlled by spark-ignition, it makes the lean combustion spark ignition engine cheaper to produce compared to a compression ignition engine, since it requires a less advanced fuel supply system. Due to decreased combustion temperatures and flammability of the lean air-fuel charge, lean combustion is less prone to self-ignition. This enables a higher compression ratio which results in higher engine efficiency. An example of the impact of lean combustion on engine fuel efficiency is visualized in Figure 2.

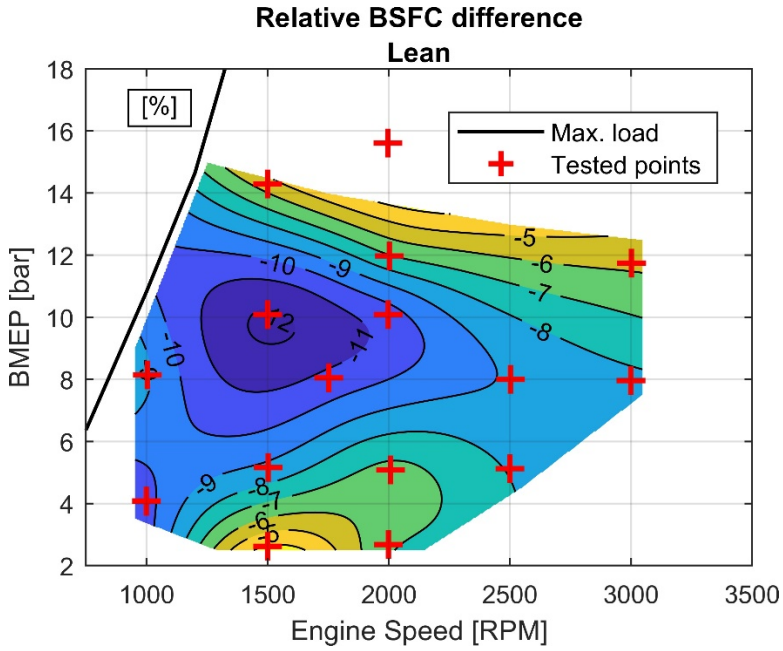

Figure 2. Relative improvement of brake specific fuel consumption (BSFC) of lean combustion compared to stoichiometric combustion, of a lean engine map.

2.2.2 Disadvantages

Due to excess oxygen in the exhausts from lean combustion, it is not possible to reduce nitrogen oxides with a regular three-way catalyst. Therefore, emissions of NO_x have become the main challenge of lean combustion concepts. Due to this aspect, the success of lean combustion relies upon the ability to achieve sufficiently low NO_x emissions, low enough so that they become negligible or manageable by a lean NOx aftertreatment system. Common to all existing lean NO_x aftertreatment systems is that they impose a penalty proportional to the NO_x emissions. The penalty consists either of fuel that must be used to regenerate the system, or by a NO_x reducing agent. Decreased exhaust temperatures due to lower combustion temperatures from lean combustion also complicate the use of catalytic after-treatment systems in general since they are reliant upon thermal energy to exceed light-off- or activation temperatures.

Nitrogen oxides are formed during combustion and are prevalent to most engine types and combustion processes. The largest source is so called thermally formed nitrogen oxides, NO_x, which originates from oxidation of atmospheric nitrogen in the inlet air. The formation of thermal NO_x is highly nonlinearly dependent on temperature, and the process is normally said to start occurring at temperatures of 1600K [34]. Since combustion temperatures decrease with increased amount of air-dilution, it is desirable to maximize air-dilution to suppress NO_x formation. An example of NO_x-emissions in relation to lambda is shown in Figure 3, which illustrates the importance of operating the engine very lean to achieve low NO_x-emissions.

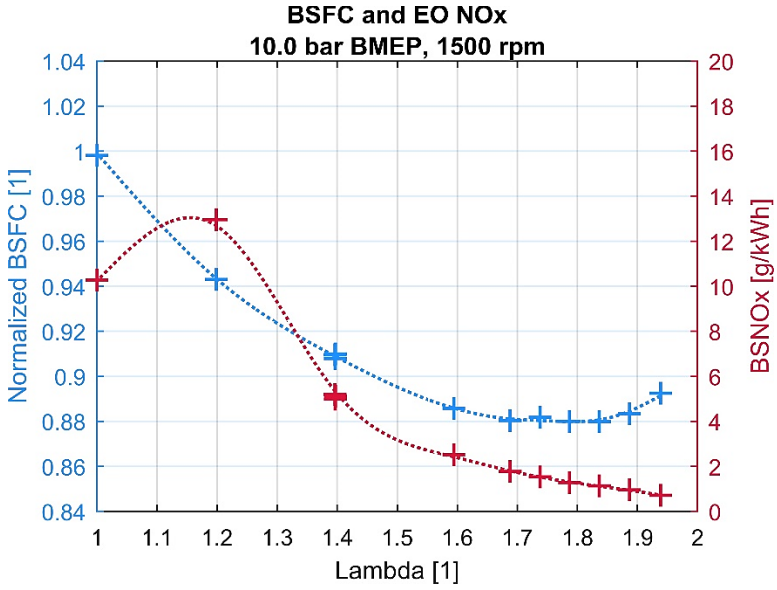

Figure 3. Brake specific NO_x emissions (BSNOx) and normalized brake-specific fuel consumption (BSFC), versus lambda. The NO_x-graph illustrates how the NO_x emissions increases when lambda is increased from stoichiometry to slightly lean, lambda = 1.2, and then steadily decreasing exceeding lambda = 1.4.

When the air-fuel ratio of the mixture is increased above stoichiometry, the flame speed decreases, which results in slower combustion. This is due to a decrease of the laminar flame speed, which denotes the speed of a flame front in a quiescent pre-mixed air-fuel mixture. The laminar flame speed, S_L, is thus adversely affected by increased air-dilution, and is also dependent upon temperature and pressure. For isooctane, the laminar flame speed can be correlated according to Heywood as [34]:

$$S_L = S_{L,0}\left(\frac{T_u}{T_0}\right)^{\alpha}\left(\frac{P_u}{P_0}\right)^{\beta}$$
$$\alpha = 2.18 - 0.8(\phi - 1) \qquad (2)$$
$$\beta = -0.16 + 0.22(\phi - 1)$$

ϕ denotes the relative fuel-air ratio, normally called equivalence ratio, which is the inverse of relative air-fuel ratio, lambda. Ideally, the flame speed and corresponding release of heat is very rapid to achieve stable and efficient combustion. When the combustion duration is extended, less chemical energy can be converted into useful mechanical work. If the combustion process is too long, some heat will create negative work during the compression phase and/ or some heat will be released to late during expansion and will be wasted to the exhaust. Not only does the flame speed decrease, but the diluted air-fuel mixture becomes more difficult to ignite. Additionally, when very diluted, pre-mixed combustion becomes very susceptible to variations, creating instability, which will be discussed further in the following section.

2.2.3 The Lean Limit

The amount of air-dilution that can be utilized is limited by the so called lean-limit. Theoretically, an air-fuel mixture will sustain a propagating flame until the flammability limit is exceeded – either too rich (rich flammability limit) or too lean (lean flammability limit). The lean flammability limit, LFL, is temperature dependent and can be described by the modified Burgess-Wheeler equation:

$$\frac{LFL(T)}{LFL(T_0)} = 1 - \frac{\overline{C}_{p,fuel-air}}{LFL(T_0)(-\Delta H_c)}(T - T_0) \tag{3}$$

Where $\overline{C}_{p,fuel-air}$ is the total ideal gas heat capacity and ΔH_c is enthalpy of combustion [36]. In practice however, the lean flammability limit is never reached in engine operation but instead governed by the lean stability limit, usually referred to as only the lean limit. The lean limit is commonly defined as the threshold of which, when exceeded, the combustion instability becomes unacceptably high. Combustion instability is also known as cyclic dispersion, which denotes the variation between combustion cycles. Due to some factors with a degree of randomness in their behavior, influencing the combustion process, the combustion varies from cycle to cycle, resulting in different work outputs and emissions. The variation in work output is primarily affected by variations in flame initiation, speed of combustion and total heat released. Thus, unlike what might be expected, it is not the flammability limit that constitutes the lean limit, but it is the degree of variation or instability between combustion cycles that determines how much air-dilution that can be added to the combustion chamber.

Combustion instability is present to some degree in all reciprocating IC-engines, but in regular engine designs and operation its presence is hardly noticed and is of little primary importance. There are different ways of how to measure the combustion stability, and there are likewise various threshold values applied in the scientific community and industry. The instability is defined statistically, and the most commonly applied measurement is the coefficient of variation of indicated mean effective pressure, which is simply a normalized standard deviation of the measure of work output, NMEP;

$$CoV_{NMEP} = \frac{\sigma_{NMEP}}{\mu_{NMEP}} \cdot 100\ [\%] \tag{4}$$

At high loads, when the mean NMEP is high, the influence of the standard deviation diminishes, why it might be suitable to adopt the standard deviation directly as a measurement of dispersion at high loads. Consequently, at low loads, when the average NMEP becomes low, the standard deviation term becomes dominating, resulting in large CoV values despite low dispersion. Instead, it may be preferable to use a suitable value of standard deviation as threshold for the low load stability as well. Values of CoV of NMEP varies between applications and manufacturers but is usually found within the interval of 2-5% and sometimes up to 10% for special applications [37]. Another important statistical quantity that can be used to assess instability is the lowest normalized value;

$$LNV_{NMEP} = \frac{\min(NMEP)}{\mu_{NMEP}} \cdot 100\ [\%] \tag{5}$$

LNV of NMEP is a number that identifies misfires or partial burns. CoV and LNV are usually correlated to some extent, but an engine can produce high CoV numbers if the combustion is consistently fluctuating with moderate amplitude, creating high standard deviation but modest minimum values in relation to the average. It is also possible that the engine combustion is stable, resulting in low CoV, but occasionally misfire or burn partially which is detected as a low minimum value which consequently results in a low LNV. A partial burn or misfire is particularly undesirable since it can be sensed by the driver as a random vibration in the car. It also results in drastically increased emissions of unburnt fuel, dependent on the severity of the partial burn or misfire, and a corresponding loss in efficiency. A general guideline is that the number of LNV should not fall below 85% to be detectable. To stretch the lean limit, it may be acceptable to allow lower numbers, presuming the emissions and efficiency do not suffer. At low loads, it is also accustomed to adopting lower LNV threshold values due to the low mean values of NMEP. An example of curves of CoV and LNV of NMEP versus relative air-fuel ratio lambda is presented in Figure 4 which illustrates the similar trends between CoV and LNV, and also depicts the sharp rise in instability in the vicinity of the stability limit.

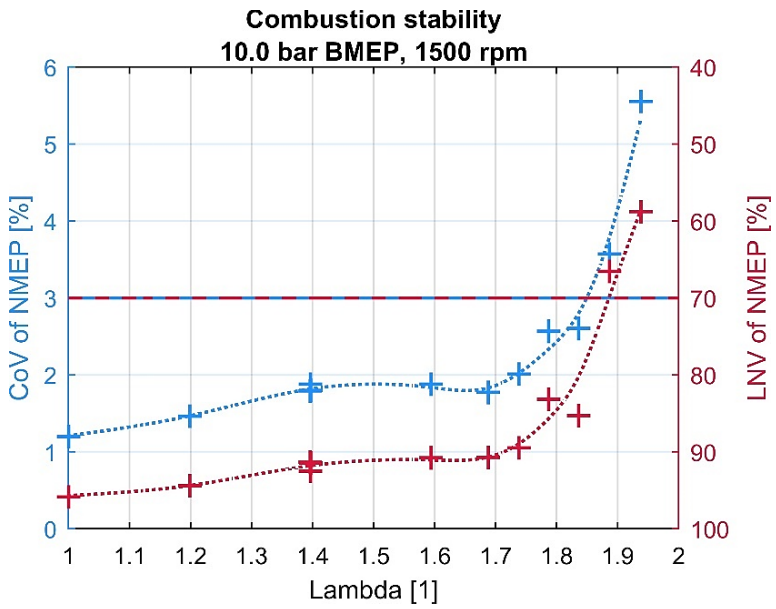

Figure 4. Example of CoV and LNV of IMEP versus lambda. A stability limit of 3% CoV of NMEP and 70% LNV of NMEP is shown in the graph.

2.2.4 Sources of dispersion

The sources of combustion dispersion are, and have been for some time, quite well known to the research community and industry, yet the phenomenon persist to pose challenges since countermeasures to counteract dispersion proves complicated. Dispersion, also known as cyclic dispersion, combustion instability and combustion variety, is not unique to lean combustion but is persistent to all types of internal combustion in reciprocating engines. When adopting weak combustion however, such as air-diluted pre-mixed combustion, the susceptibility to variations becomes higher. Figure 5 illustrates the influence of air-dilution on dispersion of combustion. The shaded areas corresponding to each graph shows the standard deviation of each combustion event, which increases steadily when air-dilution, lambda, is increased. Additionally, the corresponding COV of NMEP is visualized as the red graph. At lambda = 1.85, the dispersion becomes so high that the CoV of NMEP exceeds the stability limit of 3%.

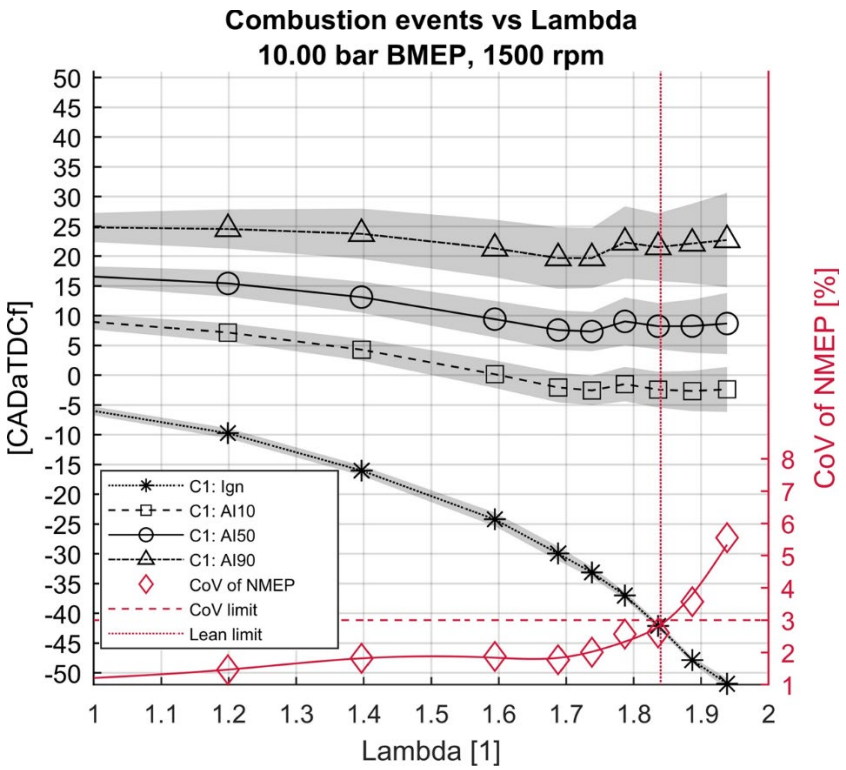

Figure 5. Combustion characteristic of a lambda sweep at 1500 rpm and 10 bar BMEP. Shaded areas represent standard deviation. As can be seen, the shaded areas grows wider when lambda is increased, and at lambda = 1.85 the dispersion of combustion becomes large enough to cause the CoV of NMEP to exceed the limit of 3%.

In-homogeneities

One potential source of dispersion is in-homogeneous air-fuel mixture. In-homogeneities are also partly known as stratification. If a volume fraction of the combustion chamber receives a larger share of fuel compared to the other fraction, the local air-fuel ratio will differ between the two portions. If the volume fraction with least fuel is located at the location of the spark at the timing of ignition, the initial flame propagation will be slower or potentially fail since there is less fuel than anticipated for the spark plug to ignite. In the next combustion cycle, the situation might be the complete opposite and the richer volume fraction of the air-fuel mixture may be located suitably near the spark plug, resulting in rapid initial flame propagation. The combustion process is particularly sensitive to in-homogeneities at the ignition event, but in-homogeneities can also affect the following flame propagation and completeness of combustion.

Berckmüller et al. studied the correlation between fuel distribution and heat release development in an optical engine, measuring fuel concentration by planar LIF with a fuel tracer [38]. The engine was a port injected Honda VTEC-E using swirl and a stratified charge. They highlighted that the initial flame development will be a function of laminar flame speed, which in turn depends on the local air-fuel ratio. It could be shown that the local fuel concentration at the vicinity of the spark plug had a strong correlation to the

initial flame development and corresponding peak cylinder pressure. The measurements also showed strong fluctuations of the local fuel concentrations at the spark plug. They also concluded that for convection of the flame to be successful, favorable mixtures were required downstream of the initial flame, but once the flame front was developed it was less sensitive to local variations in the bulk. This indicated that fluctuations of the fuel concentration in the vicinity of the spark plug are a major cause of the cyclic variations in combustion for lean mixtures.

Residuals

The combustion chamber is generally incapable of expelling the complete volume of residuals that remains after combustion since the combustion chamber has a dead volume at top dead center. Additionally, the pressure in the exhaust port is in most scenarios higher than the pressure in the intake, potentially driving the exhaust backwards into the intake. The residuals consist of hot, inert gas of mostly nitrogen, carbon dioxide and water vapor. These gases do not necessarily mix well with fresh charge that is displaced into the combustion chamber during the intake stroke. If a volume fraction containing higher amounts of residuals is present in the vicinity of the spark plug at the ignition event, the ignition process can be affected. These inert residual gases are known to decrease the flame speed in engines which is why the presence of residuals near the spark-plug at ignition is disadvantageous for initial flame development [39]. The distribution of the residuals at the combustion event is not necessarily the same from cycle to cycle. Berckmüller et al. studied the dispersion of residuals in an engine by using NO as a tracer measured by planar LIF [38]. They could measure clear cyclic variation of the distribution of NO, but the concentration of NO in the residual gases was inconsistent. Since the total amount of NO was dependent from the quality of the previous combustion cycle, it diminished the correlation of distribution and dispersion of combustion. The engine was a four valve Honda VTEC-E operating with swirl. Johansson tried a similar technique by using water vapor as the tracer and two-photon excitation in planar LIF which displayed correlation between presence of residual gases at the spark plug and dispersion of combustion [40]. The engine used by Johansson was a two-valve engine with pancake combustion chamber, thus less representative of more modern four valve pent-roof cylinder heads. In a study conducted by Keck et al., it was shown that there still remained significant cyclic dispersion despite that the charge was completely premixed, which indicates stratified residuals that effect the flame development [41].

Flow

Inside the combustion chamber, a complicated flow structure occurs that has great influence on the combustion event. The flow structure can with simplified terms be described as a sum of large structures and small structures. The large flow pattern has an integral length scale similar to that one of the combustion chamber itself, while the smaller scales are turbulent fluctuations. Turbulent flow is random by nature, which means that locally the flow is unpredictable despite that the large flow structure appears consistent. If the local flow field at the location of the ignition event varies from cycle to cycle, it can consequently have implications on the ignition and flame development. The flow is sensitive and there are multiple factors that, additional to the randomness of the

turbulence itself, affect the flow pattern on different scales. Pulses in inlet manifold and exhaust manifold, vortices created by various hardware components disturbing the flow, and characteristics of the remaining residuals from the previous cycle are examples of such features that could affect the flow. Krüger et al investigated the flow structures in a stratified spray-guided direct injected optically accessible engine and found that inside the combustion chamber, there were up to four different large scale flow structures that by competing and interacting created instabilities [42]. Wang et al. showed that inconsistent flow patterns at the early flame development could spontaneously reverse the flame direction in the combustion chamber of the optically accessible engine they investigated [43]. More studies such as the ones conducted by Aleiferis et al. where flame images were taken inside an optical accessible combustion chamber showed great variations of the flame development properties which were connected to dispersion of large scale flow structures [44, 45]. Strong correlations between initial flame development volume and the resulting IMEP could also be demonstrated. It can be expected that there is interaction between the flow field and distribution of both residuals and fuel, as highlighted by Johansson [40].

Temperature

Like air-fuel ratio, the laminar flame speed is heavily dependent upon temperature of the unburnt gases. The gas temperatures inside the combustion chamber is not necessarily homogeneous, but rather in-homogeneous or stratified. One source of temperature stratification is the hot residual gases that may exceed 1200K. If residual gases remain and is not well mixed, it will result in in-homogeneous temperature distribution. Additionally, heat exchange from the hot cylinder walls to the cold, fresh gases during the intake stroke may also cause uneven distribution of heat in the charge. If the local temperature in the vicinity of the spark plug varies from cycle to cycle, it will result in cyclic dispersion of laminar flame speed. An example of the influence of different temperatures on laminar flame speed of gasoline is illustrated in Figure 6. Notably, the laminar flame speed varies significantly in relation to temperature changes.

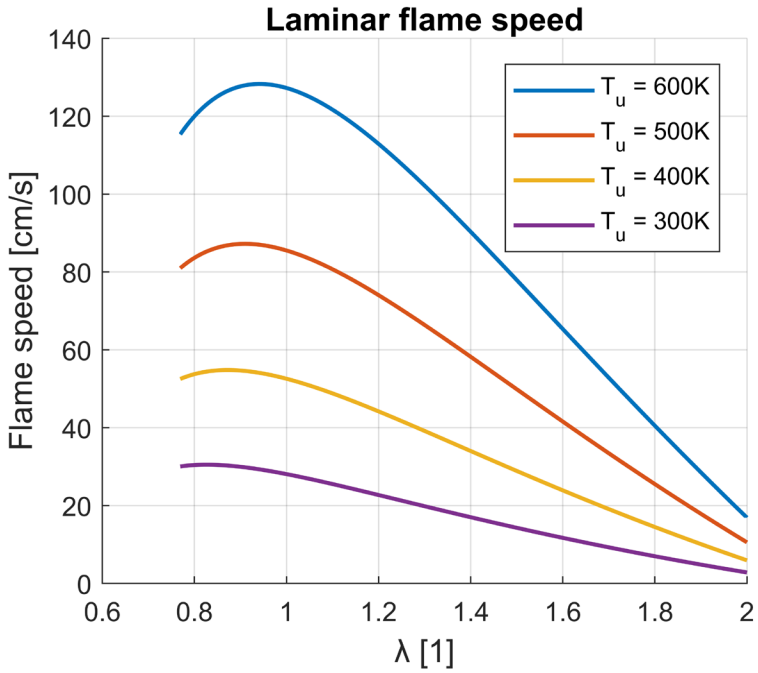

Figure 6. Laminar flame speed versus relative air-fuel ratio lambda and at various temperatures of the unburnt gas, derived from Equation 2 which is similar to the results of Amirante et al. [46]. The graph illustrates the decline of laminar flame speed when the fuel-air ratio and temperature decreases.

Hardware instability

Lack of repeatability of hardware components are also potential sources or dispersion. Examples of such are the fuel injector, that might change behavior slightly between cycles, resulting in different fuel distributions. The ignition system may cause inconsistent spark discharge. The inlet and exhaust valves may open slightly different due to vibrations, alterations in the mechanism, oil pressure and fluctuations in the cam-phasing of cam-trains with variable valve actuation. The throttle valve may vary in position, affecting flow in the inlet manifold and potentially downstream. Signals from sensors such as the exhaust oxygen sensor, air mass or air pressure sensors may vary. Additional to individual hardware dispersion, there may also be fluctuations in the control system of the engine. Hardware fluctuations are seldomly investigated as a source of dispersion and ideally the combustion should simply obey the inputs to the combustion chamber. Nevertheless, if fluctuations in control and hardware interact with random fluctuations, a bad combustion cycle may become worse and increase the total impact of cyclic dispersion.

2.3 Homogeneous Lean Combustion

In contrast to stratified lean combustion, homogeneous lean combustion is realized by combustion of a homogeneously pre-mixed air-fuel mixture. By creating a high degree of homogeneity and a very lean global air-fuel ratio, it is possible to achieve lean

combustion that produce low NO_x emissions [47]. This is a vital characteristic of homogeneous lean combustion that makes it the most popular lean combustion concept in recent years. Lean homogeneous combustion is also advantageous in terms of soot emissions. The premixed lean flame produces less soot compared to both stoichiometric-, stratified lean- and diffusion combustion, since fuel and air is well mixed and there is excess air available to guarantee high degree of oxidation of the fuel molecules.

There are however reasons why homogeneous lean combustion has not been extensively utilized previously. The homogeneous lean mixture will inevitably experience lower flame speeds of the flame kernel, compared to a well-designed stratified lean combustion system that ignites a richer mixture. The lower flame speeds lead to prominent difficulties in achieving ignition and flame propagation. Therefore, means of improving ignition and flame propagation and suppression of cyclic dispersion of homogeneous lean mixtures in SI-engines has been extensively investigated by researchers in recent years.

2.3.1 State of the art in homogeneous lean combustion research

To improve of lean combustion, measures have been developed to minimize cyclic dispersion, improve combustion speed and mitigate emissions of nitrogen oxides. The two attributes that obtain most focus is the cyclic dispersion and combustion speed. Additionally, simultaneously achieving NO_x mitigation is crucial.

It is well established that the ignition properties have large influence on the combustion of lean mixtures. Generally, when the mixture is made weaker, the minimum ignition energy demand increases which is why increased spark energy is required. Effects of increased ignition energy on stability and dilution limit of spark-plug based ignition systems have been presented by several studies [48, 49]. It has also been shown that increased velocity of the flow, in relation to the spark, increases the minimum ignition energy demand due to cooling and flame stretch [10]. The position of the spark plug electrodes, electrode gap and the shape of the spark plug has also been proven to influence ignition behavior. Aleiferis et. al demonstrated that a perpendicular position of the spark plug ground electrode in relation to the flow was the most beneficial to support flame development [44]. Lee and Boehler compared different spark plug geometries and concluded that a single ground electrode and sharp electrode tips was the most beneficial from constant volume combustion vessel experiments [50]. By perpendicular positioning and sharp electrodes, the interaction between the gas flow and spark increases. If there is gas flow and sufficient spark current, the spark may be deflected increasing the spark volume thus the exchange of energy to the gas [51]. Consequently, sharper electrodes and deflection of the arc may decrease heat losses from the spark and flame kernel to the electrodes [52].

There are various ignition systems supporting extended spark energy such as high energy ignition coils and dual coil ignition systems. The dual coil system (DCI) and similar ones has the advantage that they can sustain a consistent yet pulsating spark current for an extended duration of time which increases interaction and energy transfer to the gas [53]. Additionally, by extended duration of the spark, the chances that an ignitable mixture passes by the spark gap during ignition increases in an in-homogeneous mixture. Other

types of ignition systems have been proposed, such as the high-frequency ignition system [54, 55]. High-frequency ignition (HFI), also known as corona discharge-ignition, utilizes high voltage alternating current with a single electrode with several electrode tips, which discharges into the gas. Prior to formation of an arc, the polarity of the electrode is reversed which means that no current flow occurs. Depending on the impedance and geometry of the electrode tips, the HFI system can induce energy into a large volume which theoretically suppresses local effects of in-homogeneities. A comparison of DCI and HFI is visualized in Figure 7.

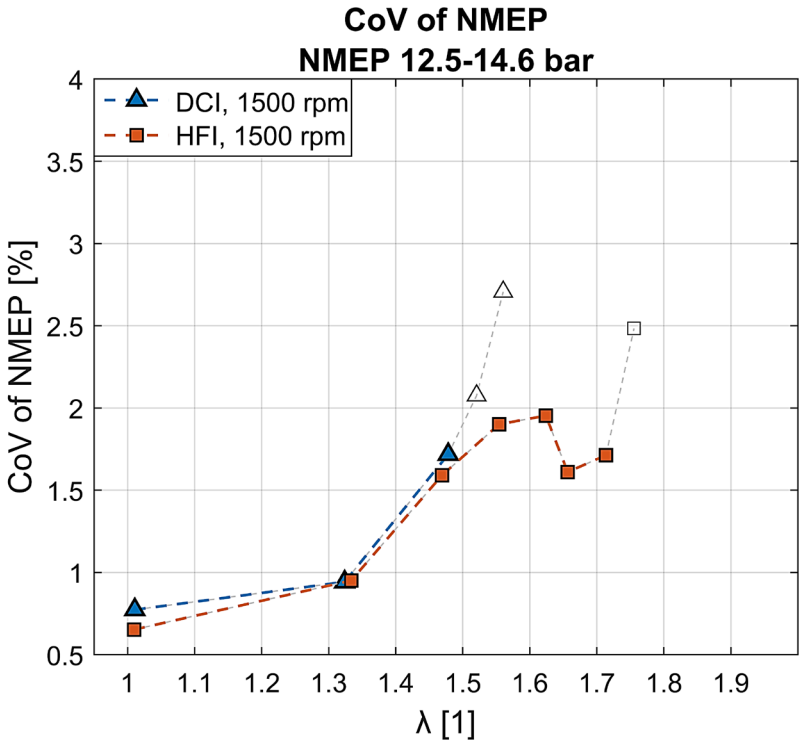

Figure 7. Example of the difference in lean limit between a dual coil ignition system and a high frequency ignition system. As can be seen, it was possible to extend the lean limit 0.25 lambda units using the HFI system. The stability limit was set to 2% CoV of NMEP.

Jet-ignition is another type of system that has been proposed lately, which has shown great potential in suppressing dispersion and improving burn rates [56]. There are different types of jet-ignition systems depending on the characteristics of the jet, but the working principals is not uncommon to the pre-chamber technology of the seventies. The difference is much smaller pre-chambers in the jet-systems, smaller orifices to promote high velocities and turbulence, and the pre-chambers are fed by modern electronic direct injectors.

Increasing turbulence is a common approach of increasing combustion speed. The laminar flame speed is adversely affected by increased air dilution, but the turbulent flame speed is increased by increased turbulence intensity. A simple relation between

laminar flame speed, turbulence intensity and turbulent flame speed has been proposed by Damköhler [57]:

$$S_T = S_L + u' \tag{6}$$

This relation has since been extended by many researchers and in practice the turbulent flame speed is subject to very complex mechanisms not captured by this proposed relation. The main weakness is that the model predicts flame propagation even when the laminar flame speed is zero. However, the equation illustrates the importance of increased turbulence intensity to increase flame speed of air-diluted combustion. Turbulence promotes the flame speed by wrinkling the flame front which in turns increases the flame front area. As stated by Kiyota et al., turbulence is subject to dissipation and it is therefore desirable to preserve the bulk flow motion and convert the bulk eddy into turbulence in the late compression stroke before combustion [4]. To achieve this, it is necessary to induce kinetic energy in the bulk flow during the intake stroke. This can be done by promoting bulk flow patterns such as swirl or tumble. Tumble is most common amongst modern four-valve pent-roof cylinder head engines, while swirl more common on older two-valve engines and stratified combustion systems. It is also possible to mix the two, creating so called slant-swirl or swumble [58]. Modern four-valve combustion chambers have limited surface available for squish generated turbulence, and therefore the combustion chamber is preferably design to crush the bulk flow in the late compression stroke to convert the large eddy into smaller scale eddies [59, 60].

Increasing bulk flow kinetic is normally accomplished by redesigning the intake ports. A tumble port is straightened to direct the flow towards the exhaust side of the combustion chamber, and sometimes the port cross sectional area is made smaller to increase the gas velocity. Redesign towards a tumble port is however subject to increased port friction, compared to a conventional filling port, which results in increased pumping losses [35]. Current trends in combustion chamber design requires decreased included valve-angles to make the pent-roof flatter to allow for higher compression ratios and lower surface to volume ratios. Decreased included valve angles create additional challenges to promote tumble flow. Additionally, it may be challenging to design a port which sufficiently promotes bulk flow kinetic energy at lower mass flows, which simultaneously allows for high flows at peak power. Variable tumble systems have been proposed as a solution to this problem, such as tumble-plates or tumble-flaps that partially blocks the inlet port which increases the gas velocity and targeting the top side of the valve to promote tumble motion at part load [61]. An example of such a system is the system used by the author in campaign 2, which is shown in Figure 8. It should be noted however, that heavily increased motion may increase wall wetting by centrifugation of the fuel droplets, and also potentially increase thermal losses to the cylinder walls due to higher convection. As was shown by Krüger et al., it is also crucial to suppress competing flow structures to avoid flow instability which otherwise may promote cyclic dispersion [42].

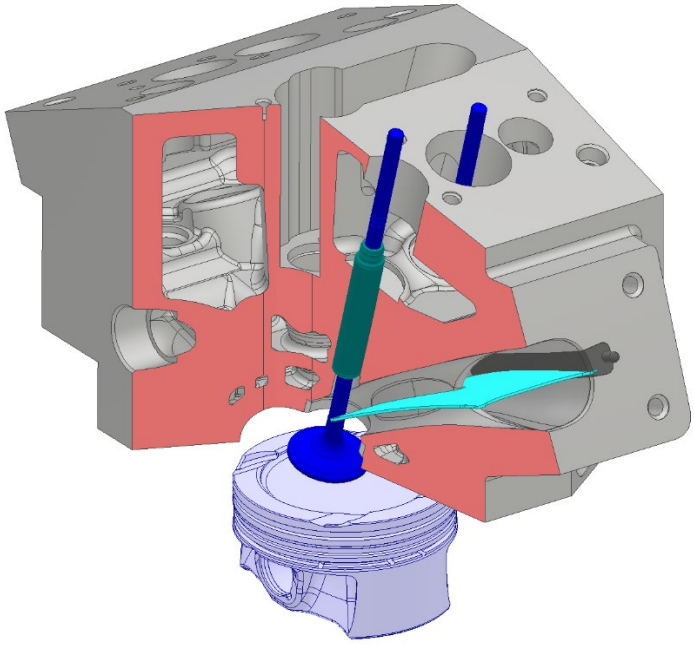

Figure 8. Section view of a CAD-model of a cylinder head with fitted tumble plate (colored cyan). By blocking the lower side of the plate, the inlet port area reduces by 50% which increases the gas velocity during intake and improves targeting towards the top side of the inlet valve plate. This technique was used in the single-cylinder engine of campaign 2.

Additionally, excessive turbulence levels may wrinkle and stretch the initial flame kernel and quench it instead of promoting propagation [62]. Similarly, high turbulence that causes high flame stretch, denoted by a high Karlovitz number, may also cause a quench of the developed flame as highlighted by Moriyoshi et al. [63]. When there is high turbulence present at the ignition event, the initial flame is more likely to be quenched due to convection and heat losses of the flame kernel. Similarly, if the turbulence is too high, flame propagation can be obstructed and quenched, reducing combustion efficiency, which results in a larger amount of unburned fuel and increased hydrocarbon emissions.

Since the flame speed is dependent on temperature, it has been proven beneficial to increase the charge temperature to reduce cyclic dispersion and increase combustion speed. This can be accomplished by increasing the temperature of the inlet air, at the expense of decreased volumetric efficiency [64]. Increased charge temperature prior to ignition may also be accomplished by increased compression ratio, which was realized already in the sixties by Bolt and Holkeboer [9]. Increasing compression ratio also has the advantage that the top dead volume decreases which in turn decreases the amounts of trapped residuals during gas. Increased compression ratio may however increase the surface to volume ratio, which in turn increases heat losses. By improper design, the piston may impair the flow and reduce the turbulence at top dead center. It is also likely to achieve increased flame to wall interaction which severely deteriorates flame

development, why careful design of the piston should be considered when increasing the compression ratio [65]. Additionally, increased compression ratio may be introduced at the cost of increased tendency of knocking combustion which diminishes high load efficiency. Since the charge temperature is of great importance to ignitability it is also desirable to have a late ignition timing, close to top dead center. An earlier spark timing, sometimes necessitated by slow flame development, experience lower temperatures and densities. This occurs since the temperature and pressure build up from compression by the piston is lower, the earlier the spark occurs. Therefore, promoting flame kernel development and combustion speed is a necessity to avoid excessive spark timings. Figure 9 demonstrates the great effect that air-dilution has on the initial flame development.

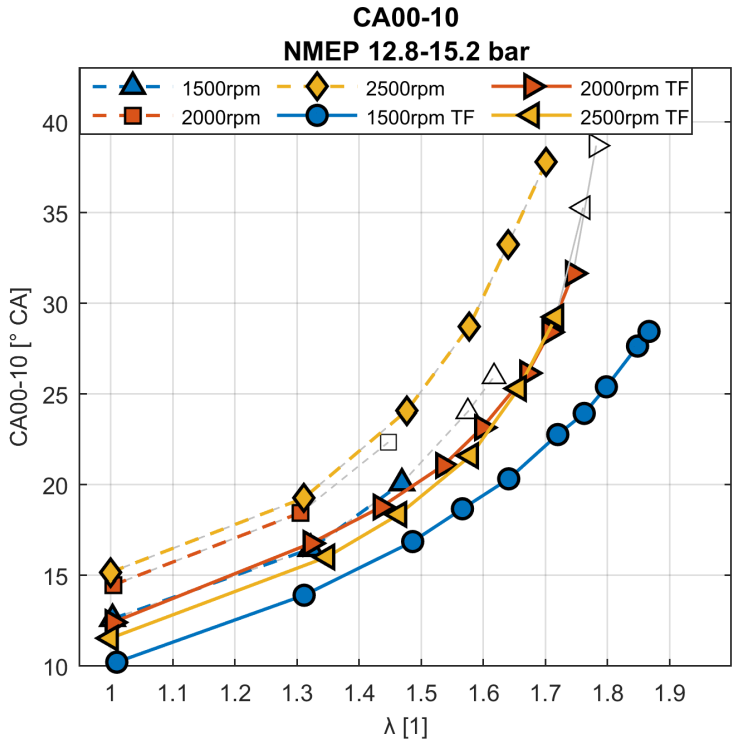

Figure 9. Computed initial flame development, defined as the duration between start of ignition and 10% mass fractions burned of the fuel, calculated from the heat release of the indicated cylinder pressure. The graphs illustrate the great increase of flame development when increasing air dilution.

Homogeneity has repeatedly been highlighted as important to achieve stable lean combustion. Homogeneity is highly dependent on the fuel injection system and injection strategy. Hanabusa et al. conducted a study where port injection and direct injection was compared which clearly showed that fluctuation of air-fuel ratio near the spark plug decreased with port injection [66]. It is therefore tempting to consider port injection prior to direct injection in a lean combustion system, at the expense of decreased volumetric efficiency and potentially reduced compression ratio due to higher tendency of knocking

combustion, which obstruct the overall desire of increased fuel efficiency. Port fuel injection has the advantage that the injection rate can be low since there is available time for air-fuel mixing in the inlet port. Additionally, it is possible to target the inlet valve, which is hot, which in turn improves vaporization. Direct injection requires higher injection rates since there is limited time for air fuel mixing. Injection is normally done during the intake stroke to maximize mixing. Higher injection rates require higher injection pressures, also necessitated to achieve high degree of atomization of the fuel. The main advantage of direct injection is that the fuel sources energy from the combustion chamber to be vaporized, which decreases chamber temperatures. Decreased temperatures improve volumetric efficiency and mitigates knock, at the expense of lesser homogeneity.

To conclude, the ongoing research suggest that lean combustion is promoted by maximized homogeneity and minimal residual gases. A large source of dispersion is the flow structure, which is preferably guided to be as uniform as possible to avoid competing flow structures. Compression ratio is favorably increased to promote flame speed, but care should be applied to piston design to minimize surface to volume ratio and allow flame development without wall-interaction. Theory of turbulent combustion and experimental investigations suggest that high kinetic energy should be induced in the bulk flow. The ignition process is benefitted from high gas velocity in relation to the spark to maximize interaction volume, but the turbulent fluctuations should be kept low to minimize flame kernel quenching. Combustion of the bulk necessitates high turbulence intensity at top dead center. The design of the combustion chamber and ports therefore requires a balance between strong bulk flow with minimal turbulence intensity for ignitability and strong turbulence to rapidly combust the bulk, without quenching the end gas. Increasing turbulence requires promoted bulk flow in the combustion chamber to increase the kinetic energy. Increased bulk flow is normally accomplished at the expense of increased port friction and decreased volumetric efficiency, which is a drawback in lean combustion systems since lean combustion requires higher air mass flow compared to stoichiometric combustion. In test campaign 1, a prototype 2-stage serial turbocharger was utilized to increase the air mass flow capabilities of an engine to achieve lean combustion at operating conditions where standard gas-exchange systems cannot deliver excess air to the combustion. An image of the turbocharger used is presented in Figure 10.

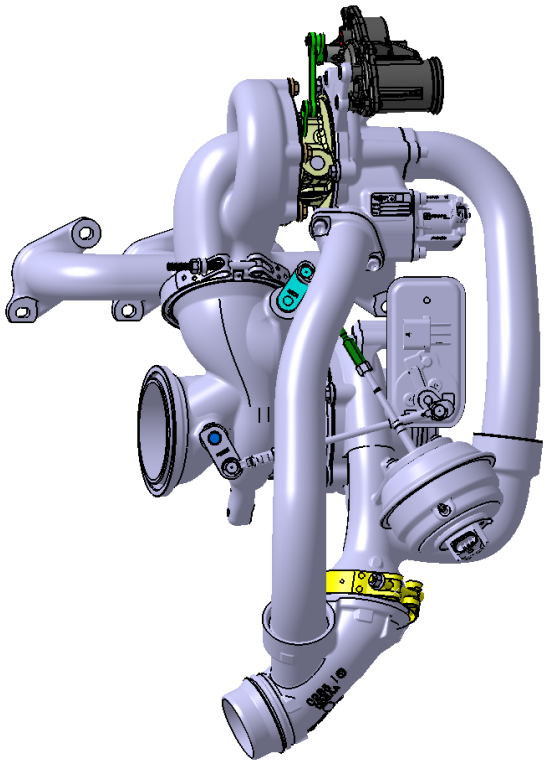

Figure 10. CAD-image of the turbocharger used in test campaign 1 to increase air mass flow rates to extend lean combustion capabilities

2.3.2 Knock and high load lean combustion

Knocking combustion is considered one of the main obstacles improving SI-engine efficiency. Knock is considered as an abnormal combustion event that threatens the integrity of the engine. Knock is also sometimes referred to as ringing. The name originates from the distinct knocking or ringing sound that is emitted from an engine when significant knock occurs. Knock originates from the auto-ignition of the unburnt end-gas during combustion. Pressure and temperature build up, together with potential radiation from the flame front, trigger ignition of so-called exothermic centers which consists of small volumes of higher reactivity compared to the mean end-gas properties. The exothermic centers are created by fuel rich pockets, collection of hot residual gases or hot spots on the combustion chamber walls [67]. The auto-ignition triggers a very rapid release of heat with a corresponding high-pressure gradient equated with shockwaves oscillating in the natural frequencies of the combustion chamber, usually in the frequency band of 5-50kHz. The pressure waves are normally attributed by moderate pressure amplitudes, not challenging to the combustion chamber integrity. Instead, the rapid heat release and consequent compression of the end-gas due to sequential ignition of exothermic centers result in high heat-flux between the combustion products and the combustion chamber walls which thermally stresses the material [68]. Additionally,

focusing of the shockwaves in crevices might occur which potentially lead to cracked ring-lands.

The occurrence of knock is strongly dependent on the reactivity, pressure and temperature of the end-gas and can be described by the characteristic time delay of auto ignition as proposed by Heywood [34]:

$$\tau = C_1 P^{-n} e^{\left(\frac{C_2}{T}\right)} \quad (7)$$

If the time-delay of auto-ignition is longer than the time that is required for the flame to consume the end-gas, auto-ignition do not occur. Therefore, it is desirable to increase the auto-ignition delay time and decrease combustion duration, without causing excessive increase in temperature and pressure.

The end-gas reactivity can be decreased by dilution by air or exhaust gas recirculation. Addition of excess air was investigated by Grandin and Ångström as a mean of reducing high load enrichment in a turbocharged engine, together with cooled exhaust gas recirculation [69]. The attempt at utilizing excess air as a diluent, replacing enrichment at high load, proved un-fruitful since the addition of air could not recover sufficient spark advance to compensate for slower combustion and increased cyclic dispersion. The amount of air-dilution that was implemented was modest however, not exceeding a relative air-fuel ratio of lambda = 1.2 since the gas exchange-system consisted of a regular turbocharger. Additionally, Grandin et al. studied the effect of the different diluents on end-gas heat release prior to auto-ignition to assess the influence of different chemistries [70]. Notably, when diluting with air, the highest knock intensities were encountered, explained by that the increase of specific heat ratio led to increased compression temperatures. Similarly, Grandin et al. applied rather low amounts of excess air in this study as well, peaking at a relative air-fuel ratio of lambda = 1.3. Topinka et al. reported similar conclusions of that leaning out the air-fuel mixture required slightly increased octane rating requirement [71].

If the relative air-fuel ratio lambda is increased beyond lambda = 1.3, a substantial cooling effect is obtained which influences the knocking properties. Doornbos et al. conducted a study to investigate the effects of high amounts of air-dilution on knocking combustion [54]. The study revealed non-linear effects on knock tendency, were an increase of lambda from stoichiometric to slightly lean of lambda = 1.2 increased the tendency of knocking, confirming the observations made by Grandin et al. However, when lambda was further increased beyond lambda = 1.4, a significant drop in knock tendency was achieved. Doornbos et al. operated their test engine at 1500 rpm and a load of 11 bar NMEP. Another study, conducted by Stokes et al. in the 2000's aimed at realizing knock mitigation by lean boosting in a downsized engine [72]. They conducted an experimental study in a single-cylinder research engine with artificial boosting and could demonstrate lean combustion within the stability limits up to a load of 14 bar NMEP. However, it was not stated at which air-dilution rates nor was the corresponding NO_x-emissions presented. Ratnak et al. also conducted a study of boosted lean combustion on higher loads [73]. They operated their test engine at a speed of 4000 rpm and up to loads of 11 bar NMEP, with limited dilution rates of lambda = 1.3. Bunce and

Blaxill reported loads up to 14 bar BMEP, with higher levels of air dilution at lambda = 1.6 which is one of the most promising results found in the literature regarding high load lean operation [56]. Consequently, they reported moderate NO_x emissions despite high load lean combustion. Bunce and Blaxill did however utilize turbulent jet ignition rather than regular spark ignition, explaining the extended lean combustion capabilities compared to conventional spark-ignition lean.

From the studies reviewed, it has repeatedly been reported that it is possible to apply lean charges to high load engine operation but with mixed results. However, if the dilution rates are moderate, it will most likely result in very high NO_x emissions exceeding 10 g/kWh, due to insufficient combustion cooling. Most researches report limited air-dilution rates, possibly explained by limited air-supply and impaired combustion stability.

2.4 Research question

Much of the body of the literature has presented studies of homogeneous lean combustion on low to intermediate loads to improve part-load fuel efficiency of spark-ignited engines. The current trends towards downsizing and a selection of studies that has reported high load lean combustion suggest that utilization of homogeneous lean combustion can be expanded to high specific loads to substantially improve overall engine fuel efficiency. This leads to the following research questions:

- Is it possible to sustain high load homogeneous lean combustion in a modern combustion system by utilizing a lean optimized turbocharger, and by doing so, improve the fuel economy?
- How much can the engine loads be increased while sustaining lean combustion?
- How does high load combustion conditions influence the combustion of a homogeneous lean charge?
- What is the influence of excess air on auto-ignition on high load lean operation?
- What constitutes potential high load lean limitations?

3 Method

Experimental research has been conducted to answer the proposed research questions and achieve the goals. The experimental work has been divided in two experimental campaigns; the first utilizing a modified multi-cylinder engine; the second utilized a single cylinder research engine with artificial boosting.

3.1 Experimental setups

3.1.1 Experimental campaign 1 – Turbocharged multi-cylinder engine

In campaign 1, the target was to verify the hypothesis that lean combustion can be sustained in- and benefitted from, a downsized boosted lean combustion system. The corresponding results have been published in paper 1. To do this, a self-sustaining multi-cylinder engine, complete with boosting system and exhaust aftertreatment system, was utilized, to mimic realistic conditions. Self-sustaining refers to that the engine and auxiliaries are stand-alone and do not need any external power-supply or air for example.

The engine used was a modified Volvo Cars two-liter in-line four-cylinder direct injected spark-ignited turbocharged engine rated to 187kW and 350Nm. Details of the engine is given in Table 1 and a schematic layout is presented in Figure 11. The engine was equipped with a prototype regulated two-stage serial turbocharger with a high-pressure stage consisting of a variable nozzle turbine, and a low-pressure stage consisting of a waste-gated turbine. The high-pressure stage was equipped with an active bypass valve to control exhaust flow between the two turbine stages at various conditions. The turbocharger system was designed to meet the high demands on air mass flow to achieve highly diluted lean combustion exceeding lambda 2 at low speed between medium torque levels up to maximum torque, and to deliver an approximate air mass flow sustaining lambda 1.4 at peak power. The VNT high-pressure turbine was primarily optimized to operate at the challenging intermediate torque levels above 7 bar NMEP where a naturally aspirated engine normally reaches its lean load limit, and 11-13 bar NMEP where the main turbocharger normally starts to deliver significant boost. The two turbines can work in series delivering the high dilution rates stated, but at higher speed the VNT turbine must be bypassed to avoid excessive restriction of the exhaust. More detailed data of the prototype turbocharger is not available due to disclosure of the producer and the design and assessment of the turbocharger system is consequently out of scope of this thesis.

Additionally, the engine was equipped with a high energy dual coil ignition system. The ignition system was fitted to increase spark energy and spark duration to improve lean charge ignition, thus improving combustion stability and lean limit. The reader is referred to Alger. et. al for more details of dual coil systems [53]. The main working principal of the system is that the two parallel coils works in series to sustain a continuous arc between the spark plug electrodes. After discharge of the first coil, before all available coil energy is emitted, the second coil discharges and the first coil is reloaded. By this method, a continuous, but pulsating, current can be sustained in the spark plug gap.

The engine was fitted with a complete exhaust aftertreatment system to account for pressure drop and to characterize aftertreatment conditions during lean operation. The aftertreatment system consisted of a standard three-way catalyst close-coupled to the second turbine, and a downstream active urea-SCR. The SCR-system was not activated during campaign 1 but served only to achieve realistic exhaust conditions.

Table 1. Engine specifications of campaign 1

Engine type	VEA Gen I, VEP4 MP
Number of cylinders	Four, in-line
Displaced volume	1969 cc
Bore / Stroke	82 mm / 93.2 mm
Compression ratio	10.8:1
Valve train	DOHC, 16 valves
Intake camshaft	Variable 0-48° CA advance
Exhaust camshaft	Variable 0-30° CA retard
Ignition system	DCI, standard J-gap spark plugs
Fuel system / Injection pressure	DI / 200 bar
Fuel	Gasoline RON95 E10
Start of injection	-308° to -340° ATC
Boosting system	2-stage regulated turbocharger
Rated power/ Rated torque	187 kW / 350 Nm
Stoichiometric air/ fuel ratio	14.01:1

The engine was fitted with a variety of sensors to sample temperature, pressures and to receive in-cylinder indicated pressure signals. The engine was positioned in a test cell and connected to an AVL Elin 315 static dynamometer to control engine speed and load during tests. An emission sample was extracted after the second turbine to receive engine out raw emissions and the emissions were analyzed using a standard emission rack. More details about the measurement equipment is given in Table 2.

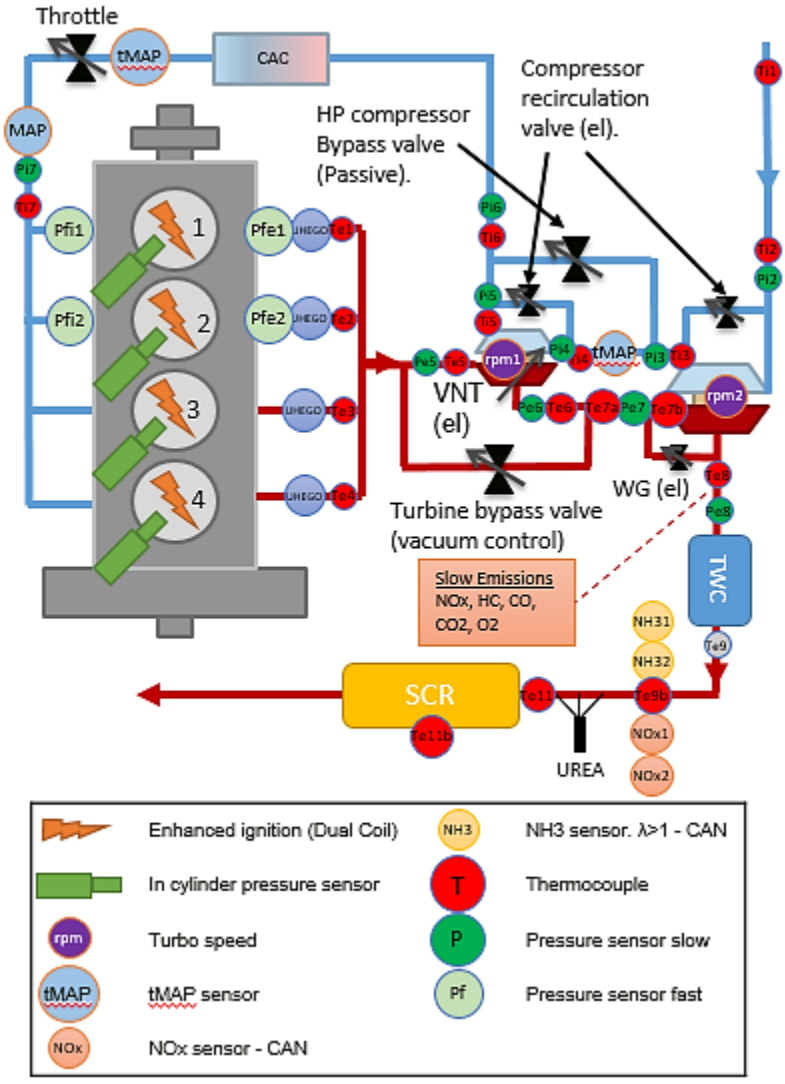

Figure 11 . Engine layout of campaign 1

Table 2. Acquisition specifications of campaign 1

Cylinder pressure sensors	Kistler 6045AU20
Cylinder pressure amplifiers	Kistler 5011
Crank angle decoder	AVL 365C
Indicating acquisition	AVL Indimaster 670
Indicating acquisition	AVL Indicom 1.6
Pressure transducers	Trafag CMP 8270
Temperature probing	Thermocouples type K
CO_2	Non-dispersive infrared detector
CO	Non-dispersive infrared detector (0-500ppm + 0-5%)
O2	Paramagnetic oxygen analyser
HC	Flame ionization detector
NO_x	Two channel chemiluminescence detector ($NO+NO_x$)
Lambda	Broadband exhaust gas oxygen sensor
Fuel mass flow	Micromotion Coriolis fuel meter

Emission species were measured to assess combustion efficiency, the influence of air-dilution on noxious emissions of NO_x, HC and CO. Consequently, the emission species were used to compute the Brettschneider lambda to validate the broadband lambda-sensor readings.

3.1.2 Campaign 2 – Single cylinder research engine

Campaign 2 was conducted to continue to investigate the results obtained from campaign 1 and the corresponding results have been published in paper 2. In campaign 2, a single cylinder research engine was used as the unit under test. The single cylinder engine provides easier control of the engine settings, calibration and eliminates potential interactions and maldistributions that may occur in a multi-cylinder engine. The single cylinder engine also allows complete decoupling of the hot and cold parts of the gas-exchange system which allows extended studies on gas-exchange phenomena. Details of the engine is listed in Table 3 and a schematic of the setup is presented in Figure 12.

The single cylinder research engine was used to further investigate high load lean combustion, where the multi-cylinder proved inadequate. To sustain high load lean operation, the engine was connected to an external air-supply delivering a maximum of 2 bar gauge boost pressure and maximum mass flow far exceeding the requirements. The boost pressure was accompanied by an exhaust pressure valve that could simulate turbine pressure drop of a turbocharger. This is particularly important to account for to avoid

unrealistic scavenging and positive pump work which effects the net efficiency of the combustion cycle. Throughout the experiments performed in the single-cylinder engine, the exhaust pressure was maintained the same as the inlet pressure.

The engine was fitted with a variable tumble device consisting of a divider plate inserted into the inlet ports, of which the lower half of the ports could be blocked by a throttle to target the top side of the valves and increase gas velocity. Like the multi-cylinder engine, the single-cylinder engine was also fitted with a dual coil ignition system to extend ignition energy and spark duration.

Table 3. Engine specifications of campaign 2

Engine type	Single-cylinder research engine, AVL 5411
Displaced volume	475 cc
Bore / Stroke	82 mm / 90 mm
Compression ratio	10:1
Combustion chamber	Pent roof
Tumble ratio	1.5/ 2.5 at open/ closed flap
Variable tumble	Tumble Flap, 0/50% blocked area
Valve train	DOHC, 4 valves
IVC	-141° ATC @ 1 mm lift
EVO	137° ATC @ 1 mm lift
Overlap	23° CA @ 0 mm lift
Ignition system	DCI, standard J-gap spark plugs
Fuel system / Injection pressure	DI / 200 bar
Fuel	Gasoline RON95 E10
Stoichiometric air/ fuel ratio	14.01:1
Start of injection	-310° ATC
Boosting system	2 bar gauge, external supply

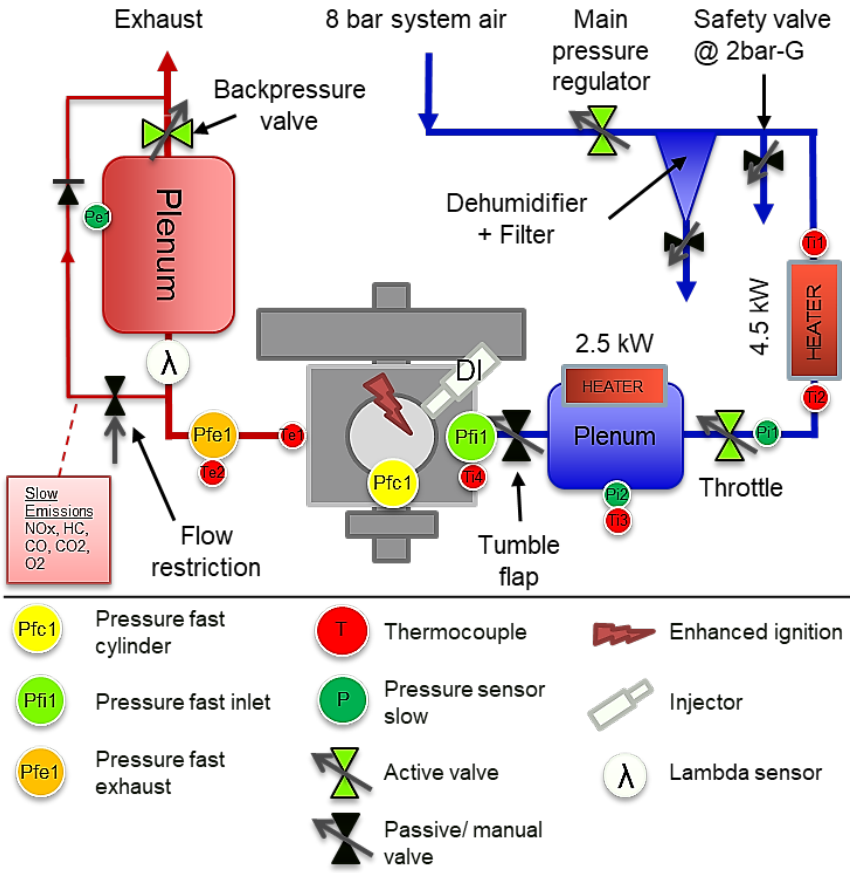

Figure 12 . Engine layout of campaign 2

Details of the acquisition system is listed in Table 4. Like experimental campaign 1, the main emissions species from the exhaust were measured to assess influence of lean combustion on emission characteristics. The concentrations of emission species were also used to estimate combustion efficiency and compute the Brettschneider lambda value.

Table 4. Acquisition specifications of campaign 2

Cylinder pressure sensors	AVL GH14DK (M5)
Cylinder pressure amplifiers	Kistler 5011
Crank angle decoder	AVL 365C
Indicating acquisition	AVL IndiModul
Indicating acquisition	AVL Indicom 2.6
Pressure transducers	Trafag 8862 + 8863
Temperature probing	Thermocouples type K
CO_2	Non-dispersive infrared detector
CO	Non-dispersive infrared detector (0-5000ppm + 0-5%)
O2	Paramagnetic oxygen analyser
HC	Flame ionization detector
NO_x	Two channel chemiluminescence detector ($NO+NO_x$)
Lambda	Broadband exhaust gas oxygen sensor, Horiba MEXA110
Fuel mass flow	Micromotion Coriolis fuel meter

3.2 Combustion diagnostics

Online software of the acquisition units provided online computed combustion measures on cycle basis based upon simplified approaches that were used for calibration during the tests. The online software also accounted for pegging of the cylinder pressure transducers, which was performed by using the thermodynamic approach. When air is added to stoichiometric combustion, the thermodynamic properties of the cylinder charge and corresponding combustion changes, which is not accounted for in the online software computations of heat release. Therefore, measured cylinder pressures obtained from experiments were postprocessed using more refined computational methods to obtain the combustion attributes. Since lean combustion is strongly related to unsteady phenomena, it is important to accurately capture the characteristics of each combustion cycle during a measurement interval.

3.2.1 Heat release

By using the first law of thermodynamics, assuming no mass-transfer over the combustion chamber control volume, the chemical heat release or gross heat release can be computed as:

$$\frac{dQ_{ch}}{d\theta} = \frac{\gamma}{\gamma - 1} P \frac{dV}{d\theta} + \frac{1}{\gamma - 1} V \frac{dP}{d\theta} + \frac{dQ_{ht}}{d\theta} \tag{8}$$

Assuming no mass-transfer means that blow by, the gas leakage through the piston rings, in neglected. For the formula to succeed one must know the combustion chamber pressure, volume, ratio of specific heats of the gases and the heat losses in the crank angle domain. Heat losses can be approximated by means of modelled correlations or complex simulations. One may also simplify the formula by disregarding the heat loss and only compute the net heat release:

$$\frac{dQ_{net}}{d\theta} = \frac{\gamma}{\gamma - 1} P \frac{dV}{d\theta} + \frac{1}{\gamma - 1} V \frac{dP}{d\theta} \tag{9}$$

The net heat release is more commonly known as the apparent heat release. Computing the net heat release assumes an adiabatic process and is directly proportional to the measured quantities of pressure and volume. It is not representative of the actual release of heat inside the combustion chamber, but it is representative of the useful heat converted into work. During both campaign 1 and campaign 2, the net heat release was utilized as the measure of heat release rate. Finally, the ratio of specific heats, gamma, must be known in order to compute the heat release.

$$\gamma = \frac{c_p}{c_v} \tag{10}$$

The ratio of specific heats is dependent on the properties of the gases inside the combustion chamber, and it also changes by temperature. For quick assessments, the ratio of specific heats may be set to a constant value of approximately 1.32 for pre-mixed SI-engines.

3.2.2 Estimation of ratio of specific heats

Polytropic approach

Various proposals have been presented in literature of how to estimate the ratio of specific heats. By assuming adiabatic compression and expansion, the ratio of specific heat equals the polytropic coefficient. The polytropic coefficient may consequently be computed from the compression and expansion curves respectively, using a least squares method to estimate the polytropic constant, a method proposed by Dahl [74] which in turn was inspired by Tunestål [75].

$$PV^{\kappa} = C \tag{11}$$

The polytropic relation do not hold during the combustion event however, and therefore the polytropic coefficient is interpolated between the coefficient of compression and expansion respectively. Since the polytropic coefficient is computed from the measured pressure, it automatically incorporates changes in the specific heats from altering the air-fuel ratio. This method was used during campaign 1 to compute the heat release.

Ceviz-Kaymaz

Another method was proposed by Ceviz and Kaymaz to directly estimate the ratio of specific heats [76]. The ratio of specific heats is computed separately for unburned and burned gases and are given by functions defined by Ceviz and Kaymaz which are dependent upon both air-fuel ratio and gas temperature. The average ratio of specific heats is then proportional to mass fractions burnt:

$$\gamma = MFB\gamma_b + (1 - MFB)\gamma_u \tag{12}$$

To compute the ratio of specific heats for the two gases, the cylinder temperature needs to be known. Assuming consistency of the ideal gas law, one can estimate the average cylinder temperature as:

$$T_{cyl}(\theta) = T_{cyl,ivc}\frac{\left(P_{cyl}(\theta) \cdot V_{cyl}(\theta)\right)}{P_{cyl,ivc}V_{cyl,ivc}} \tag{13}$$

Consequently, the gas temperature at inlet valve closing must be known to estimate the gas temperatures. This can be estimated by measuring the inlet air temperature just before entering the combustion chamber. During the intake stroke the fresh charge will interact with the combustion chamber walls hence presumably increase in temperature, why heat conduction should be taken into account. If the engine is direct injected, the cooling effect of the vaporization of the fuel should also be considered. Computation of heat transfer and vaporization may however be considered excessive and variations in the range of 10 K of the temperature estimation has negligible influence on the resulting estimation of specific heats. Ideally, the temperature should also be computed separately for unburned and burned gases, why the estimation of cylinder mean temperature should be seen as a simple approximation. Grandin for instance suggested the use of a fixed value of temperature increase, added to the inlet air temperature of 40K [77].

To compute the resulting ratio of specific heats, the mass fractions burned must already be known, why the heat release must be iteratively computed using the method suggested by Ceviz and Kaymaz. This method was used during campaign 2 to compute the heat released. It was considered more accurate compared to the polytropic approach since the ratio of specific heat is given during the combustion event and not interpolated as the polytropic approach requires. The polytropic approach is presumably more effective on rapid combustion such as HCCI (homogeneous charge compression ignition) where the interpolation has little influence on the heat release curve. When addressing slow heat release which is obtained from spark ignited diluted combustion, an interpolation which is non-representative may cause larger errors compared to a direct estimation of the specific heats, such as the Ceviz and Kaymaz method.

3.3 Dilution and how it is measured

This thesis main subject is dilution, why it deserves additional attention. Dilution is a general term, denoting gases that are present in the combustion chamber in addition to a stoichiometric air and fuel mixture. In most cases, there will remain some amount of combustion residuals from the previous cycle due to the inability to expel the gases that

remain within the top dead volume of the combustion chamber. The residuals from stoichiometric combustion are mostly constituted by N_2, CO_2 and H_2O. This is utilized in modern engines with variable valve actuations which increases the valve overlap in low loads to increase dilution by internal residuals, thus reducing pumping losses. Conversely, it is also possible to design the gas exchange system in such way that in higher load points a tuned inlet runner and beneficial pressure ratio between inlet and exhaust allows for scavenging of the residuals. This is sometimes referred to as air short-circuiting. Any dilution by external means, such as air-dilution, adds up to the total dilution factor. The amount of internal residuals are difficult to measure directly but can be estimated if the displaced mass of air of a combustion cycle is known and the corresponding mass trapped inside the combustion chamber is known. This can be estimated by simulations. Additionally, if scavenge occurs, the air-fuel ratio in the cylinder becomes difficult to measure, since some of the air escapes into the exhaust which makes the in-cylinder charge richer than intended.

The amount of air-dilution is commonly presented as the relative air-fuel ratio known as lambda. It may also be presented as the relative fuel-air ratio, equivalence ratio, phi. The amount of air dilution can be measured by various means from the exhaust. The most common way is to utilize a so-called lambda-sensor, which is universally known as a universal heated exhaust gas oxygen sensor (UHEGO) or broadband oxygen sensor. The broadband UHEGO, as opposed to the narrowband version, can sense the air to fuel ratio in a wide band. It works by measuring acquired current to pump oxygen to or from an exhaust gas measurement chamber to maintain stoichiometric air fuel ratio. As reference, a measurement cell called a Nernst cell, senses the potential between ambient air and the measurement chamber which should be proportional to a certain voltage. This measurement cell, consisting of a zirconium membrane, is sensitive to pressure and will overestimate the oxygen content at higher exhaust pressures. It is therefore important to account for the pressure difference between the exhaust gases and the ambient air. In the multi-cylinder engine of campaign 1, the broadband oxygen sensor is positioned after the second turbine and before the three-way catalyst. At this position, the pressure varies only little with exception of high power of which the pressure drop of the after-treatment system might become considerable. In the single cylinder engine of campaign 2, the broadband oxygen sensor was positioned in the exhaust runner, prior to the exhaust surge tank and exhaust pressure valve. Therefore, the sensor used in the single-cylinder engine experienced high exhaust pressures proportional to the boost pressures utilized. The signal from the oxygen sensor was therefore empirically compensated by a formula which takes into account the oxygen concentration and exhaust pressure.

By extracting an emission sample and analyze the sample by emission instruments, it is also possible to calculate the air to fuel ratio. One such method is given By the Brettschneider equation, which requires the exhaust concentrations of CO, CO_2, NO and HC, together with the fuel properties of hydrogen to carbon ratio and oxygen to carbon ratio. The method depends on accurate measurements of the four species and is more susceptible to measurement errors compared to an oxygen sensor. The air-fuel ratio can also be measured by measuring the fuel mass flow and air mass flow simultaneously. Difficulties in measuring air mass flow accurately usually renders this methodology

impractical, but in laboratory environments high precision air-flow meters can be utilized. Normally, production engines are equipped with a hot wire anemometry sensor that detects the air mass flow that is used for air mass-flow estimates.

During the experimental campaigns, broadband exhaust gas oxygen sensors were primarily used to measure the air-fuel ratio. The validity was verified by comparing with the computed Brettschneider lambda.

3.4 Knock characterization

To evaluate knock, it is useful to separate the knock signal from the combustion cycle signal. It is also beneficial to exclude the knock signal form the pressure trace when performing heat release estimations since the chock-waves caused by knock do not represent burn rates. The knock signal consists of high frequency pressure waves, received by the combustion chamber pressure transducer, and is in the frequency band of approximately 5kHz up to 50kHz. To separate the high frequency knock signal from the low frequency combustion cycle, a filter can be utilized. The challenge becomes to find a filter that has minimum ripple, sharpest cut-off and imposes no phase shift to the data. The lowest frequencies of the knock signal tend to be similar to the highest frequencies of the combustion process, why it can be sometimes difficult to separate knock and combustion, and therefore a sharp cut-off is desirable. An example of two frequency spectrums from lean combustion, one combustion cycle with no detectable knock and one cycle with heavy knock, is shown in Figure 13.

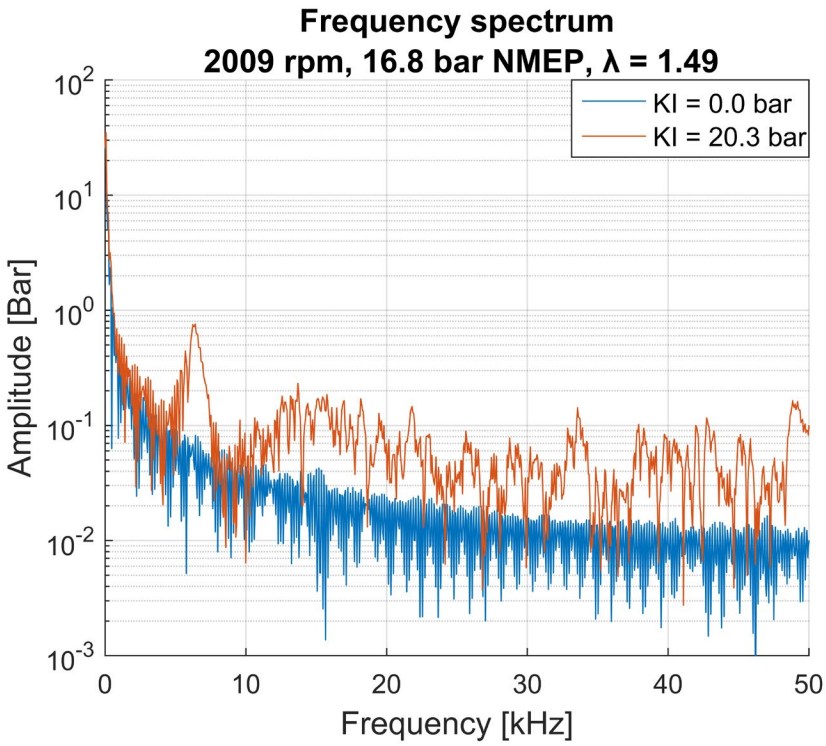

Figure 13. Fourier transformed pressure signals from a knocking combustion cycle and a non-knocking combustion cycle. As can be seen the lowest knock amplitudes starts at approximately 5kHz, which is close, or interacts with, the frequencies obtained from the heat release.

Two methods have been utilized. In campaign 1, a Butterworth filter of the fourth order was utilized. The filtering was done during post processing. Since the signal was finite, it could be filtered two times in opposite directions to eliminate the phase distortion introduced by the Butterworth filter. In campaign 2, a finite impulse response filter based upon a Hanning window was utilized. The finite impulse response filter provides a steeper cut-off compared to the Butterworth, and due to the symmetry of the filter no phase shift is introduced.

3.5 Data acquisition and evaluation

Measurements were exclusively conducted under steady state conditions. Before each measurement, temperatures were verified to be stable. Temperature readings are subject to high inertial effects and are therefore appropriate indicators of steady state. By measuring during steady state conditions, statistical quantities such as CoV and LNV can be appropriately acquired. If the conditions are non-steady, i.e. transient, it will likely influence the stability of the combustion thus impairing the statistical quantities.

Measurements were acquired by simultaneously measuring the indicating system and time-resolved data. The indicating system recorded 300 consecutive cycles in campaign 1 form the multi-cylinder engine and 60 seconds for the time-resolved data. In campaign 2,

500 cycles were recorded from the single-cylinder engine and the time-resolved data was recorded over 30 seconds. The measurement-duration of the time-resolved data was decreased in campaign 2 to match the maximum measurement duration of the indicating system, that is 30 seconds at the minimum speed of 1000 rpm. Additionally, in campaign 2 the engine was operated mostly with prominent knock without any knock-mitigation system active, why a decrease in measurement duration was considered necessary to minimize the chances of engine failure. The time-resolved data was then averaged to discriminate against signal noise. All the cycles recorded by the indicating systems were used to compute the statistical quantities of combustion such as LNV and CoV of NMEP.

The indicating systems recorded pressure signals at 0.1° CA resolution in the window of -50° to 90° ATC and with a resolution of 1°CA the rest of the cycle. High resolution in the combustion window is necessary to capture the higher frequencies obtained by knocking combustion, were literature suggests at least 0.25° CA resolution. Additionally, higher resolution improves accuracy of heat release determination.

Drifts and dispersion of the measurement setup were accounted for by daily measuring a reference engine load-point. In campaign 1, a load-point of 1500 rpm and 10 bar BMEP was chosen which also served as warm-up. In the single cylinder engine, both a motored measurement and a fired one was taken after each start-up. The reference load point of the single cylinder engine was 1500 rpm and 5.5 bar NMEP. The single-cylinder engine was pre-heated by its auxiliary rig-system which made any warm-up running obsolete. Additionally, daily calibration of the exhaust gas meters was conducted using zero and span-gases to account for any drift and potential contamination of the instruments.

Ideally, all measurements are repeated at least three times to estimate the measurement errors. This is however sometimes impractical due to cost and time-constraints if many experiments are to be performed. Instead, daily repetitions can be used to estimate the repeatability of the setup and measurement devices. Simultaneously, the repetitions allow modelling and determination of influence of the time-variable. Additionally, three repeated measurements or more in each design of experiment such as a parameter-sweep provides an estimation of the error relative to the observed effects which can be used to determine significance. This is a simplification, since it cannot be guaranteed that the dispersion is the same if the conditions are changed, but the practice is commonly used to decrease experimental effort. An example of repeated measurement in a parameter sweep of lambda is illustrated in Figure 14.

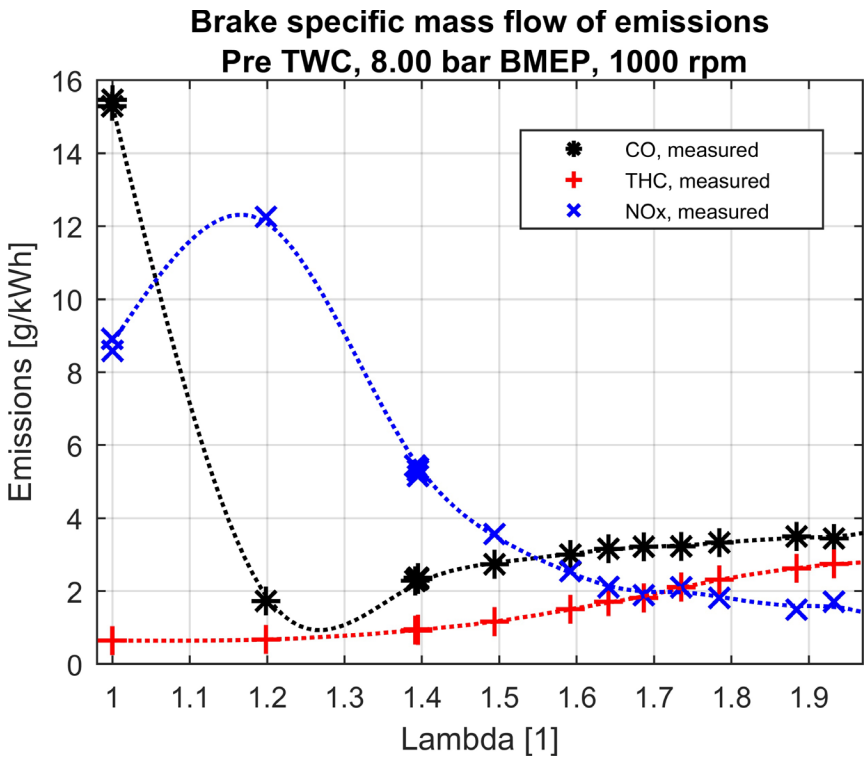

Figure 14. Resulting emissions from a lambda-sweep. Repetitions have been included at lambda = 1 and lambda = 1.4 to visualize the dispersion of the measurements to assure that the dispersion do render the observed trends insignificant. As can be seen, the dispersion relative to the large changes in emission with respect to lambda is small.

Measurements were generally conducted by performing so called lambda sweeps. A lambda sweep includes a measurement at stoichiometry, followed by increments of lambda until the stability limit has been exceeded. Where appropriate, the order of which lambda that was tested was randomized. It should be noted however that randomize the order increases the stabilization- and tuning duration. An advantage of the lambda sweep is that the stoichiometric point is included, which means that the results of lean combustion can be compared relatively to stoichiometric combustion. As could be seen in Figure 14, the dispersion in relation to the effect of lambda was very small. This observation was very similar for all investigated load-points and investigated parameters and the significance did not have to be questioned.

4 Contributions to the field

In the work performed to produce this thesis, the author was responsible for planning of the experimental work and designing and assembling of the experimental setups. The author was also responsible for performing the measurements, processing of the generated data, analyzing the generated data and the general writing of the two papers included in this thesis.

4.1 Paper I

"Homogeneous Lean Combustion in a 2lt Gasoline Direct Injected Engine with an Enhanced Turbo Charging System"

In this paper, one of the world's first downsized engines equipped with a 2-stage turbocharger designed to sustain high air-dilution rates over a wide range of loads and speeds were developed and assessed. The target was to expand the homogeneous lean operating window up to engine loads of approximately 16 bar BMEP which is sufficient to cover approximately 90% of the driving conditions of regular driving represented by the worldwide harmonized light vehicle test procedure (WLTP). This is to maximize the fuel efficiency benefits that are available from lean combustion, together with minimizing the need for mode switches between lean and stoichiometric combustion.

The demonstrator engine was fitted with a high energy ignition system and a lean NO_x aftertreatment system to obtain representable exhaust back-pressures. The setup was probed with sensors to measure critical pressures and temperatures throughout the gas exchange system and combustion chambers. By steady state mapping of the engine, a lean map could be created which was used to study the characteristics of lean combustion in the test engine versus engine speed and load.

From the lean map, it could be concluded that homogeneous lean combustion at a turbocharged operating point of 10 bar BMEP and 1500 rpm could realize a peak 12% fuel efficiency benefit by knock mitigation and reduced heat losses compared to stoichiometric combustion. This would not be possible without the boosting capabilities. Throughout the majority of the lean map, the NO_x emissions could be reduced down to a range of 1-2 g/kWh. This is slightly higher than the targeted sub 1 g/kWh NO_x. This is partly explained by that the engine combustion system, apart from the ignition system, was completely stock and not adapted for lean combustion. Thus, the required air-fuel ratios to reduce the NO_x below the target could not be sustained.

Contradictory to the expectations, the engine could not sustain lean combustion at loads higher than 13 bar BMEP with acceptable combustion stability. This was not due to inability of the turbocharger to deliver required air, but the explanation was rather due to that the combustion stability deteriorated. The expected knock mitigation effect of air-dilution was insufficient to allow for sufficient spark advance to compensate for the slower combustion. This led to the conclusion that later spark advance of lean combustion increases the effective instability of NMEP. This discovery of a lean load limit will constitute a limitation to high load lean combustion.

4.2 Paper II

"Investigation of Homogeneous Lean SI Combustion in High Load Operating Conditions"

The indication of a lean load limit, discovered in campaign 1 and published in paper I, necessitated further investigations to understand why this phenomenon occurred. Prior to the first test campaign, the hypothesis was that the knock mitigation effect by operating very lean, that had been demonstrated by previous studies, was sufficient to allow for high pressure lean combustion at loads as high as 16 bar BMEP. Test campaign 1 proved this hypothesis wrong, thus more experiments were performed in a supercharged single-cylinder research engine to investigate the load limit further. The single-cylinder engine allowed decoupling from the gas-exchange characteristics obtained when utilizing a turbocharger to deliver boost pressure. To operate very lean at high loads, a boost system was designed and built that utilized compressed air at 8 bar which was then regulated down to boost pressure levels by a regulator and modulated to surge tank pressure by a throttle valve. The single cylinder engine was additionally equipped with a high energy ignition system and an inlet port tumble plate to increase the tumble gas motion in the combustion chamber.

By performing lambda- and ignition sweeps, the relation between combustion instability and knock could be investigated at various spark advances and air-dilutions. Various loads and speeds were included, together with default tumble and enhanced tumble by using the tumble plate. The engine speed has a substantial effect on the gas motion, and the trends in relation to the engine load is valuable to understand how the lean load limit occurs.

Form the test data, a definition of the lean load limit could be achieved as "the convergence of the stability boundary and knock boundary" which eliminates valid options of spark advance and corresponding combustion phasing [78]. In stoichiometric, un-diluted combustion, the stability limit does not occur, why the spark advance and corresponding combustion phasing can be retarded to reduce peak pressure of the combustion to mitigate knock. This is not always possible with lean combustion, since the stability limit dictates how much spark retard is possibly without exceeding the combustion stability threshold.

The lean load limit limited the engine load to approximately 13-14 bar NMEP, which is similar to the result obtained in paper I. By increased tumble using the tumble plate, the load could be increased up to slightly above 16 bar NMEP which is close to the initial load target of the multi-cylinder engine. The use of the tumble plate introduced increases of pumping losses, in the order of 0.5% units, and heat losses, in the order of 1% units, which was much smaller than expected since the substantial throttling of the intake port should increase the port friction considering the high mass-flows, and the stronger gas motion was anticipated to increase heat flux to the engine walls during combustion. By adopting techniques to improve the combustion chamber gas motion, it has been demonstrated that lean combustion can be sustained at considerably higher loads than is possible with low gas motion.

5 Future work

The work of this thesis has primarily focused on homogeneous lean combustion in high load application. More research is needed on the core subject of cyclic dispersion and flame propagation which has received lesser attention in this work. The literature has highlighted the influence of residuals in cyclic dispersion. It is therefore desirable to determine the quantity of residuals in the combustion chamber which in turn will reveal the total combustion chamber dilution factor of residuals and excess air. This can be done by 1-D simulations of the gas exchange using a tool such as the Gamma Technologies Suite, where the model is calibrated by indicated pressures received from experiments.

A substantial amount of the data that was produced by running experiments in the single cylinder research engine in campaign 2 has not been analyzed. More experiments including comparison between dual coil ignition and high frequency ignition were performed both on high and low engine loads. Additionally, other factors such as valve overlap, exhaust pressure and intake air temperature were tested but not analyzed which may prove useful in continuing the investigation of high load lean combustion.

Interaction between combustion and exhaust after-treatment is another aspect of interest to realize clean tailpipe emissions and legislation compliance. Therefore, part of the next step in the research of lean combustion is to study the corresponding particulate emissions and how they can be filtrated from the exhaust. Lean combustion exhaust poses challenges to filtration techniques since the amount of particulate emissions is low compared to stoichiometric combustion. The exhaust gases are additionally colder and contains excess oxygen and these factor's influence on passive oxidation in a particulate filter is of interest to investigate for future lean particulate filtration in spark-ignited engines.

The capability of reducing NO_x emissions from the engine out exhaust is a crucial element in realizing clean tailpipe emissions. A promising technology that provides lean NO_x after-treatment is selective catalytic reduction (SCR). Active SCR-technology is well known and is already commercialized on the market together with diesel engines. However, very few studies on lean spark-ignited combustion with active SCR-technology has been reported. The active SCR-technology is very important since it is a flexible system that has high potentials of reducing NO_x-emissions in a wide range of operating conditions, without causing a fuel penalty. The active SCR-system utilizes a NO_x-reducing agent containing urea, known as AdBlue, instead of regeneration by rich engine operation. Therefore, it is possible to optimize between fuel efficiency and reducing agent consumption rather than solely optimize the engine towards low engine out NO_x emissions. Further research on the SCR system is intended to study how effectively NO_x can be reduced at various operating strategies of a lean combustion SI-engine.

References

1 "CO2 emissions from cars: the facts," Transport & Environment 2018, Available: https://www.transportenvironment.org/sites/te/files/publications/2018_04_CO2_emissions_cars_The_facts_report_final_0_0.pdf.

2 P. Mock, Ed. *EUROPEAN VEHICLE MARKET STATISTICS*. International Council on Clean Transportation, 2020.

3 Bae, C. and Kim, J., "Alternative fuels for internal combustion engines", *Proceedings of the Combustion Institute* 36:2017, doi:10.1016/j.proci.2016.09.009.

4 Kiyota, Y., Akishino, K., and Ando, H., "Concept of Lean Combustion by Barrel-Stratification", SAE Technical Paper 920678, 1992, doi:10.4271/920678.

5 Johansson, A. N., Hemdal, S., and Dahlander, P., "Experimental Investigation of Soot in a Spray-Guided Single Cylinder GDI Engine Operating in a Stratified Mode", SAE Technical Paper 2013-24-0052, 2013, doi:10.4271/2013-24-0052.

6 International Council on Clean transportation. (2019, 05-27). *CO2 EMISSION STANDARDS FOR PASSENGER CARS AND LIGHT-COMMERCIAL VEHICLES IN THE EUROPEAN UNION*. Available: https://theicct.org/sites/default/files/publications/EU-LCV-CO2-2030_ICCTupdate_201901.pdf

7 Hopkinson, B., "Hopkinson, Bertram. "The Effect of Mixture Strength and Scavenging upon Thermal Efficiency", *Proceedings of the Institution of Mechanical Engineers* 74(1):1908,

8 Ricardo, H. R., "Some Experiments on Supercharging in a High-Speed Engine", *Proceedings of the Institution of Automobile Engineers* 15(1):1920,

9 Bolt, J. A. and Holkeboer, D. H., "Lean Fuel/Air Mixtures for High-Compression Spark-Ignited Engines", SAE Technical Paper 620524, 1962, doi:10.4271/620524.

10 Bolt, J. A. and Harrington, D. L., "The Effects of Mixture Motion Upon the Lean Limit and Combustion of Spark-Ignited Mixtures", SAE Technical Paper 670467, 1967, doi:10.4271/670467.

11 Environmental Protection Agency. (May 19, 2020). *Timeline of Major Accomplishments in Transportation, Air Pollution, and Climate Change*. Available: https://www.epa.gov/transportation-air-pollution-and-climate-change/timeline-major-accomplishments-transportation-air

12 Lee, R. C. and Wimmer, D. B., "Exhaust Emission Abatement by Fuel Variations to Produce Lean Combustion", SAE Technical Paper 680769, 1968, doi:10.4271/680769.

13 Tanuma, T., Sasaki, K., Kaneko, T., and Kawasaki, H., "Ignition, Combustion, and Exhaust Emissions of Lean Mixtures in Automotive Spark Ignition Engines", SAE Technical Paper 710159, 1971, doi:10.4271/710159.

14 Yagi, S., Date, T., and Inoue, K., "NOx Emission and Fuel Economy of the Honda CVCC Engine", SAE Technical Paper 741158, 1974, doi:10.4271/741158.

15 Noguchi, M., Sanda, S., and Nakamur, N., "Development of Toyota Lean Burn Engine", SAE Technical Paper 760757, 1976, doi:10.4271/760757.

16 Scussel, A. J., Simko, A. O., and Wade, W. R., "The Ford PROCO Engine Update", SAE Technical Paper 780699, 1978, doi:10.4271/780699.
17 Germane, G. J., Wood, C. G., and Hess, C. C., "Lean Combustion in Spark-Ignited Internal Combustion Engines - A Review", SAE Technical Paper 831694, 1983, doi:10.4271/831694.
18 "General Motors Believes it has an Answer to the Automotive Air Pollution Problem," in *The Blade: Toledo*, ed, 1974.
19 Engh, G. T. and Wallman, S., "Development of the Volvo Lambda-Sond System", SAE Technical Paper 770295, 1977, doi:10.4271/770295.
20 Volvo Car Sverige AB, Newsroom. (2002, 05-19). *The prize winner - Lambda Sond*. Available: https://www.media.volvocars.com/se/sv-se/media/pressreleases/5249
21 Ingesson, G., Yin, L., Johansson, R., and Tunestal, P., "Evaluation of Nonlinear Estimation Methods for Calibration of a Heat-Release Model", *SAE Int. J. Engines* 9(2):2016, doi:10.4271/2016-01-0820.
22 Stokes, J., Lake, T. H., Christie, M. J., and Denbratt, I., "Improving the NOx/Fuel Economy Trade-Off for Gasoline Engines with the CCVS Combustion System", SAE Technical Paper 940482, 1994, doi:10.4271/940482.
23 Kuwahara, K., Ueda, K., and Ando, H., "Mixing Control Strategy for Engine Performance Improvement in a Gasoline Direct Injection Engine", SAE Technical Paper 980158, 1998, doi:10.4271/980158.
24 Kano, M., Saito, K., Basaki, M., Matsushita, S., and Gohno, T., "Analysis of Mixture Formation of Direct Injection Gasoline Engine", SAE Technical Paper 980157, 1998, doi:10.4271/980157.
25 Wirth, M., Mayerhofer, U., Piock, W. F., and Fraidl, G. K., "Turbocharging the DI Gasoline Engine", SAE Technical Paper 2000-01-0251, 2000, doi:10.4271/2000-01-0251.
26 Ortmann, R., Arndt, S., Raimann, J., Grzeszik, R., and Würfel, G., "Methods and Analysis of Fuel Injection, Mixture Preparation and Charge Stratification in Different Direct Injected SI Engines", SAE Technical Paper 2001-01-0970, 2001, doi:10.4271/2001-01-0970.
27 DieselNet Technology Guide. (2020, 05-20). *NOx Adsorbers*. Available: https://dieselnet.com/tech/cat_nox-trap.php
28 Chambon, P., Huff, S., Norman, K., Edwards, K. D., Thomas, J., and Prikhodko, V., "European Lean Gasoline Direct Injection Vehicle Benchmark", SAE Technical Paper 2011-01-1218, 2011, doi:10.4271/2011-01-1218.
29 Enderle, G. V., Merdes, N., Kreitmann, F., and Weller, R., "The new 2.0l turbo engine from the MercedesBenz 4-cylinder engine family," presented at the 2nd Aachen Colloquium China, 2012.
30 Pauly, T., Franoschek, S., Hoyer, R., and Eckhoff, S., "Cost and Fuel Economy Driven Aftertreatment Solutions -for Lean GDI-", SAE Technical Paper 2010-01-0363, 2010, doi:10.4271/2010-01-0363.
31 Inoue, T., Matsushita, S., Nakanishi, K., and Okano, H., "Toyota Lean Combustion System - The Third Generation System", SAE Technical Paper 930873, 1993, doi:10.4271/930873.

32 Zelenyuk, A. *et al.*, "Detailed characterization of particulate matter emitted by lean-burn gasoline direct injection engine", *Int. J. Engine Research* 18(5-6):2016, doi:10.1177/1468087416675708.
33 Parks, J. E., Storey, J. M. E., Prikhodko, V. Y., Debusk, M. M., and Lewis, S. A., "Filter-Based Control of Particulate Matter from a Lean Gasoline Direct Injection Engine", SAE Technical Paper 2016-01-0937, 2016, doi:10.4271/2016-01-0937.
34 Heywood, J. B., *Internal Combustion Engine Fundamentals*. McGraw-Hill inc., 1988.
35 Berntsson, A. W., Josefsson, G., Ekdahl, R., Ogink, R., and Grandin, B., "The Effect of Tumble Flow on Efficiency for a Direct Injected Turbocharged Downsized Gasoline Engine", *SAE Int. J. Engines* 4(2):2011, doi:10.4271/2011-24-0054.
36 Rowley, J. R., Rowley, R. L., and Wilding, W. V., "Estimation of the lower flammability limit of organic compounds as a function of temperature", *Journal of Hazardous Materials* 186:2011, doi:10.1016/j.jhazmat.2010.11.039.
37 Matthias, N., Wallner, T., and Scarcelli, R., "Analysis of Cyclic Variability and the Effect of Dilute Combustion in a Gasoline Direct Injection Engine", *SAE Int. J. Engines* 7(2):2014, doi:10.4271/2014-01-1238.
38 Berckmuller, M., Tait, N. P., and Greenhaigh, D. A., "The Influence of Local Fuel Concentration on Cyclic Variability of a Lean Burn Stratified-Charge Engine", SAE Technical Paper 970826, 1997, doi:10.4271/970826.
39 Metghalchi, M. and Keck, J. C., "Burning Velocities of Mixtures of Air with Methanol, Isooctane, and Indolene at High Pressure and Temperature", *Combustion and Flame* 48:1982, doi:10.1016/0010-2180(82)90127-4.
40 Johansson, B., "Cycle to Cycle Variations in S.I. Engines - The Effects of Fluid Flow and Gas Composition in the Vicinity of the Spark Plug on Early Combustion", SAE Technical Paper 962084, 1996, doi:10.4271/962084.
41 Keck, J. C., Heywood, J. B., and Noske, G., "Early Flame Development and Burning Rates in Spark Ignition Engines and Their Cyclic Variability", SAE Technical Paper 870164, 1987, doi:10.4271/870164.
42 Krüger, C., Schorr, J., Nicollet, F., Bode, J., Dreizler, A., and Böhm, B., "Cause-and-effect chain from flow and spray to heat release during lean gasoline combustion operation using conditional statistics", *Int. J. Engine Research* 18(1-2):2017, doi:10.1177/1468087416686721.
43 Wang, Y. *et al.*, "Investigation of Flow Conditions and Tumble near the Spark Plug in a DI Optical Engine at Ignition", SAE Technical Paper 2018-01-0208, 2018, doi:10.4271/2018-01-0208.
44 Aleiferis, P. G., Taylor, A. M. K. P., Whitelaw, J. H., Ishii, K., and Urata, Y., "Cyclic Variations of Initial Flame Kernel Growth in a Honda VTEC-E Lean-Burn Spark-Ignition Engine", SAE Technical Paper 2000-01-1207, 2000, doi:10.4271/2000-01-1207.
45 Aleiferis, P. G., Taylor, A. M. K. P., Ishii, K., and Urata, Y., "The nature of early flame development in a lean-burn stratified-charge spark-ignition engine", *Combustion and Flame* 136(3):2004, doi:10.1016/j.combustflame.2003.08.011.

46 Amirante, R., Distaso, E., Tamburrano, P., and Reitz, R. D., "Laminar flame speed correlations for methane, ethane, propane and their mixtures, and natural gas and gasoline for spark-ignition engine simulations", *Int. J. Engine Research* 18(9):2017, doi:10.1177/1468087417720018.

47 Hanabusa, H., Kondo, T., Hashimoto, K., Sono, H., and Furutani, M., "Study on Homogeneous Lean Charge Spark Ignition Combustion", SAE Technical Paper 2013-01-2562, 2013, doi:10.4271/2013-01-2562.

48 Doornbos, G., Hemdal, S., and Dahl, D., "Reduction of Fuel Consumption and Engine-Out NOx Emissions in a Lean Homogeneous GDI Combustion System, Utilizing Valve Timing and an Advanced Ignition System", SAE Technical Paper 2015-01-0776, 2015, doi:10.4271/2015-01-0776.

49 Kolodziej, C. P., Pamminger, M., Sevik, J., Wallner, T., Wagnon, S. W., and Pitz, W. J., "Effects of Fuel Laminar Flame Speed Compared to Engine Tumble Ratio, Ignition Energy, and Injection Strategy on Lean and EGR Dilute Spark Ignition Combustion", *SAE Int. J. Fuels Lubr.* 10(1):2017, doi:10.4271/2017-01-0671.

50 Lee, Y. G. and Boehler, J. T., "Flame Kernel Development and its Effects on Engine Performance with Various Spark Plug Electrode Configurations", SAE Technical Paper 2005-01-1133, 2005, doi:10.4271/2005-01-1133.

51 Shiraishi, T., Teraji, A., and Moriyoshi, Y., "The Effects of Ignition Environment and Discharge Waveform Characteristics on Spark Channel Formation and Relationship between the Discharge Parameters and the EGR Combustion Limit", *SAE Int. J. Engines* 9(1):2015, doi:10.4271/2015-01-1895.

52 Hayashi, N., Sugiura, A., Abe, Y., and Suzuki, K., "Development of Ignition Technology for Dilute Combustion Engines", *SAE Int. J. Engines* 10(3):SAE Technical Paper 2017-01-0676, 2017, doi:10.4271/2017-01-0676.

53 Alger, T., Gingrich, J., Mangold, B., and Roberts, C., "A Continuous Discharge Ignition System for EGR Limit Extension in SI Engines", *SAE Int. J. Engines* 4(1):2011, doi:10.4271/2011-01-0661.

54 Doornbos, G., Hemdal, S., Denbratt, I., and Dahl, D., "Knock Phenomena under Very Lean Conditions in Gasoline Powered SI-Engines", *SAE Int. J. Engines* 11(1):03-11-01-0003, 2018, doi:10.4271/03-11-01-0003.

55 Suess, M., Guenthner, M., Schenk, M., and Rottengruber, H.-S., "Investigation of the potential of corona ignition to control gasoline homogeneous charge compression ignition combustion", *Proceedings of the Institution of Mechanical Engineers, Part D: Journal of Automobile Engineering* 226(2):2012, doi:10.1177/0954407011416905.

56 Bunce, M. and Blaxill, H., "Sub-200 g/kWh BSFC on a Light Duty Gasoline Engine", SAE Technical Paper 2016-01-0709, 2016, doi:10.4271/2016-01-0709.

57 Glassman, I. and Yetter, R. A., *Combustion*, 4 ed. Elsevier, 2008.

58 He, Y., Selamet, A., Reese, R. A., Vick, R. K., and Amer, A. A., "Effect of Intake Primary Runner Blockages on Combustion Characteristics and Emissions with Stoichiometric and EGR-Diluted Mixtures in SI Engines", SAE Technical Paper 2007-01-3992, 2007, doi:10.4271/2007-01-3992.

59 Neußer, H.-J. and Geiger, J., "Continuous Variable Tumble - A New Concept for Future Lean Burn Engines", SAE Technical Paper 960607, 1996, doi:10.4271/960607.
60 Larsson, T. *et al.*, "The Volvo 3-Litre 6-Cylinder Engine with 4-Valve Technology", SAE Technical Paper 901715, 1990, doi:10.4271/901715.
61 Ogink, R. and Babajimopoulos, A., "Investigating the Limits of Charge Motion and Combustion Duration in a High-Tumble Spark-Ignited Direct-Injection Engine", *SAE Int. J. Engines* 9(4):2016, doi:10.4271/2016-01-2245.
62 Zhang, A. *et al.*, "The Impact of Spark Discharge Pattern on Flame Initiation in a Turbulent Lean and Dilute Mixture in a Pressurized Combustion Vessel", *SAE Int. J. Engines* 6(1):2013, doi:10.4271/2013-01-1627.
63 Moriyoshi, Y., Kuboyama, T., Kaneko, M., Yamada, T., and Sato, H., "Fuel Stratification Using Twin-Tumble Intake Flows to Extend Lean Limit in Super-Lean Gasoline Combustion", SAE Technical Paper 2018-01-1664, 2018, doi:10.4271/2018-01-1664.
64 Sjöberg, M., Zeng, W., Singleton, D., Sanders, J. M., and Gundersen, M. A., "Combined Effects of Multi-Pulse Transient Plasma Ignition and Intake Heating on Lean Limits of Well-Mixed E85 DISI Engine Operation", *SAE Int. J. Engines* 7(4):2014, doi:10.4271/2014-01-2615.
65 Yamakawa, M. *et al.*, "Combustion Technology Development for a High Compression Ratio SI Engine", *SAE Int. J. Fuels Lubr.* 5(1):2012, doi:10.4271/2011-01-1871.
66 Hanabusa, H., Kondo, T., Hashimoto, K., and Furutani, M., "Study on Cyclic Variations of Laminar Flame Speed in Homogeneous Lean charge Spark Ignition Combustion", SAE Technical Paper 2016-01-2173, 2016, doi:10.4271/2016-01-2173.
67 Grandin, B., Denbratt, I., Bood, J., Brackmann, C., and Bengtsson, P.-E., "The Effect of Knock on the Heat Transfer in an SI Engine: Thermal Boundary Layer Investigation using CARS Temperature Measurements and Heat Flux Measurements", SAE Technical Paper 2000-01-2831, 2000, doi:10.4271/2000-01-2831.
68 Burgdorf, K. and Denbratt, I., "Comparison of Cylinder Pressure Based Knock Detection Methods", SAE Technical Paper 972932, 1997, doi:10.4271/972932.
69 Grandin, B. and Ångström, H.-E., "Replacing Fuel Enrichment in a Turbo Charged SI Engine: Lean Burn or Cooled EGR", SAE Technical Paper 1999-01-3505, 1999, doi:10.4271/1999-01-3505.
70 Grandin, B. *et al.*, "Heat Release in the End-Gas Prior to Knock in Lean, Rich and Stoichiometric Mixtures With and Without EGR", SAE Technical Paper 2002-01-0239, 2002, doi:10.4271/2002-01-0239.
71 Topinka, J. A., Gerty, M. D., Heywood, J. B., and Keck, J. C., "Knock Behavior of a Lean-Burn, H2 and CO Enhanced, SI Gasoline Engine Concept", SAE Technical Paper 2004-01-0975, 2004, doi:10.4271/2004-01-0975.
72 Stokes, J., Lake, T. H., and Osborne, R. J., "A Gasoline Engine Concept for Improved Fuel Economy –The Lean Boost Syste", SAE Technical Paper 2000-01-2902, 2000, doi:10.4271/2000-01-2902.

73 Ratnak, S., Kusaka, J., Daisho, Y., Yoshimura, K., and Nakama, K., "Experiments and Simulations of a Lean-Boost Spark Ignition Engine for Thermal Efficiency Improvement", *SAE Int. J. Engines* 9(1):2015-32-0711, 2016, doi:10.4271/2015-32-0711.
74 Dahl, D., "Gasoline Engine HCCI Combustion," PhD, Applied Mechanics, Chalmers University of Technology, Göteborg, 2012.
75 Tunestål, P., "Self-tuning gross heat release computation for internal combustion engines", *Control Engineering Practice* 17(4):Journal 2009, doi:10.1016/j.conengprac.2008.09.012.
76 Ceviz, M. A. and Kaymaz, I., "Temperature and air–fuel ratio dependent specific heat ratio functions for lean burned and unburned mixture", *Energy Conversion and Management* 46(15-16):Journal 2004, doi:10.1016/j.enconman.2004.12.009.
77 Grandin, B., "Knock in Gasoline Engines," PhD, Department of Thermo and Fluid Dynamics, Chalmers University of Technology, Göteborg, 2001.
78 Clasen, K. and Koopmans, L., "Investigation of Homogeneous Lean SI Combustion in High Load Operating Conditions", SAE Technical Paper 2020-01-0959, 2020, doi:10.4271/2020-01-0959.

Symbols and Acronyms

0	Denotes start or reference condition
b	Burned
C	Empirical constant
c_p	Specific heat at constant pressure (J/kgK)
c_v	Specific heat at constant pressure (J/kgK)
H_c	Combustion enthalpy
n	Empirical exponent
P	Pressure
Q_{ch}	Chemical heat, gross heat
Q_{fuel}	Available heat of injected fuel
Q_{ht}	Heat loss
Q_{net}	Net heat
S_L	Laminar flame speed
S_T	Turbulent flame speed
T	Temperature
u	Unburned
u'	Turbulence intensity
V	Volume
γ	Specific heat ratio, c_p/c_v
η_t	Ideal thermal efficiency
θ	Crank angle
κ	Polytropic exponent
λ	Relative air-fuel ratio
μ	Average
σ	Standard deviation
τ	Auto ignition delay
φ	Equivalence ratio, relative fuel-air ratio

ATC	After top center
BMEP	Brake mean effective pressure
BSFC	Brake specific fuel consumption
BTC	Before top center
CA	Crank angle (degrees)
CA00	0% mass fraction burned = spark timing
CA10	10% mass fraction burned
CA50	50% mass fraction burned
CA90	90% mass fraction burned
CAaTDCf	Crank angle (degrees) after top dead center firing
CO	Carbon monoxide
CO2	Carbon dioxide
CoV	Coefficient of variation
CR	Compression ratio
Cyl	Cylinder
DCI	Dual coil ignition
DI	Direct injection
DISI	Direct injection spark ignition
DOHC	Double over-head camshafts
E10	10% Ethanol
EVC	Exhaust valve closing
EVO	Exhaust valve opening
H_2O	Water
HC	Hydrocarbon
HCCI	Homogeneous charge compression ignition
HFI	High frequency ignition
HLC	Homogeneous lean combustion
ICE	Internal combustion engine
ICE	Internal combustion
IVC	Inlet valve closing
IVO	Inlet valve opening

KI	Knock intensity
KO	Knock onset
KT	Knock tendency
Lambda	Relative air-fuel ratio
LFL	lower flammability limit
LIF	Laser induced fluorescence
LNV	Lowest normalized value
MBT	Maximum brake torque
MFB	Mass fraction burned
N2	Nitrogen
NMEP	Net (indicated) mean effective pressure
NOx	NO + NO2, nitrogen oxides
RON	Research octane number
SCR	Selective catalytic reduction
SI	Spark ignition
Std	Standard deviation
TC	Top center
TDC	Top dead center
TF	Tumble flap
THC	Total hydrocarbon
TWC	Three-way catalyst
UHEGO	Universal heated exhaust gas oxygen sensor
WG	Waste-gate
WLTP	Worldwide harmonized light vehicle test procedure
VNT	Variable nozzle turbine
VTEC	Variable valve timing & lift electronic control

Appended papers I - II

Paper I

2018-01-1670 Published 10 Sep 2018

Homogeneous Lean Combustion in a 2lt Gasoline Direct Injected Engine with an Enhanced Turbo Charging System

Kristoffer Clasen and Lucien Koopmans Chalmers University of Technology

Daniel Dahl Volvo Car Corp.

Citation: Clasen, K., Koopmans, L., and Dahl, D., "Homogeneous Lean Combustion in a 2lt Gasoline Direct Injected Engine with an Enhanced Turbo Charging System," SAE Technical Paper 2018-01-1670, 2018, doi:10.4271/2018-01-1670.

Abstract

In the quest for a highly efficient, low emission and affordable source of passenger car propulsion system, meeting future demands for sustainable mobility, the concept of homogeneous lean combustion (HLC) in a spark ignited (SI) multi-cylinder engine has been investigated. An attempt has been made to utilize the concept of HLC in a downsized multi-cylinder production engine producing up to 22 bar BMEP in load. The focus was to cover as much as possible of the real driving operational region, to improve fuel consumption and tailpipe emissions. A standard Volvo two litre four-cylinder gasoline direct injected engine operating on commercial 95 RON gasoline fuel was equipped with an advanced two stage turbo charger system, consisting of a variable nozzle turbine turbo high-pressure stage and a wastegate turbo low-pressure stage. The turbo system was specifically designed to meet the high demands on air mass flow when running lean on higher load and speeds. Also, a dual coil ignition system was used for enhanced ignition ability and a lean NO_x emissions exhaust after-treatment system (EATS) dummy was fitted downstream the turbo to receive representative exhaust pressures and temperatures for further development purposes. The engine was mapped running lean in various load points in the operational area of interest. It was found that the engine could sustain a high degree of dilution in lower engine speeds and intermediate loads. Fuel consumption improvements of 12% were obtained running at 1500 rpm and 10 bar BMEP at lambda 1.8. At higher engine loads, above 10 bar BMEP, it was found that the combustion stability deteriorated. The ignition could not be optimized due to knocking combustion and at the same time, combustion duration, measured in crank angle degrees, increased with increasing en-leanment and engine speed, leading to late combustion phasing and large variation in cycle-to-cycle of NMEP. This is currently limiting the operational region of lean combustion of the engine used. The load limit in lean operation was investigated, assessing combustion variations and knock phenomena under different operating conditions.

Introduction

Road transportation of today is heavily dependent on the internal combustion engine (ICE) and the need for increased efficiency and reduction of harmful- and greenhouse gas emissions is of vital importance for minimizing its environmental and health impact. In 2016, about half of the new cars in Europe were powered by diesel fuel [1]. In the U.S. and Japan the market share of diesel is negligible for light duty applications [2]. For hybrid applications the SI engine is preferred due to its cost advantage over the diesel engine. Therefore, SI engines are believed to play an important role when providing highly efficient, clean and affordable propulsion with or without any degree of electrification. To realize additional improvements, unconventional combustion concepts are considered and one such concept with high potential is lean combustion, which is the topic of this paper.

The advantages of lean combustion, air-diluted combustion, are well known [3, 4, 5, 6]. As summarized by Doornbos et al. [7], lean operation allows for increased air mass flow and at part load this will result in lower pumping losses due to less throttling. The increased mass in the combustion chamber reduces the combustion temperature, which results in reduced heat losses. The ratio of specific heats increases with lean operation which results in higher ideal thermal efficiency and the increased concentration of oxygen increases combustion efficiency. The lean combustion concept has been implemented in so called CVCC engines (compound vortex controlled combustion) [8], and later in in-cylinder stratified concepts [9, 10]. Both approaches have in common that the cylinder air/fuel mixture is in-homogeneous or stratified. In stratified lean combustion a small portion of a richer mixture in the vicinity of the sparkplug is combined with a large portion of a very lean mixture resulting in an overall lean cylinder charge which is combusted. By placing the richer portion close to the spark in a SI-engine, stable ignition and onset combustion can be achieved resulting in a smooth engine operation. One drawback of a stratified charge is that the small portion with a richer mixture is believed to produce increased NOx

emissions when combusted [9]. Also, stratified combustion has been linked to an increase in soot emissions [11]. A third disadvantage of stratified lean operation is that it is limited to lower engine load due to substantially increased NO_x, soot and unburned hydrocarbons (THC) emissions in higher engine load. At higher loads it is difficult to stratify a large fuel mass mixture and maintain the intended air/fuel ratio distribution of the stratified cloud within the flammability limits, partly due to long injection durations. In downsized turbocharged engines, stratified operation can be expected to cover at most the same relative operational area compared to a corresponding non-downsized engine [12]. Homogeneous lean combustion is an alternative method to stratified lean combustion. In HLC the homogeneous, pre-mixed lean air/fuel mixture is spark-ignited directly without local fuel-enrichments, which in theory should eliminate the local temperature increase caused by the small richer portion in a lean stratified charge. The capability of HLC to produce low NO_x emissions has been verified by several studies [7, 13, 14, 15]. By diluting the air/fuel mixture, the combustion temperatures decrease and less NO_x emissions are formed. Reports on the upper load limit for an engine operated in HLC mode, fitted with a gas-exchange system capable of providing excess air at high loads, are difficult to find. Most research effort has been concentrated to the lower part-load region.

Normally NO_x, CO and THC in the exhausts are converted to N_2, H_2O and CO_2 respectively, by a three-way catalyst (TWC), an exhaust after-treatment device which is utilized on all production SI-engines in automotive applications. TWCs have close to 100% conversion efficiency when at optimum operation temperature but are only capable of reducing NO_x molecules when the engine is operated at a stoichiometric (or rich) condition. TWCs are virtually incapable of NO_x reduction with excess oxygen and low CO concentrations in the exhaust which are the exhaust conditions obtained when operating an SI-engine with lean combustion [13, 16, 17, 18]. If the engine out NO_x emissions from lean combustion cannot be decreased to sufficiently low levels, not complying with tailpipe emission legislation and environmental needs, a lean NO_x exhaust after-treatment must be introduced. Two of the available options of lean NO_x EATS are the more conventional Lean NO_x Trap (LNT) and the more recent alternative of Selective Catalytic Reduction (SCR). The LNT system is dependent on alternating between lean and rich operation, where the trapped NO_x from lean operation is reduced by heat and CO, formed during rich operation, resulting in CO_2 and N_2 tailpipe emissions. The SCR system is dependent on the addition of NH_3 which is introduced externally as a urea-solvent or more commonly known by its tradename of adBlue or diesel exhaust fluid. The urea-solvent is typically constituted by 32.5% urea and 67.5% deionized water. SCR-technology has been highlighted as one of the most promising lean NO_x EATS alternatives for diesel application but it can also be used for lean combustion SI-engines [19]. Since the SCR is not dependent on cyclic rich operation the fuel penalty of NO_x-reduction is reduced, but replaced by NH_3 consumption. To keep urea consumption of the SCR-catalyst low the engine out NO_x emissions should be reduced as much as possible. The ability of HLC to produce low NO_x emissions in combination with a SCR EATS makes it a promising concept, hence chosen for further investigation in this paper.

A homogeneous lean charge is more difficult to ignite and combusts slower when the amount of air dilution is increased. Lean conditions reduce the in-cylinder temperature while increasing pressure which slows the laminar burning velocity, placing a higher demand on the ignition system and combustion system design. When increasing the amount of air dilution, eventually a stability limit is reached, usually defined by a predetermined level of coefficient of variation (CoV) and lowest normalized value (LNV) of NMEP. The instability has been linked to variations in the early stages of combustion for premixed turbulent flames [20]. Beyond the stability limit uneven engine operation and misfires causes efficiency to deteriorate and emissions to increase. To further increase dilution tolerance, which leads to further NO_x emissions reduction, extension of the lean limit has been addressed by previous research [14, 15, 20, 21]. Most of the studies found in the literature have been focusing on low load and speed operation. In his doctoral thesis, Doornbos made various HLC experiments running at a peak load of 11 bar NMEP ranging from 1000-3000 rpm in a single-cylinder engine rig, utilizing pure spark ignition with artificial supercharging [14]. Bunce and Blaxill have performed tests up to 14 bar BMEP ranging from 2000-3000 rpm also using artificial supercharging but with a jet-ignition system [15]. Both studies concluded that air dilution was successful in mitigating knock when a relative air/fuel ratio, lambda, above approximately 1.5-1.6 was implemented. Attempts with HLC operation at similar or higher loads, utilizing a turbocharger system, have not been found in the literature. The load of 11 bar NMEP achieved by Doornbos in his experiments is merely 50% of the expected power output from the engine platform that was utilized, which leaves a large operational region un-investigated. In higher loads implications such as severe knock tendencies and boosting efficiency should be considered. Since the engine out NO_x is correlated to the amount of dilution, operating close to the lean limit to minimize engine out NO_x is desired. Depending on the dilution tolerance of the engine used, maximum dilution may result in the engine being operated at certain load-points at a relative air/fuel ratio of lambda >1.6, which requires an increase of air mass flow of 50% or more, compared to stoichiometric operation. To be able to maintain power output in lean operation the boosting capabilities must subsequently be substantially increased but at the same time available enthalpy in the exhaust will be reduced since air dilution decreases combustion temperatures and hence exhaust temperatures.

This paper describes the findings and analysis of an experimental study on a production, downsized multi-cylinder engine fitted with a prototype turbocharger system for increased boosting capability in lean operation, of which no other similar system applied to a HLC SI-engine have been previously observed by the authors. To fulfil the demands on air mass flow during HLC operation, a 2-stage turbo solution was chosen where a high-pressure turbo primarily covers low load low speed operation and an enlarged low-pressure turbo primarily covers peak torque curve and rated power. In overlapping intermediate load-points the two turbos were expected to operate in series. The aim of the study was to establish a performance map of the lean operation and determine potential boosting or combustion limits of the system. Additionally,

a target was also to identify the engine out emissions contexture, temperatures and mass-flow for further development and investigations of future lean NO_x EATS options suitable for a HLC SI-engine concept. By extending the applicable area of HLC to higher loads more HLC engine operation during real driving conditions can be achieved and the operational efficiency will be improved. In this paper the hardware developed and used will be presented, followed by experimental setup, results, analysis and discussion.

Experimental Setup

Engine

The engine hardware utilized was a production Volvo Cars two litre in-line four-cylinder direct injected spark ignited turbocharged (TC) engine rated to 187 kW and 350 Nm, that was modified by a new turbocharger, improved ignition system and a lean NO_x EATS. This type of engine is normally fitted with a single stage wastegate turbo from factory. The stock gas exchange system was only capable of sustaining lean operation up to approximately 7 bar BMEP. Therefore, to test higher load points in lean operation an enhanced boosting system was necessary Two main challenges were identified when designing the TC-system for the engine running lean on high loads. First, a lean NO_x EATS increases backpressure of the exhaust system which decreases the available pressure drop for the turbine(s). Second, available exhaust enthalpy relative to required boost will be lower in lean operation. High turbocharger efficiency is required and it should also provide boost in a broad area of the operational window.

A combustion model with estimated parameters was utilized to simulate and develop the prototype TC-system. For future purposes, the model should be calibrated against engine experiments to achieve a more accurate simulation for a future generation of a lean TC-system. According to the preliminary simulations, regulated two-stage turbocharging gave the possibility to run the engine lean in all operating conditions. Therefore, after considering several turbocharger configurations, a regulated serial 2-stage turbo was chosen for the test-engine. This turbocharger has a variable nozzle turbine (VNT) on the high-pressure (HP) stage with a bypass valve together with a wastegate (WG) turbocharger on the low-pressure (LP) stage. This configuration was chosen, dimensioned and verified by simulations to meet the high demands on air mass flow required for the engine operating lean while providing the best comprise between the low-end-torque and rated power. The simulations of this boosting configuration showed significant improvements in break specific fuel consumption (BSFC) of the test-engine operating lean in a real driving cycle and full load region. The LP stage was dimensioned to provide air dilution of lambda 2 at low speed and maximum torque and lambda 1.4 at peak power. The supplied air to the engine was believed to impose the main limitation of fulfilling the full load operation with the desired lean combustion. A gasoline engine operating lean is sensitive to air mass flow since it affects the control of torque output. If the air dilution is increased stability issues are experienced and if air dilution is decreased NO_x emissions increase. For high air mass flow control and a wide operational window, the VNT turbo was necessary for the HP stage to provide well-controlled boost in low end torque and low loads. Specifications of the test-engine can be found in Table 1. A schematic overview of the test-engine and its gas-exchange system is visualized in Figure 1.

TABLE 1 Engine properties

Engine type	VEA Gen I, VEP4 MP
Number of cylinders	Four, in-line
Displaced volume	1969 cc
Bore/Stroke	82 mm/93.2 mm
Compression ratio	10.8:1
Valve train	DOHC, 16 valves
Intake camshaft	Variable 0-48° CA advance
Exhaust camshaft	Variable 0-30° CA retard
Ignition system	DCI, standard J-gap spark plugs
Fuel system/Injection pressure	DI/200 bar
Fuel	Gasoline RON95 E10
Start of injection	308-340 CAbTDCf
Boosting system	2-stage regulated turbocharger
Rated power/Rated torque	187 kW/350 Nm
Stoichiometric air/fuel ratio	14.01:1

FIGURE 1 Schematic overview of engine, including gas-exchange, EATS, sensor and sampling extraction locations

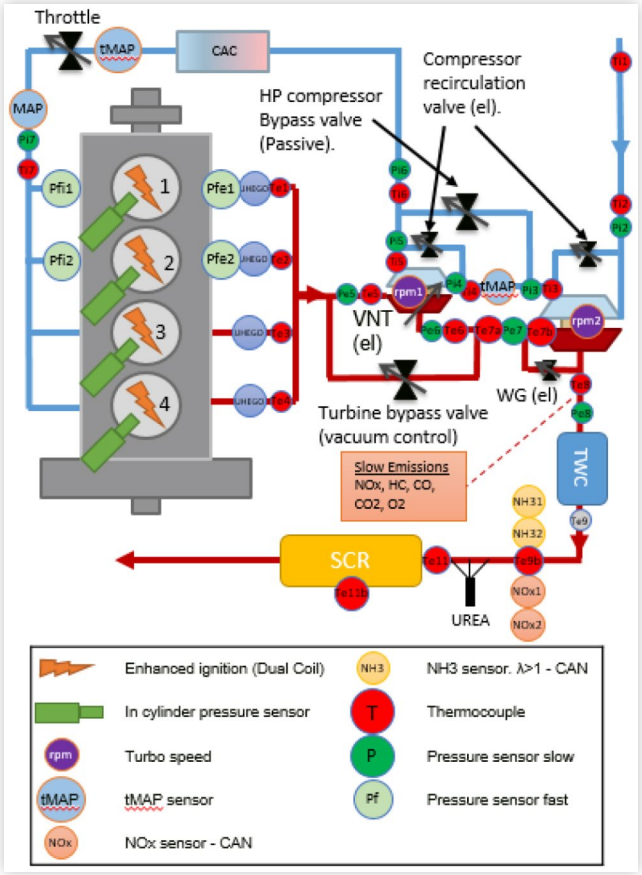

Additionally, the engine was fitted with an enhanced ignition system to increase ignition capabilities of lean charges. The system used was a dual coil ignition (DCI) system utilizing standard spark plugs. Compared to standard single coil systems, the dual coil setup is capable of both higher energy dissipation and extended spark duration due to sequential energy dissipation from the two separate coils. The DCI system was set to 2 ms spark duration and a primary current which corresponds to an estimated secondary ignition energy of 300 mJ. The spark plugs mounted were all indexed such that the ground electrodes where parallel to the crankshaft, facing backwards towards the flywheel end of the engine. Aligning all spark plugs in the same way was done to eliminate one source of cylinder to cylinder deviation, and placing the ground electrodes at 90° in relation to the tumble motion has been concluded to increase energy delivery from spark to charge resulting in a higher quality of onset combustion [7].

Conventionally, the engine was mounted and operated in a test-rig, connected to an electronic dynamometer governing engine speed and measuring output torque. All auxiliary systems belonging to the engine which are needed for conventional operation were powered by the engine alternator and battery to achieve unbiased energy consumption data. The engine was fitted with an open access prototyping ECU to allow access for sampling and changing of engine parameters. The engine was operated throughout all the tests with activated cylinder individual knock control to avoid potential engine damage due to severe knock in higher load-points.

The engine was fitted with an EATS consisting of a close-coupled TWC, a 1 m long exhaust pipe extension and a production diesel SCR-catalyst dummy. The dummy SCR-catalyst system was fitted to obtain realistic back-pressures experienced with a complete lean NO_x EATS, but without the addition of urea solvent. A fan was placed blowing towards the 1 m exhaust pipe extension to achieve realistic heat convection as would be expected in a moving vehicle. Thermocouples were inserted at various locations to be able to record internal temperatures for characterization of lean exhaust temperature conditions for future development of lean NO_x EATS. During all tests the engine ran on 95 RON gasoline with 10% ethanol.

Data Acquisition

Data was sampled using three parallel acquisition systems. Emission signals from respective instruments, fuel and dynamometer readouts were recorded using a National Instruments DAQ with a LabVIEW program. Engine parameters such as temperatures, actuator positions and pressure signals were sampled using acquisition units connected via CAN to an ETAS-box. Crank resolved pressure signals (fast pressure samples) were sampled using an AVL Indimaster 670 with AVL Indicom software.

Exhaust samples were extracted downstream of the second (LP) turbine, before the close-coupled TWC, to acquire engine out raw emissions. The sample stream was exhaled from the exhaust system via a heated hose, set to 180 °C, into a heated conditioning unit at 190 °C with heated filter and pump. Emission concentrations were analysed by separate instruments. Total hydrocarbon concentration was measured using a flame ionization detector and NOx concentration was measured using a chemiluminescence analyser. CO and CO_2 were measured using separate non-dispersive infrared radiation detectors and O_2 concentration was acquired using a magnetic susceptibility analyser.

Temperatures were measured using thermocouples type K. Fuel mass flow was measured by a Coriolis meter. Various intake and exhaust pressures were measured using Trafag CMP 8270 sensors in addition to built-in engine MAP sensors to be able to analyse the TC-system performance. In-cylinder pressures were measured from each cylinder using Kistler 6045A30U20 pressure sensors to be able to monitor combustion conditions online and for post-processing analyses. Combustion phasing used and presented are extracted from the Indicom software. Cylinder pressure sensors was flush mounted in a wide pocket between the inlet valves in the cylinder head for each cylinder. Cylinder pressure signals were sampled at 0.1° CA resolution at the main combustion event of −40° to 60° CAaTDCf, and 1° CA during the rest of the cycle. At certain load-points with a high amount of air dilution the ignition timing exceeded −40° CAaTDCf which compromises an accurate cycle-to-cycle resolved ignition (0%) to 10% mass fractions burned (MFB) analysis. No cycle-to-cycle 0-10% MFB analysis was performed in this study, therefore the violation of the high-resolution sampling window limit was not accounted for.

The relative air/fuel ratio, lambda, was primarily measured using the built-in engine broadband lambda sensor which had received an extended calibration for off-standard operating conditions. Furthermore, lambda was also estimated using the Brettschneider equation, applied to the emissions concentrations, and from the measured mass flow relation between air and fuel. The engine lambda sensor had the lowest amount of uncertainties among the three, highest repeatability and presented intermediate values whereas mass flow estimation showed up to 5% higher and emissions showed up to 5% lower lambda values compared to the sensor values. Therefore, the lambda sensor was chosen to represent the results in this paper.

Measurement Procedure

The emission measurement equipment was calibrated daily using calibration gases. After each cooldown of the engine it was heated up and a reference measurement was conducted at 1500 rpm and 10 bar BMEP on factory engine calibration settings to monitor and verify the conditions of the equipment. To take a measurement, the engine was operated at desired load-point and held until stable conditions was achieved in means of time drifting temperatures and pressures. When stable conditions were achieved, data was recorded simultaneously using the three sampling systems. Engine parameters such as temperatures, intake and exhaust pressure and emissions signals were recorded for 60 seconds and then averaged, while the fast in-cylinder pressure signal acquisition was recording during 300 consecutive engine cycles. Experiments were conducted in various campaigns

and each campaign was executed without any interruptions, i.e. shutdowns. To account for time drifts during test campaigns, pre-determined settings were repeated during each test campaign to monitor variations.

Results

Lean Map

A test campaign was conducted to map the operational window of the test-engine operated in homogeneous lean combustion mode to increase understanding of the effect of air dilution on combustion and turbocharging limitations. Engine factory settings were used for variable cam phasing, injection timing and knock control. Engine settings controlled manually were; lambda, throttle position, ignition timing and TC-system settings of WG, VNT and the active bypass valve. Ignition timing was controlled individually for each cylinder. In higher loads prone to more fluctuations of the gas-exchange system a boost regulator was used to control the VNT position to obtain more stable boost pressure than could be achieved using solely fixed settings.

Using factory calibration of the variable camshafts may have implications on the air dilution tolerance due to increased internal residual gases. Minimizing overlap at low loads, resulting in reduced internal residual gases, have been related to an increase in combustion stability during lean operation [7]. On the contrary, in higher loads where the pressure difference between intake and exhaust converges, valve overlap may result in scavenging affecting actual in-cylinder air dilution. Optimizing the valve timings for the lean map is out of scope for this paper but is essential for future improvement of HLC, especially in low load lean operation.

To determine the lean limit, maximum amount of air dilution, a stability limit of 3% CoV of NMEP was chosen for all load-points. Operating the engine above 3% CoV of NMEP resulted in rapid combustion stability deterioration and misfires indicated by falling below 70% LNV of NMEP. In each of the load-points (indicated as tested points in Figure 2 to Figure 16), a lambda sweep was performed with an increment of 0.05-0.2 lambda units. The lambda which resulted in an engine stability closest to the chosen stability limit of 3% CoV of NMEP was chosen as highest applicable lambda for each load-point and was collected into a lean map. All data visualized in the speed – load spanning lean maps is presented at the stability limit unless stated otherwise. Corresponding plots are produced directly from measured data using a 2D-interpolation over the spanned speed - load area. The highest amount of air dilution, achieved at the lean limit of each load-point, are visualized in Figure 2 as lambda values. The corresponding relative improvement in brake specific fuel consumption is presented in Figure 3.

The BSFC of the lean map was compared to engine fuel consumption obtained during lambda 1 (stoichiometric) operation on engine factory settings. The highest observed fuel consumption reduction of 12% was found at 10 bar BMEP and 1500 rpm in the lean map, where the engine could be operated at a lambda of 1.8. This in comparison with the highest achieved lambda of 2 which was recorded at 8 bar BMEP and 1000 rpm. Hence, fuel consumption reduction did not show 100% correlation to the level of air dilution. Several effects are to be considered when assessing the efficiency improvement obtained through HLC operation, amongst others: reduced pumping losses primarily in part-load, reduced in-cylinder combustion heat losses and improvement in combustion phasing.

The results from the lean operation map showed a clear load and speed dependency of the air dilution tolerance of the engine tested. Air dilution tolerance was observed to decrease

FIGURE 2 Lean map of highest achieved air dilution as relative air-fuel ratio (Lambda) below stability limit of 3% CoV of NMEP, measured by engine broadband lambda sensor. The engine is normally operated at lambda 1 (stoichiometric) conditions in the area covered by the lean map.

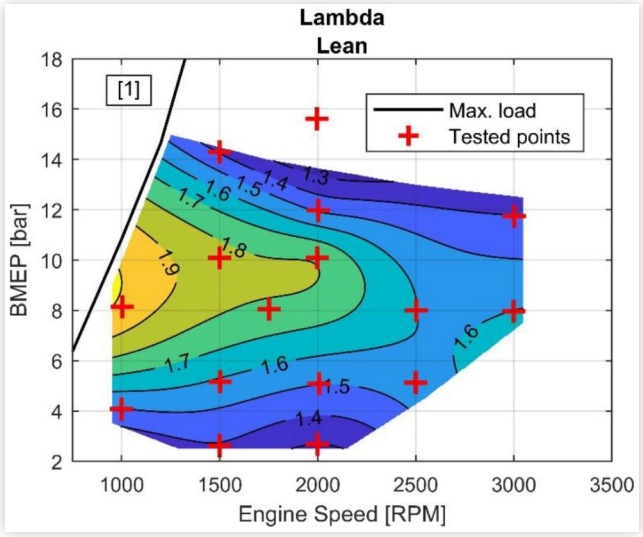

FIGURE 3 Relative brake specific fuel consumption change obtained in lean map at stability limit of 3% CoV of NMEP, compared to stoichiometric operation on engine factory settings ((F_lean - F_stoich)/F_stoich).

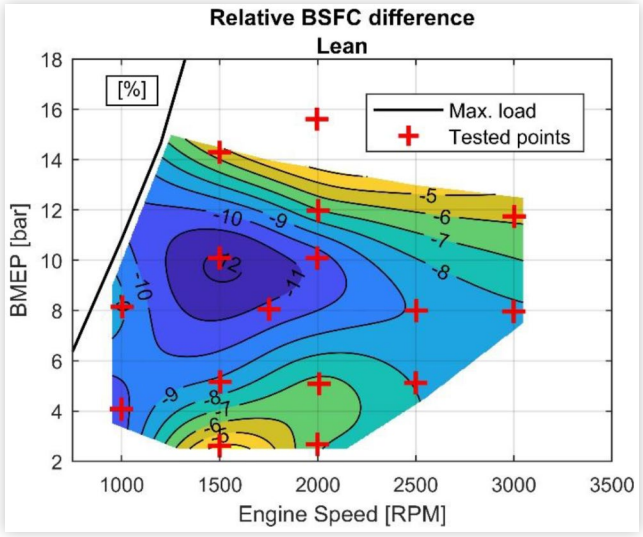

with increasing speed which can be explained by insufficient turbulence intensity increase in relation to engine speed, resulting in an increased combustion duration and instability. The reduced air dilution tolerance in relation to higher engine speed may also be attributed to increasingly unfavourable ignition conditions affecting onset combustion. In relation to load, a peak in air dilution tolerance can be observed in the region of 8-10 bar BMEP spanning from 1000-2500 rpm, visualized in Figure 2.

The engine operational point of 16 bar BMEP and 2000 rpm had been identified as an important milestone for capturing a significant part of real driving conditions for this engine type. The TC-system had therefore been designed and verified by simulations to be able to provide at least lambda 1.8 at 16 bar BMEP to comply with HLC operation in this strategic load-point. However, when the load-point of 16 bar BMEP and 2000 rpm was investigated, the combustion stability rapidly deteriorated when air dilution was added to the stoichiometric mixture and the results from that load-point was omitted. Consequently, the highest load achieved with acceptable combustion stability running lean was 14 bar BMEP and 1500 rpm, which decreased to about 13 bar BMEP at 3000 rpm. The question was raised about why the air dilution tolerance was specifically decreasing above 10 bar BMEP to result in severe combustion stability deterioration above 14 bar BMEP and 1500 rpm in HLC operation. The observed apparent load limit will be addressed and further discussed later in this paper.

Combustion Characteristics

The combustion characteristics were investigated further to increase understanding of the obtained HLC operation results seen from the lean map. Maximum brake torque (MBT) combustion phasing (AI50) of 50% MFB for this engine was pre-determined to 8° CAaTDCf. A later combustion phasing is predominantly caused by deliberately retarding the ignition to avoid knocking combustion. It should be noted that the MBT corresponding to AI50 = 8° CAaTDCf primarily applies to the engine in stoichiometric operation. Since air dilution alters the combustion characteristics such as rate of heat release, there may be a different MBT location of AI50 in lean operation. HLC operation resulted in a large extension of the operational area where the engine could be run with MBT combustion phasing, compared to stoichiometric operation. The effect of combustion phasing on engine efficiency and combustion stability are well known and a large contribution to the improvements in BSFC obtained in HLC operation in the lean map is believed to be caused by combustion phasing improvements. Combustion phasing (AI50) deviation from MBT = 8° CAaTDCf of the lean map is visualized in Figure 4 which shows near or pre MBT phasing of all part load operation up to 10 bar BMEP. This in comparison with combustion phasing (AI50) deviation from MBT at stoichiometric operation which is illustrated in Figure 5.

The improvement in combustion phasing during HLC operation, comparing Figure 4 and Figure 5, mimics trends observed primarily in intermediate load of 10 bar BMEP for relative BSFC improvement that was seen in Figure 3. At lower

FIGURE 4 Engine-average combustion phasing (AI50) deviation from MBT (8° CAaTDCf) of the lean map at stability limit of 3% CoV of NMEP. (AI50 - MBT).

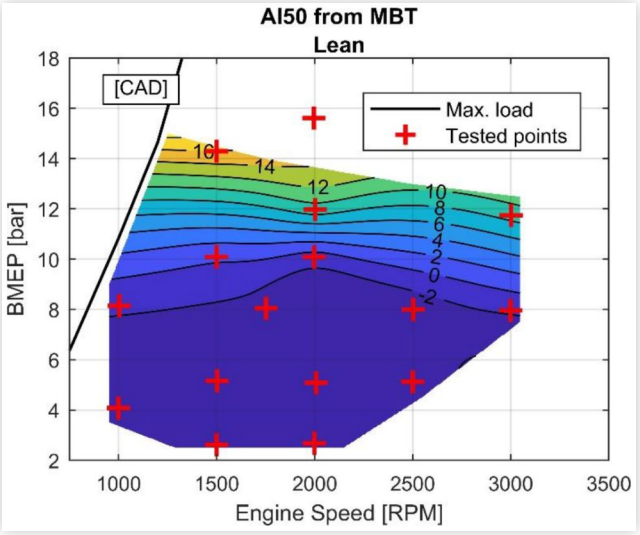

FIGURE 5 Engine-average combustion phasing (AI50) deviation from MBT (8° CAaTDCf) of stoichiometric operation map with engine factory settings. (AI50 - MBT).

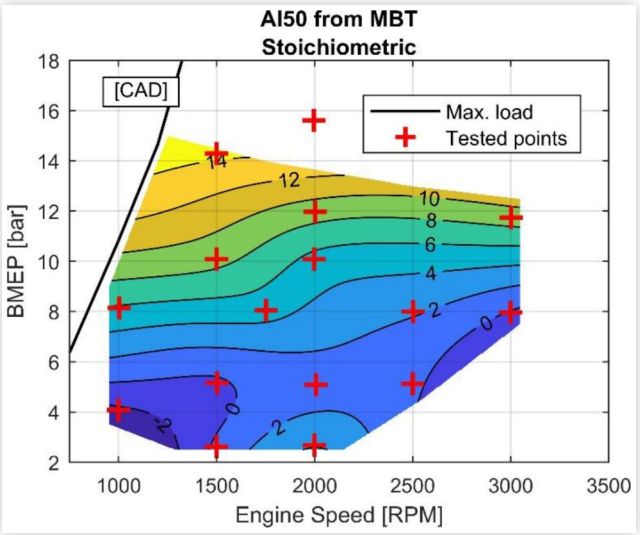

engine load the combustion phasing was already positioned at or close to MBT in stoichiometric operation which limited the effect of air dilution on combustion phasing. Most substantial improvement of AI50 was obtained at 10 bar BMEP and 1500 rpm, the very same load-point at which the highest fuel consumption benefit was achieved. At most of the lower load-points below 10 bar BMEP a combustion phasing pre MBT timing was utilized, closer to 6° CAaTDCf, to reduce cyclic variation of NMEP. Later combustion phasing was found to have a negative effect on cyclic variation of NMEP which will be discussed further later in this paper.

A disadvantage of a lean cylinder charge is its lower laminar flame speed which affects the combustion duration. It was expected that the rapid combustion duration, defined

as AI10 to AI90 (10% MFB to 90% MFB), in crank angle degrees, would increase during lean operation especially in higher engine speeds. Rapid combustion duration at HLC operation in the lean map at the stability limit is visualized in Figure 6 and the corresponding rapid combustion for stoichiometric operation is visualized in Figure 7. The deviating gradient observed in Figure 6 at 12 bar BMEP and 2000 rpm is explained by an irregularity in the data-set where the chosen load-point had slightly higher CoV of NMEP, closer to the stability limit, compared to surrounding load-points which had lower CoV of NMEP accompanied by faster combustion duration.

As expected HLC increases the combustion duration compared to stoichiometric operation and it is believed that

FIGURE 6 Engine-average rapid combustion duration of 10-90% MFB (AI10 to AI90) of the lean map at the stability limit of 3% CoV of NMEP.

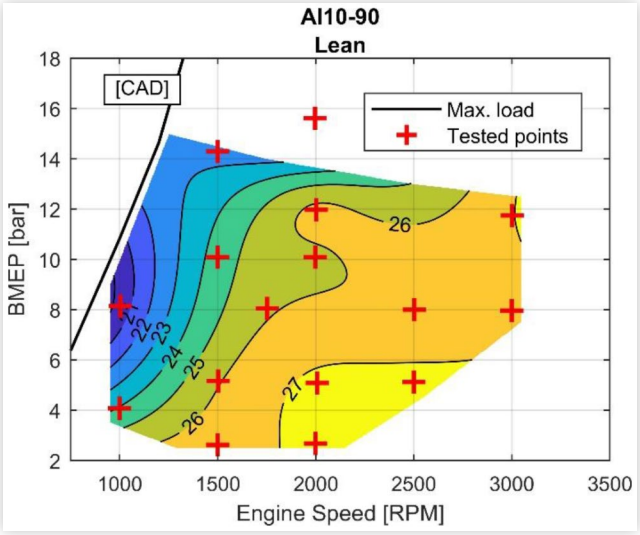

FIGURE 7 Engine-average rapid combustion duration of 10-90% MFB (AI10 to AI90) of stoichiometric operation with engine factory settings.

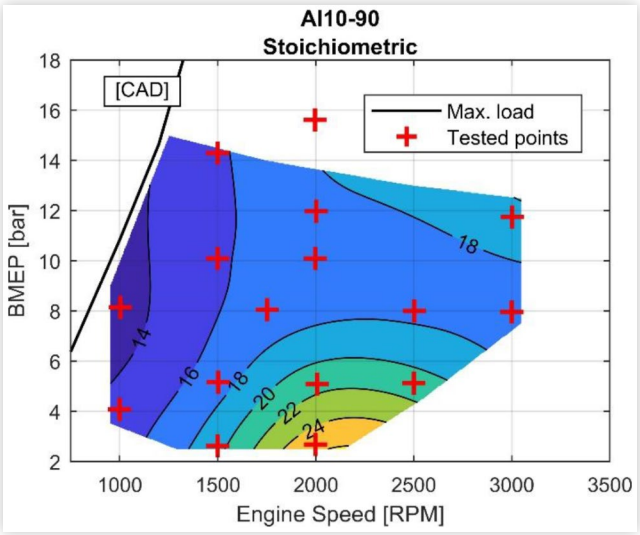

the lower efficiency gains and dilution tolerance during HLC operation at higher speeds in the lower load region below 10 bar BMEP is correlated to increased combustion duration. At the point of peak efficiency of 10 bar BMEP and 1500 rpm, the rapid combustion duration increased from 15° CA in stoichiometric operation to 24° CA in HLC operation at the stability limit. As a reference, it was concluded by Ayala et al. that when a duration of 10-90% MFB of 30° CA, at approximately 2% CoV of NMEP, were exceeded regardless of operating conditions, it had a large negative effect on efficiency and combustion stability, overruling other positive contributions to overall efficiency gains such as heat-loss reductions [22]. The whole lean map was observed to have a combustion duration of 10-90% MFB below 30° CA, but a large portion measured a duration of 26 to 28° CA. The load points with highest air dilution tolerance and highest efficiency gain of the lean map compared to stoichiometric operation had a combustion duration of less than 26° CA of 10-90% MFB. It was not verified whether the limit determined by Ayala et al. could be accurately applied to the engine of this paper, but the obtained results seen in Figure 6 suggests that improvements to decrease rapid combustion are necessary to increase dilution tolerance and efficiency in lean HLC operation. It should be noted that the lean map was defined at 3% CoV in NMEP rather than 2% as suggested by Ayala et al, and that a different approach of computing the heat release may have been applied in this paper.

Boosting Characteristics

Due to the load limit experienced, a full assessment of the turbocharger system could not be performed but results obtained from the TC-system in the lean map are presented in this section, preliminary for observations and discussions. The results obtained will be used for calibration of simulation models for the next iteration of this boosting system. The intake manifold absolute pressure of the HLC operation of the lean map at stability limit of 3% CoV of NMEP is presented in Figure 8 and the corresponding intake manifold pressure of stoichiometric operation is visualized in Figure 9.

The naturally aspirated part-load area has been reduced. The naturally aspirated upper boundary, defined by wide open throttle (WOT), was decreased from approximately 10 bar BMEP in stoichiometric operation down to 6 bar BMEP in HLC operation. Less throttling is naturally more beneficial in terms of efficiency and reduces pumping losses of the part-load operational region. As evident, boosting demand increases substantially, with a peak increase noted at 10 bar BMEP and 2000 rpm of 45%, while exhaust temperatures for the same operating conditions decrease as can be seen in Figure 10.

The relative reduction of exhaust manifold temperatures of the lean map compared to stoichiometric operation corresponds to the trends of air dilution amount seen in Figure 2. As expected, temperatures decrease significantly. At intermediate load of approximately 10 bar BMEP, a temperature reduction of more than 30% was noted, which pinpoints the challenging circumstances of decreased exhaust energy in HLC operation that must be addressed when designing a

FIGURE 8 Absolute intake manifold pressure obtained in the lean map at stability limit of 3% CoV of NMEP.

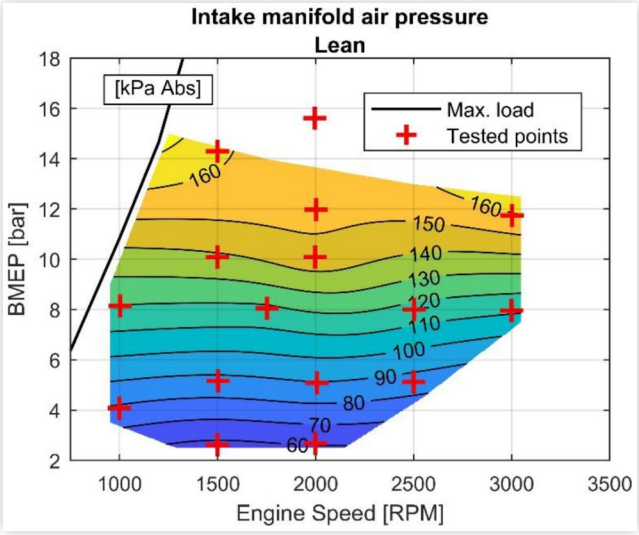

FIGURE 9 Absolute intake manifold pressure obtained in stoichiometric operation with engine factory settings.

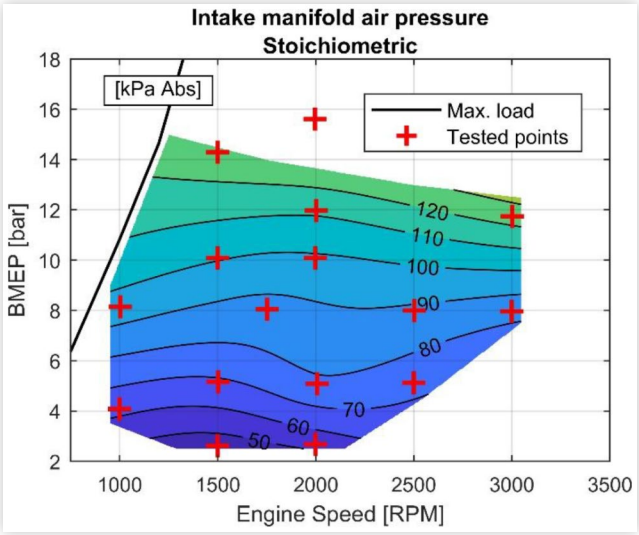

TC-system that should supply boost in higher load regions. Intake manifold pressure versus exhaust manifold pressure for the lean map was computed and visualized in Figure 11 to assess combustion conditions and performance of the TC-system.

A negative value in Figure 11 indicates higher exhaust pressure than intake pressure. From the pressure difference between inlet and outlet it was confirmed that elevated exhaust pressure was evident in a majority of the lean map. In the throttled low load area, the exhaust pressure is naturally higher than intake pressure which results in a negative pressure difference. At 1500 rpm, a strict pressure difference increase was observed between intake and exhaust which shows that the turbo system does not create excessive exhaust manifold pressure when delivering increased amount of intake manifold pressure. Due to reduced enthalpy in the exhaust in

FIGURE 10 Relative exhaust manifold exhaust temperature of lean map at stability limit of 3% CoV of NMEP vs stoichiometric operation on factory settings ((T_lean - T_stoich)/T_stoich). Temperature decrease varies from 10-32%

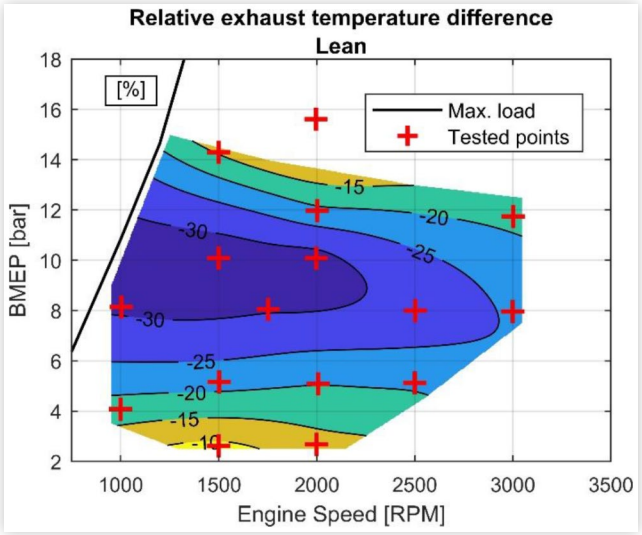

FIGURE 11 Difference between inlet air pressure and exhaust manifold exhaust pressure in lean map at stability limit of 3% CoV of NMEP (P_int - P_exh).

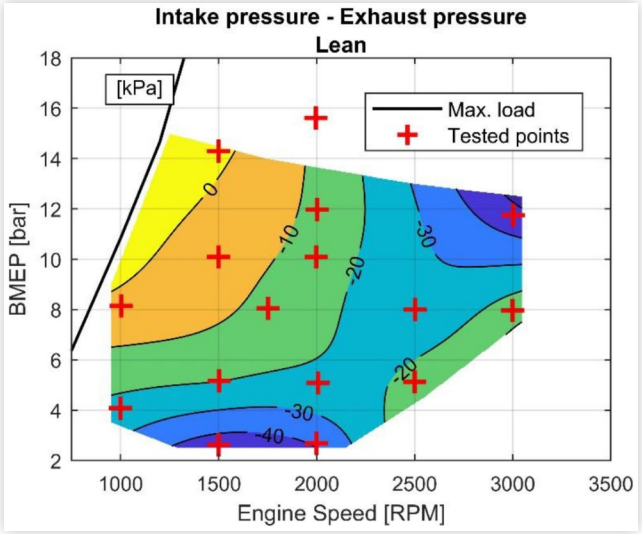

relation to increasing boost demands, it was expected to build higher exhaust pressure with increasing load, resulting in increased internal residuals which may introduce increased variations in HLC operation. Such exhaust manifold pressure increase could not be observed in the obtained lean map at the stability limit except for 12 bar BMEP and 3000 rpm. It is believed that the increase in backpressure at 12 bar BMEP and 3000 rpm was primarily caused by inefficient settings of the turbochargers. It should be considered that the amount of dilution decreases from 10 bar BMEP to 14 bar BMEP. If the amount of air dilution would increase at higher load a less favorable pressure difference might be expected. Further work

is needed to fully assess the matching of the TC-system to the obtained conditions.

To verify the impact of the gas exchange event on efficiency, the pump losses were computed as pump mean effective pressure (PMEP) from the in-cylinder pressure traces. Relative PMEP difference between stoichiometric and HLC operation at stability limit is visualized in Figure 12. Since the amount of air dilution at lower loads was not increased more than to lambda 1.4 the pumping losses were only reduced by 10%. At 8 bar BMEP and 1750 rpm, where a lambda of 1.75 was achieved in HLC operation, a peak pump loss reduction of 40% was observed. Contradictory, at 8 bar BMEP and 1000 rpm an increase in pump losses was observed. This is the load-point where the highest amount of air dilution of lambda 2 was achieved, Figure 2. The increase of pump losses at 8 bar BMEP and 1000 rpm explains why the fuel consumption reduction visualized in Figure 3 does not correspond to the amount of air dilution in the lean map. At 8 bar BMEP and 1000 rpm, the turbo system operates close to the surge line thus low turbo efficiency can be expected which could explain the pump loss increase.

Exhaust Conditions

Temperatures and emission levels at the EATS were sampled during HLC operation and compiled into lean exhaust maps. Measured engine out NO_x emissions from lean engine operation are visualized in Figure 13. Overall, NO_x emissions achieved running at the lean limit below 10 bar BMEP were in the order of 1 g/kWh. At 14 bar BMEP and 1500 rpm only a dilution level of lambda 1.4 could be achieved under the stability limit. At this engine load-point, much higher NO_x emissions, in the order of 8 g/kWh, were observed compared to the rest of the lean map. Naturally, a higher engine load is accompanied by higher intake pressure and intake temperature, cylinder pressure and cylinder temperature. The rate at which NO_x emissions are formed in an engine is known to be related to the combustion temperature. The stability limit was reached at lambda 1.4 at 14 bar BMEP and 1500 rpm, but it was believed to be insufficient for cooling down the combustion to decrease NO_x formation to a lower magnitude.

For verification, in-cylinder maximum combustion temperatures were computed from the pressure traces assuming ideal gas conditions, constant mass and a charge temperature averaged between inlet air temperature and cylinder wall temperature at inlet valve closing. This is an approximation and most likely underestimated at higher loads due to higher influence of intake temperature from compressor and charge air cooler efficiency), and higher wall temperatures, but it illustrates a valid trend. The resulting temperatures computed using Equation 1 are presented in Figure 14.

FIGURE 13 Brake specific NO_x mass flow emissions pre TWC (engine out) of the lean map.

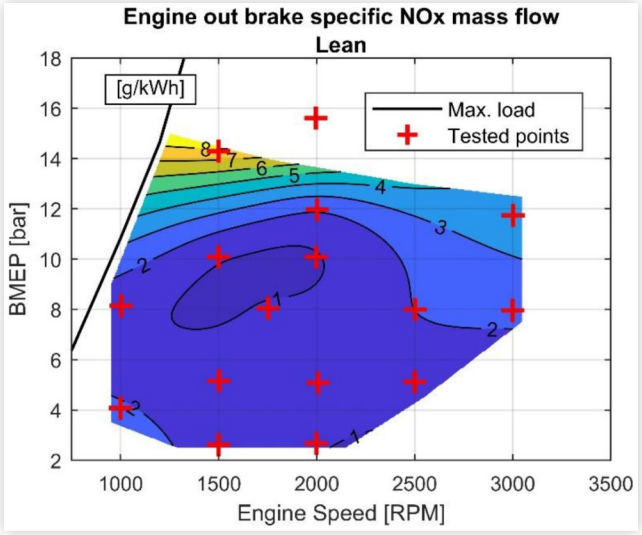

FIGURE 12 Relative pump loss difference defined as PMEP between stoichiometric operation and the lean map at stability limit of 3% CoV of NMEP.

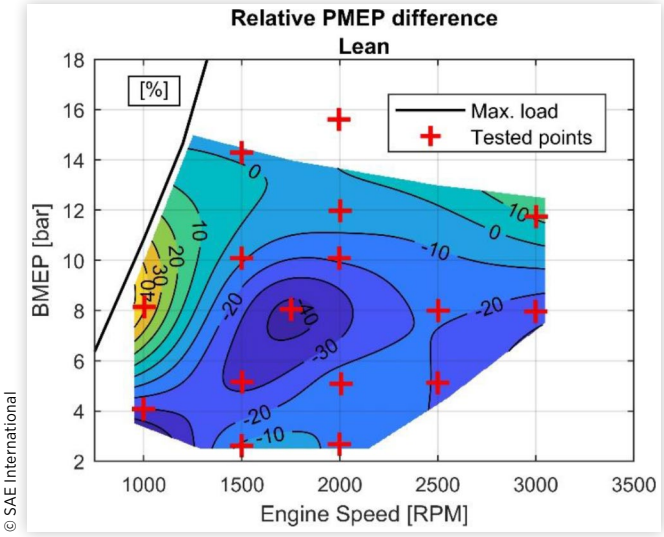

FIGURE 14 Computed engine-average in-cylinder maximum combustion temperature of the lean map at stability limit of 3% CoV of NMEP.

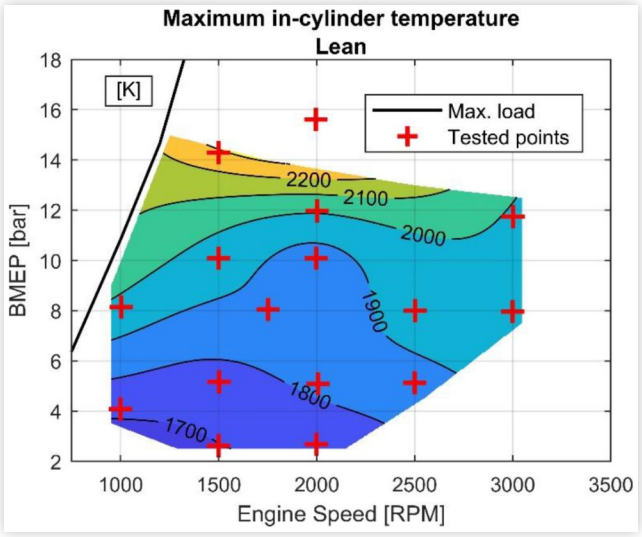

$$T_{cyl}(\theta) = T_{cyl,ivc} \frac{\left(P_{cyl}(\theta) \cdot V_{cyl}(\theta)\right)}{P_{cyl,ivc} V_{cyl,ivc}} \quad (1)$$

The same amount of air dilution was achieved both at 2.62 bar BMEP and 14 bar BMEP at 1500 rpm. The computed maximum cylinder temperatures show the difference between these two load-points despite the same amount of excess air which explains the large difference in engine out NO_x emissions. A low level of engine out NO_x emissions is crucial to keep the cost of the exhaust after-treatment down and NO_x conversion high. More air dilution, and an increased lean limit, at 14 bar BMEP and 1500 rpm is preferable to make it a viable load-point in the lean map in real applications considering the engine out NO_x emissions.

Exhaust temperatures were investigated to judge the effects on catalyst conversion efficiency potentials. Naturally, air dilution alters exhaust conditions compared to stoichiometric operation and as mentioned earlier in this paper, increasing the amount of air dilution decreases exhaust temperatures and increases mass flow. The preliminary engine simulations used prior to the engine tests for development of the TC-system, of which the results are not published, indicated very low post-turbines temperatures at low engine load which introduced uncertainties of whether the operational temperature range of a lean NO_x EATS would correspond to the exhaust temperatures produced during HLC engine operation. With exhaust temperatures below 200 °C the NO_x conversion efficiency of SCR-catalysts tested by J. Theis became very poor [23]. The SCR-catalyst type considered by the authors to use together with the test-engine in future applications had an operational temperature range of 200-650 °C as a reference and was positioned downstream the TWC. Temperatures were sampled using the previously described test-setup to answer if HLC operation exhaust flow would comply with the intended Lean NO_x EATS temperature demands. Resulting temperatures at TWC inlet position are illustrated in Figure 15 and temperatures at the SCR-catalyst inlet position in Figure 16.

FIGURE 15 TWC inlet exhaust temperature (engine out temperature) of the lean map at stability limit of 3% CoV of NMEP.

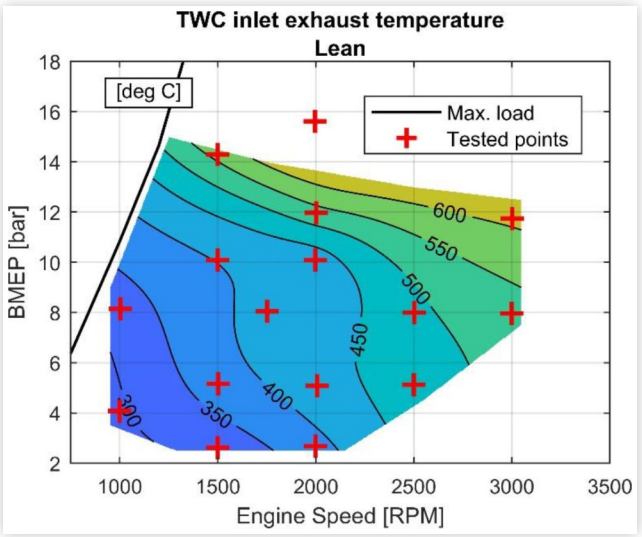

FIGURE 16 SCR dummy inlet exhaust temperature of the lean map at stability limit of 3% CoV of NMEP.

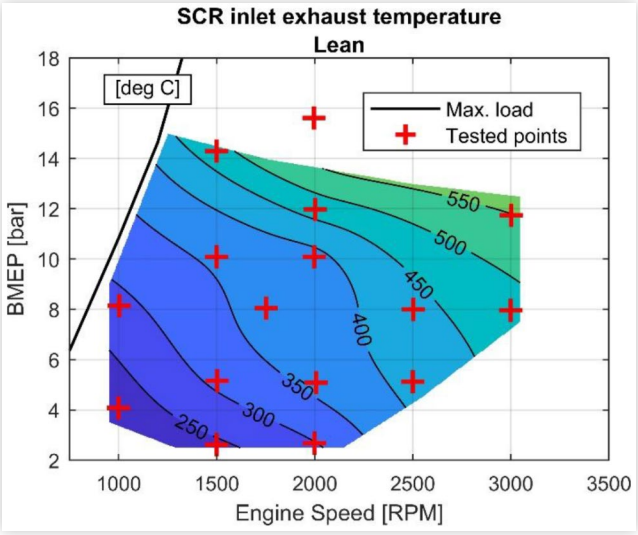

Temperatures observed over the whole mapped operational area were found to comply with both TWC light-off of 250 °C and lean NO_x EATS temperature operational range. At lower loads an increase of SCR-catalyst inlet exhaust temperature was observed when more air dilution was added. It was believed that this contradiction was caused by increased exothermic reactions in the TWC due to increased engine out total hydrocarbon emissions.

Engine out emissions from a lambda sweep at a low load of 2.62 bar BMEP and 1500 rpm can be seen in Figure 17. The plots in Figure 17 are presented as g/kWh instead of concentrations, since the change of air dilution during lambda sweeps biases exhaust emission concentrations. Increased

FIGURE 17 Engine out CO, THC and NOx emissions as brake specific mass flow, plotted vs lambda at 2.62 bar BMEP and 1500 rpm. Three repetitions included at lambda 1.3. All corresponding lines are fitted spline-curves.

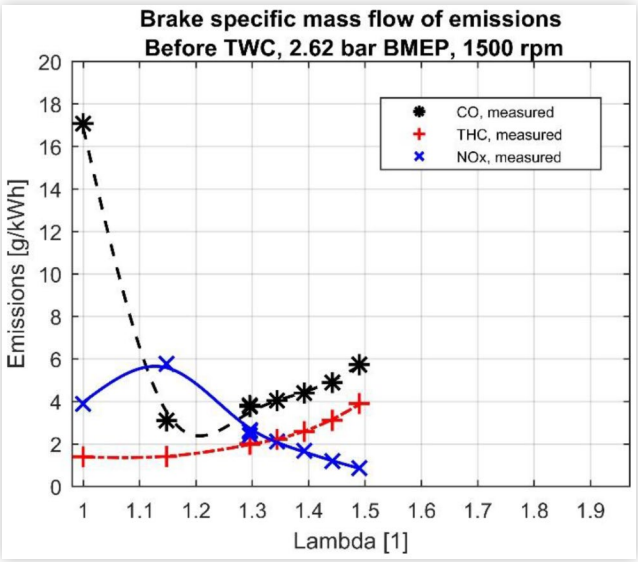

hydrocarbon emissions in lean combustion has previously been observed [15, 18, 24] and explained as a result of increased combustion instability and slower combustion rate [25]. The corresponding exhaust temperatures of the lambda sweep visualized in Figure 17 can be seen in Figure 18.

Figure 18 shows that the SCR-catalyst inlet exhaust temperatures follow the TWC outlet exhaust temperature trend. The TWC inlet exhaust temperature is decreasing with increasing air dilution as can be expected, while TWC outlet exhaust temperature increases. The difference between TWC inlet and outlet exhaust temperature converges from a difference of approximately 100 °C at stoichiometric operation to only 10 °C at maximum lambda achieved at this load-point of 2.62 bar BMEP and 1500 rpm.

Total hydrocarbon emissions increased with added air dilution for all load-points, while the effect on increased exhaust temperature after TWC was more apparent at 4 bar BMEP and 1000 rpm, 2.62 bar BMEP and 2000 rpm, and 5 bar BMEP at 1500 and 2000 rpm. Higher loads showed little or no increase of post TWC temperatures with added air dilution. Engine out emissions of a lambda sweep at 10 bar BMEP and 1500 rpm is visualized as emissions in Figure 19 and corresponding temperatures in Figure 20.

All emissions follow similar trends at 10 bar BMEP and 1500 rpm as the observed trends for 2.62 bar BMEP. The emissions showed lower levels for CO and THC and higher levels for NO_x at the 10 bar BMEP sweep. The increase of TWC outlet exhaust temperature for 2.62 bar BMEP and 1500 rpm when increasing lambda from 1 to 1.15 is unclear if it can be motivated by THC emissions since the amount of THC emissions stays stable in that lambda range. If the implied effect of exothermic reactions is neglected, and it is assumed that TWC outlet and SCR-catalyst inlet exhausts experience the same temperature decrease as TWC inlet of approximately 50 °C, then the resulting SCR-catalyst inlet temperature would fall below the threshold of 200 °C.

FIGURE 18 Exhaust temperatures sampled at 5 various locations between engine exhaust manifold and SCR-catalyst inlet, plotted vs lambda at 2.62 bar BMEP and 1500 rpm. Three repetitions included at lambda 1.3. All corresponding lines are fitted spline-curves.

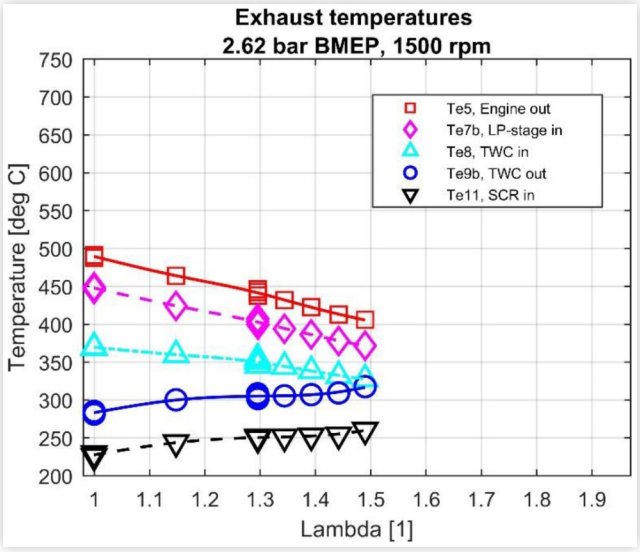

FIGURE 19 Engine out CO, THC and NOx emissions as brake specific mass flow, plotted vs lambda at 10 bar BMEP and 1500 rpm. Three repetitions included at lambda 1.4. All corresponding lines are fitted spline-curves.

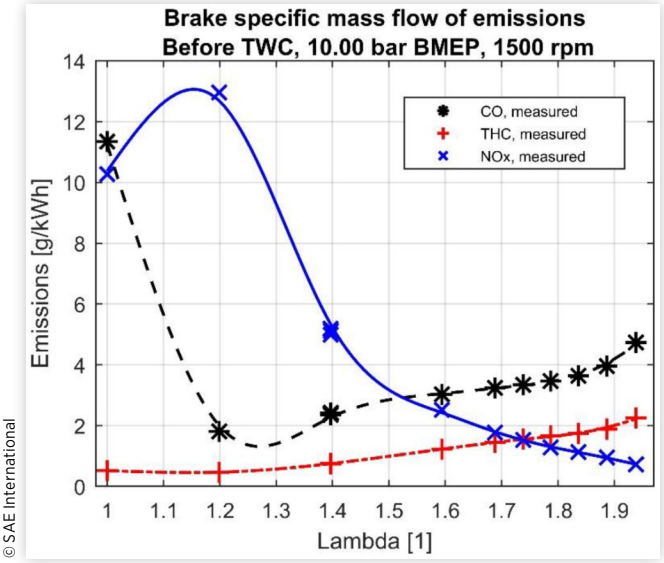

FIGURE 20 Exhaust temperatures sampled at 5 various locations between engine exhaust manifold and SCR-catalyst inlet, plotted vs lambda at 10 bar BMEP and 1500 rpm. Three repetitions included at lambda 1.4. All corresponding lines are fitted spline-curves.

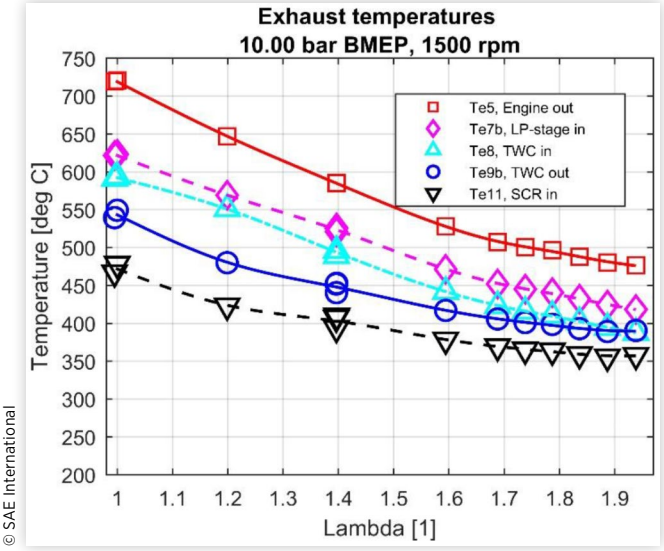

Load Limit

At loads above 12-14 bar BMEP the air dilution tolerance rapidly deteriorated. At 14 bar BMEP and 1500 rpm, the engine could only sustain lambda 1.4 with an acceptable combustion stability, which is believed to be insufficient to

fully gain the benefits of air dilution such as improved combustion phasing and reduced engine out NOx emissions. At 16 bar BMEP and 2000 rpm lean operation was virtually impossible due to a rapid increase of combustion instability when increasing lambda above stoichiometry. To further investigate the lean-load limit, the combustion phasing and knock limitation was investigated.

The effects of different levels of air dilution on the combustion phasing of 50% MFB (AI50) for different engine loads are presented in Figure 21 and Figure 22 for 1500 rpm and 2000 rpm respectively. The lambda- and load-sweeps clearly shows how the combustion phasing can be advanced with increased air dilution, especially for 10 bar BMEP, at both speeds of 1500 and 2000 rpm. On the contrary, above 10 bar BMEP, at 1500 rpm, combustion phasing was instead delayed with increased air dilution. Around 12 bar BMEP, for both speeds, an equilibrium was obtained where air dilution had little effect on combustion phasing and the initial late combustion phasing of 15-18° CAaTDCf at stoichiometric operation could not be improved. Combustion phasing was manually set by adjusting spark advance and was set to achieve MBT of AI50 where applicable and close to the knock limit otherwise. Late combustion causes loss of torque which must be compensated for by increased cylinder pressure to maintain power output. Late combustion may also result in lower peak pressure and combustion temperature unfavorable for HLC. A majority of the previous research studied have only focused on lower loads up to 5 bar BMEP, a load where MBT spark timing is permitted at most cases due to the absence of knock limitations [13, 20]. The relation between deviation of AI50 from the MBT position and its implication on resulting NMEP will not be considered in such cases.

To further investigate the combustion process, the sampled individual in-cylinder pressure signals were analyzed. A program was developed in MATLAB that computed heat release, determined combustion phasing and other parameters for each cycle. Due to the presence of knock,

FIGURE 21 Engine average combustion phasing (AI50) over 300 cycles vs lambda and load at constant speed of 1500 rpm.

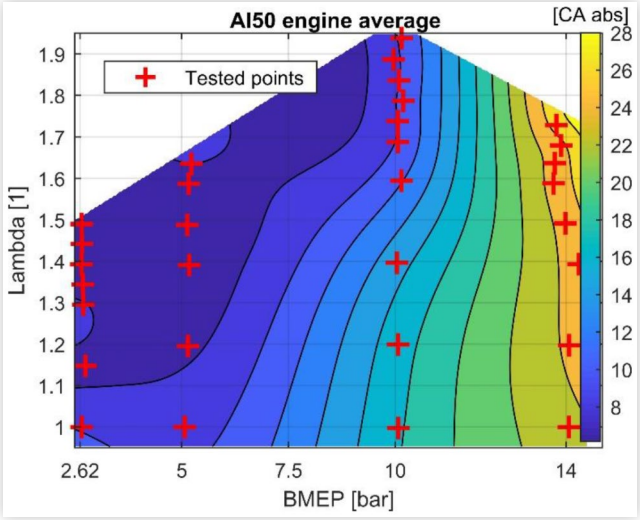

FIGURE 22 Engine-average AI50 of 300 combustion cycles vs lambda and load at constant speed of 2000 rpm.

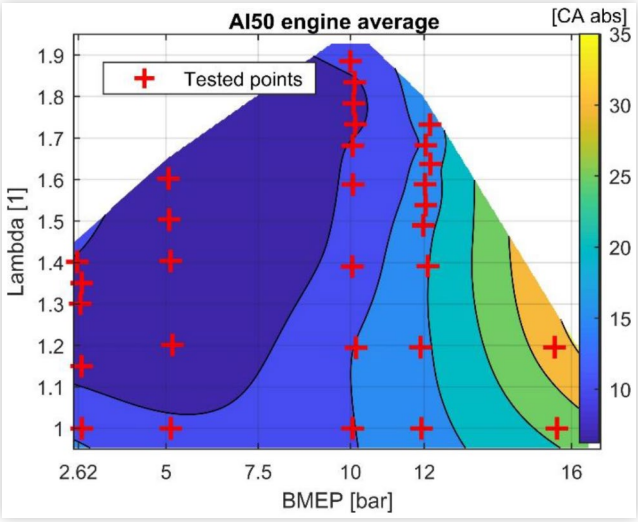

the pressure-signal was split in high- and lowpass by using a Butterworth 4:th order band pass filter with cut off frequency of 5 kHz for an engine speed of 1500 rpm. A regular band pass filter may introduce a phase shift of the signal and for more accurate estimation of parameters such as knock onset one may refer to a method utilizing wavelet transforms to split the signal, a method that has been successfully implemented before [26, 27]. Net heat release, or apparent heat release, was computed according to Equation 2 using the low pass pressure signal. The equation can be found in ICE fundamentals [28]. The net heat release disregards any losses and only consider the pressure obtained by measurement.

$$\frac{dQ}{d\theta} = \frac{\gamma - 1}{\gamma} P \frac{dV}{d\theta} + \frac{1}{\gamma - 1} V \frac{dP}{d\theta} \tag{2}$$

To compensate for variations in the ratio of specific heats γ, due to various operating conditions with different amount of air dilution, adiabatic conditions were assumed and γ was replaced by the polytrophic coefficient κ. κ was determined before and after combustion for each cycle using a least mean square method and linearly interpolated during the combustion event as suggested by Dahl [29]. A knock threshold of 0.3 bar was chosen. Each cycle with an amplitude of the high pass signal exceeding the threshold was determined as a knocking cycle. The location of knock onset (KO) was determined at zero level of the first pressure fluctuation exceeding the threshold. Knock intensity (KI) was calculated as the maximum amplitude of the high pass signal. Knock tendency (KT) has been computed for each sample of 300 engine cycles and was defined as the number of detected knocking cycles divided by the total number of cycles.

The combustion phasing AI50 was compared to NMEP to investigate possible relations. Only one cylinder was investigated and cylinder 2 was chosen since it had shown the largest cyclic variations for most load-points tested. Combustion phasing data presented were computed using the developed program. The result is visualized in Figure 23 for four loads at a constant speed of 1500 rpm and various air dilutions defined

FIGURE 23 IMEP (net) versus combustion phasing (CADaTDCf) for four different loads, one increment of lambda above stability limit of 3% CoV of NMEP.

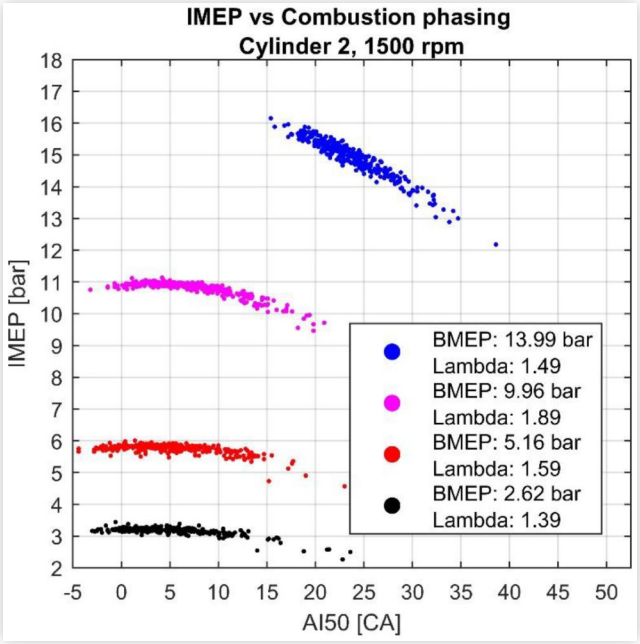

by lambda. Lambda for each load-point is one increment of either 0.05 or 0.1 above the stability limit of 3% CoV of NMEP. The main idea was to visually assess the cyclic distribution of combustion events and its effect on NMEP.

Figure 23 illustrates the wide distribution of AI50 obtained for each of the four load levels included. This variation of AI50 is inherent for lean combustion near the stability limit and similar variations were observed for all load-points tested. AI50 of 2.62, 5 and 10 bar BMEP have an average combustion phasing at or near MBT of 8° CAaTDCf, with even distribution before and after. For the 14 bar BMEP case, the combustion phasing is overall much later since spark timing could not be advanced any further because of knock limitations. The distribution of AI50 is similar for all four load levels, despite the later average phasing of 14 bar BMEP, with a majority of AI50 concentrated to a span of approximately 15° CA and a few later combustion cycles trailing behind. The absolute deviation of NMEP is also similar for the three lower loads of 2.62, 5 and 10 bar BMEP. However, since the combustion phasing AI50 is much later for the 14 bar BMEP load, the variation of AI50 has a much larger impact on variation, or absolute deviation, of NMEP, compared to the lower loads. The relative instability defined by CoV is despite this similar for all four load levels of Figure 23 since CoV is normalized to the mean NMEP.

Combustion mass-fraction-burned parameters were plotted in Figure 24 as a function of lambda for 10 bar BMEP and 14 bar BMEP respectively, with a constant speed of 1500 rpm, to further investigate the effects of air dilution on combustion and to compare the two highest load points measured. The presented results in Figure 24 were obtained and computed for cylinder 1 but the trends were similar for all four cylinders. At 10 bar BMEP increasing en-leanment

FIGURE 24 Ignition, AI10, AI50 and AI90 of a lambda sweep at 10 and 14 bar BMEP and 1500 rpm. Shaded areas show standard deviation for the corresponding graph

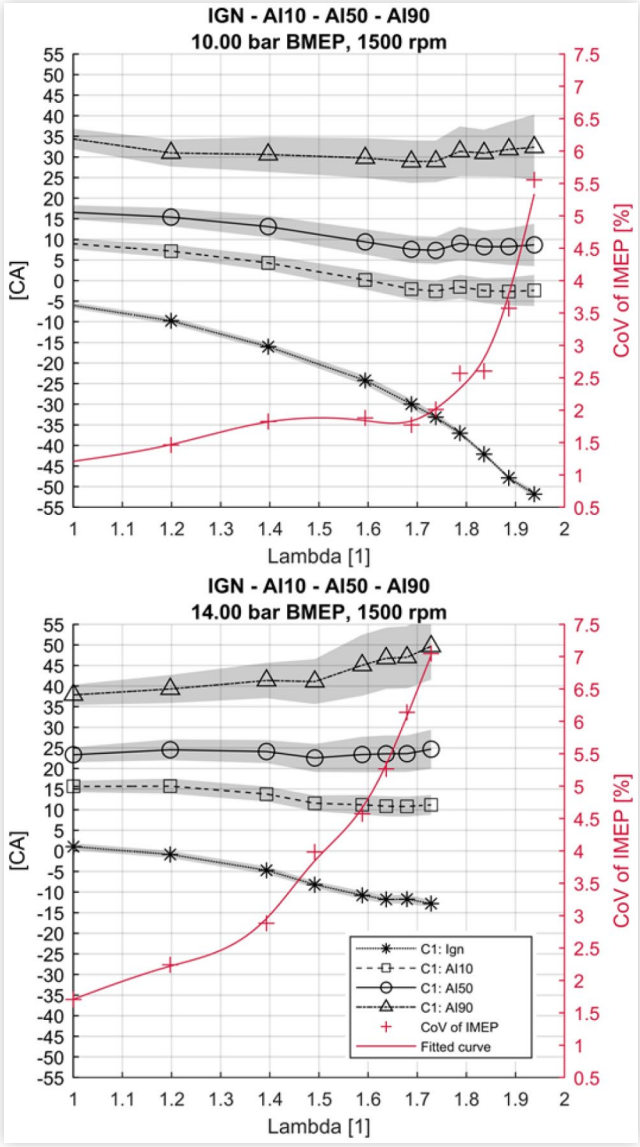

from lambda 1 allowed for earlier ignition and position of AI50 close to MBT timing could be reached at lambda 1.6. However, from lambda 1.7 and higher, further en-leanment did not advance the combustion phasing AI50 but it remained constant. Instead, combustion duration and especially the combustion duration between ignition and 10% MFB (AI10) dramatically increased, which also led to higher, and intolerable, CoV of NMEP. At 14 bar BMEP, increased en-leanment from lambda 1 did allow for a small ignition advance but the location of combustion phasing AI50 could not be advanced due to knock limiting the spark advance. Instead, the prolonged combustion duration resulted in a rapid increase in CoV of NMEP for higher air dilution. If the combustion phasing would be advanced for the 14 bar BMEP load, the combustion stability could be improved substantially. Alternatively, if the cyclic variation of AI50 was reduced the engine could operate leaner with late combustion.

At both 10 and 14 bar BMEP, knock and knock control dictated available spark advance. As discussed earlier, the late combustion and torque loss is compensated with increased boost which potentially further increases the knock tendency. Knock intensity versus knock onset after 50% MFB (AI50) have been plotted for 10 and 14 bar BMEP at 1500 rpm and the results are visualized in Figure 25 and Figure 26.

Despite that AI50 was advanced approximately 7° CA when air-diluting from lambda 1 to lambda 1.8 at 10 bar BMEP and 1500 rpm, knock tendency and knock intensity decreased while knock onset after AI50 was delayed. A more random distribution of the occurrence of knock was observed in HLC operation compared to lambda 1 but despite a general lower knock tendency and intensity with increased lambda, some outliers with high knock intensity could be observed. Similarly, at 14 bar BMEP, knock tendency decreased and knock onset was delayed with increased lambda, but no distinct reduction of knock intensity could be observed. Running 14 bar BMEP, lower overall knock tendency compared to 10 bar BMEP was experienced. The distribution of knock intensity and onset was also found to be less concentrated for the previous case.

The more random and less dense distribution of knock occurring in HLC operation correlates with the corresponding unsteady combustion. The close-to-average combustion cycles of a sample population in HLC have lower combustion temperature due to the air dilution and are hence less prone of knocking compared to stoichiometric operation. However, since the combustion phasing is generally advanced in HLC and the variation of the heat release increases this results in a few random cycles with very early heat release indicated by early 10% and 50% MFB position compared to the average, providing higher pressures and temperatures consequently.

FIGURE 25 Knock intensity as a function of knock onset delay after AI50 in CADaTDCf, over 300 cycles and four cylinders. Knock tendency and AI50 averaged over engine and cycles. 10 bar BMEP and 1500 rpm.

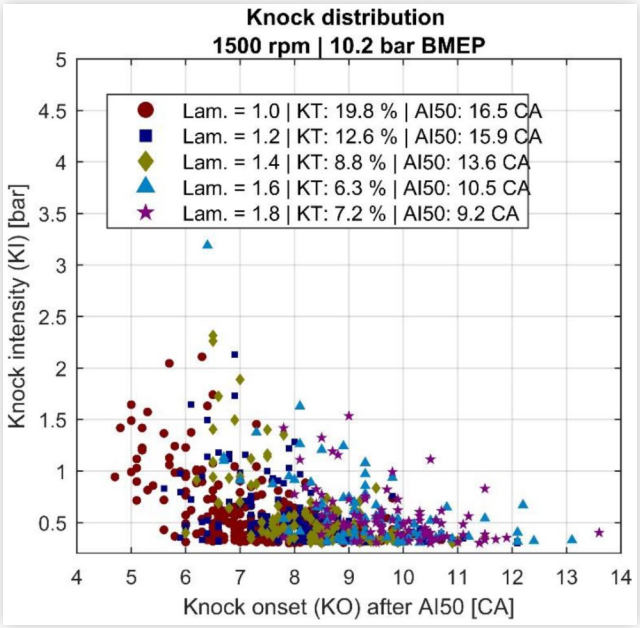

FIGURE 26 Knock intensity as a function of knock onset delay after AI50 CADaTDCf, over 300 cycles and four cylinders. Knock tendency and AI50 averaged over engine and cycles. 14 bar BMEP and 1500 rpm.

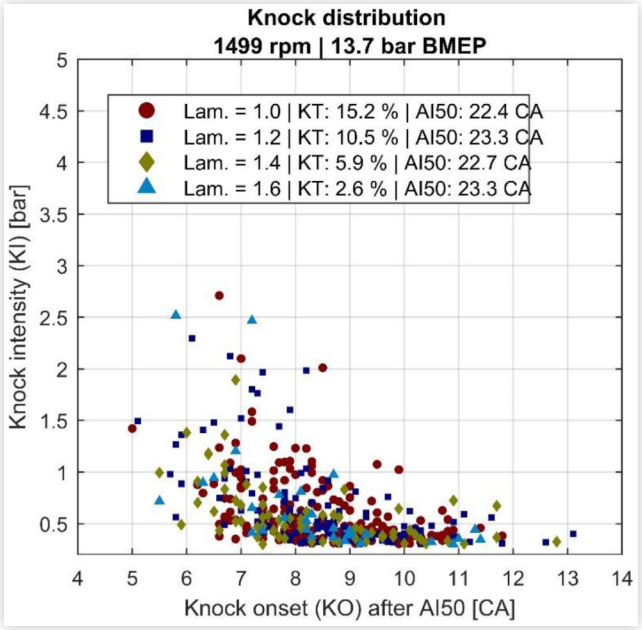

This may explain why there are still a small portion of knocking combustion cycles with high knock intensity occurring at HLC, despite the much lower knock tendency.

The more random nature of knock in HLC operation makes it more difficult to predict and control. Also, a decrease in knock detection accuracy of the standard knock detection system can be expected when operating lean since the knock frequencies change due to changes of the natural frequencies in the combustion chamber. One solution to prevent early combustion cycles, thus reducing high knock intensity, is to decrease the cyclic dispersion of the heat release, in the same manner as when increasing the lean combustion stability limit itself. If similar knock tendency and intensity as in stoichiometric operation can be tolerated in lean operation, a more aggressive ignition advancement could potentially be implemented to reduce cyclic dispersion of NMEP without improving cyclic dispersion of heat release but this could have implications such as increased knock intensity of the early combustion cycles remaining. Enforcing increased spark advance necessitates either recalibration or deactivation of the knock control.

Conclusions

In this paper a homogeneous lean combustion engine concept utilizing enhanced boosting has been implemented and tested as a further step towards introducing HLC in production. A study covering key operational load-points and additional ones was conducted from which a lean map could be created. The lean map showed general trends where a peak of performance increase where found at 1500 rpm and 10 bar BMEP.

Combustion phasing improvements of close to MBT timing could be realized due to air dilution in the lower half of the engine map which contributes to the peak BSFC reduction of 12% obtained in the lean map. Additionally, the region of naturally aspirated operation was decreased by approximately 4 bar BMEP which reduced pumping losses in part load. Lean combustion could be sustained up to 14 bar BMEP which is a significant improvement attributed to the enhanced boosting system, compared to stock engine performance which normally sustain only up to 7 bar BMEP.

Obtained boost pressures did not directly correspond to the amount of air dilution. Significant efficiency increases were obtained in HLC operation, varying over the load-speed region investigated in this paper, which reduced the boost demand compared to what was expected. It could not be concluded whether the turbo system could deliver boost at high loads of 16 bar BMEP and above due to combustion limitations.

Increased air dilution increases the hydrocarbon emissions and exothermal reactions in the TWC. The temperature at the TWC exhaust is therefore increasing at higher lambda for lower loads and speeds. This could be beneficial for the efficiency of the NO_x after-treatment system, positioned downstream of the TWC. Temperatures at various locations of the EATS were found to comply with the temperature ranges of the after-treatment catalysts. Engine out NO_x emissions could be reduced to a magnitude of 1 g/kWh for most of the lean map, except for the higher loads above 10 bar BMEP.

Sufficient spark advance could not be obtained due to knock limitations when loads above 10 bar BMEP were investigated. This resulted in late combustion and due to the inherent increase of cycle to cycle variation of onset combustion and combustion phasing with increased air dilution, the combustion instability defined by variations in NMEP increased rapidly. With current cyclic dispersion of combustion phasing, it may be concluded that HLC is unfavourable in combination with late combustion. The cyclic dispersion of combustion phasing needs to be decreased to reduce impact on CoV of NMEP. Alternatively, the combustion phasing needs to be advanced by means of knock mitigation to allow for earlier spark to decrease the impact of cyclic dispersion of combustion phasing on CoV of NMEP.

Two main areas of interest have been identified, low load HLC and 75% load HLC. Low load operation has the highest time density during driving and this area requires combustion enhancement to increase air dilution tolerance. High load has lower time density but HLC can provide substantial fuel consumption benefits during transients and vehicle acceleration, provided that sufficient air dilution can be applied to improve combustion phasing and lower NO_x emissions as was demonstrated in intermediate load. Increasing the lean load limit would decrease the number of mode switches required between HLC and lambda 1 during driving. However, high load HLC requires opposite conditions of low load in means of knock prevention which imposes a conflict of interest between high and low load HLC.

From the results obtained, it may be concluded that by utilizing enhanced boosting and increased ignition energy, the production engine utilized in this paper was well capable of sustaining extended HLC operation compared to an unmodified engine. The demonstrated fuel consumption improvements and mostly low NO_x emissions in relation to the small modifications implemented to current engine architecture indicates opportunities of HLC as a concept in future production engines.

References

1. eurostat, "Passenger Cars in the EU," 2018, http://ec.europa.eu/eurostat/statistics-explained/index.php/Passenger_cars_in_the_EU#Further_Eurostat_information.
2. European Vehicle Market Statistics, "International Council on Clean Transportation Europe," 2017, [Online], http://eupocketbook.org/.
3. Gomez, A.J. and Reinke, P.E., "Lean burn: A Review of Incentives, Methods, and Tradeoffs," SAE Technical Paper 880291, 1988, doi:10.4271/880291.
4. Meier, R.C., "Development of a Lean Burn/Lean Reactor Engine System through the Application of Engine Dynamometer Mapping Techniques," SAE Technical Paper 770300, 1977, doi:10.4271/770300.
5. Germane, G.J., Wood, C.G., and Hess, C.C., "Lean Combustion in Spark-Ignited Internal Combustion Engines - A Review," SAE Technical Paper 831694, 1983, doi:10.4271/831694.
6. Quader, A.A., "What Limits Lean Operation in Spark Ignition Engines-Flame Initiation or Propagation?" SAE Technical Paper 760760, 1976, doi:10.4271/760760.
7. Doornbos, G., Hemdal, S., and Dahl, D., "Reduction of Fuel Consumption and Engine-out NOx Emissions in a Lean Homogeneous GDI Combustion System, Utilizing Valve Timing and an Advanced Ignition System," SAE Technical Paper 2015-01-0776, 2015, doi:10.4271/2015-01-0776.
8. Yagi, S., Date, T., and Inoue, K., "NOx Emission and Fuel Economy of the Honda CVCC Engine," SAE Technical Paper 741158, 1974, doi:10.4271/741158.
9. Kiyota, Y., Akishino, K., and Ando, H., "Concept of Lean Combustion by Barrel-Stratification," SAE Technical Paper 920678, 1992, doi:10.4271/920678.
10. Hardalupas, Y., Taylor, A.M.K.P., Whitelaw, J.H., Ishii, K. et al., "Influence of Injection Timing on In-Cylinder Fuel Distribution in a Honda VTEC-E Engine," SAE Technical Paper 950507, 1995, doi:10.4271/950507.
11. Johansson, A.N., Hemdal, S., and Dahlander, P., "Experimental Investigation of Soot in a Spray-Guided Single Cylinder GDI Engine Operating in a Stratified Mode," SAE Technical Paper 2013-24-0052, 2013, doi:10.4271/2013-24-0052.
12. Wirth, M., Mayerhofer, U., Piock, W.F., and Fraidl, G.K., "Turbocharging the DI Gasoline Engine," SAE Technical Paper 2000-01-0251, 2000, doi:10.4271/2000-01-0251.
13. Hanabusa, H., Kondo, T., Hashimoto, K., Sono, H. et al., "Study on Homogeneous Lean Charge Spark Ignition Combustion," SAE Technical Paper 2013-01-2562, 2013, doi:10.4271/2013-01-2562.

14. Doornbos, G., "Lean Homogeneous Combustion and NOx Emission Control for SI-Engines," Ph.D., Applied Mechanics, Chalmers University of Technology, Göteborg, 2017.
15. Bunce, M. and Blaxill, H., "Sub-200 g/kWh BSFC on a Light Duty Gasoline Engine," SAE Technical Paper 2016-01-0709, 2016, doi:10.4271/2016-01-0709.
16. Doornbos, G., Hemdal, S., Dahl, D., and Denbratt, I., "Transient Responses of Various Ammonia Formation Catalyst Configurations for Passive SCR in Lean-Burning Gasoline Engines under Various Real Engine Conditions," SAE Technical Paper 2016-01-0935, 2016, doi:10.4271/2016-01-0935.
17. Doornbos, G., Adams, E., Carlsson, P., Dahl, D. et al., "Comparison of Lab Versus Engine Tests In the Development of a Highly Efficient Ammonia Formation Catalyst for a Passive SCR System," SAE Technical Paper 2015-24-2504, 2015, doi:10.4271/2015-24-2504.
18. Pauly, T., Franoschek, S., Hoyer, R., and Eckhoff, S., "Cost and Fuel Economy Driven Aftertreatment Solutions -for Lean GDI," SAE Technical Paper 2010-01-0363, 2010, doi:10.4271/2010-01-0363.
19. Nishiyama, H., Tanaka, Y., Adachi, T., Kawamura, S. et al., "A Study on the Improvement of NOx Reduction Efficiency for a Urea SCR System," SAE Technical Paper 2015-01-2014, 2015, doi:10.4271/2015-01-2014.
20. Ayala, F.A. and Heywood, J.B., "Lean SI Engines: The Role of Combustion Variability in Defining Lean Limits," SAE Technical Paper 2007-24-0030, 2007, doi:10.4271/2007-24-0030.
21. Sjöberg, M., Zeng, W., Singleton, D., Sanders, J.M. et al., "Combined Effects of Multi-Pulse Transient Plasma Ignition and Intake Heating on Lean Limits of Well-Mixed E85 DISI Engine Operation," *SAE Int. J. Engines* 7(4), 2014, doi:10.4271/2014-01-2615.
22. Ayala, F.A., Gerty, M.D., and Heywood, J.B., "Effects of Combustion Phasing, Relative Air-Fuel Ratio, Compression Ratio, and Load on SI Engine Efficiency," SAE Technical Paper 2006-01-0229, 2006, doi:10.4271/2006-01-0229.
23. Theis, J.R., "SCR Catalyst Systems Optimized for Lightoff and Steady-State Performance," SAE Technical Paper 2009-01-0901, 2009, doi:10.4271/2009-01-0901.
24. Sellnau, M., Foster, M., Moore, W., Sinnamon, J. et al., "Second Generation GDCI Multi-Cylinder Engine for High Fuel Efficiency and US Tier 3 Emissions," *SAE Int. J. Engines* 9(2), 2016, doi:10.4271/2016-01-0760.
25. William, P., Attard, and Blaxill, H., "A Lean Burn Gasoline Fueled Pre-Chamber Jet Ignition Combustion System Achieving High Efficiency and Low NOx at Part Load," SAE Technical Paper 2012-01-1146, 2012, doi:10.4271/2012-01-1146.
26. Borg, J.M., Saikalis, G., Oho, S., and Cheok, K.C., "Knock Signal Analysis Using the Discrete Wavelet Transform," SAE Technical Paper 2006-01-0226, 2006, doi:10.4271/2006-01-0226.
27. Burgdorf, K. and Karlström, A., "Using Multi-Rate Filter Banks to Detect Internal Combustion Engine Knock," SAE Technical Paper 971670, 1997, doi:10.4271/971670.
28. Heywood, J.B., *Internal Combustion Engine Fundamentals* (McGraw-Hill inc., 1988).
29. Dahl, D., "Gasoline Engine HCCI Combustion," Ph.D., Applied Mechanics, Chalmers University of Technology, Göteborg, 2012.

Contact Information

Kristoffer Clasén
+4631-772 14 19
clasen@chalmers.se

Acknowledgments

The work performed to create this paper was conducted within a project called UPGRADE - "High efficient Particulate free Gasoline Engines". This project has received funding from the European Union's Horizon 2020 Research and Innovation program under grant agreement 724036

The authors would like to thank Arvin Aghaali for providing background, details and insights about the prototype turbo-system utilized.

Abbreviations

AI10 - 10% mass fraction burned
AI50 - 50% mass fraction burned
AI90 - 90% mass fraction burned
BMEP - Break mean effective pressure
BSFC - Brake specific fuel consumption
CA - Crank angle (degrees)
CAaTDCf - Crank angle (degrees) after top dead center firing
CAbTDCf - Crank angle (degrees) before top dead center firing
CoV - Coefficient of variation
DAQ - Data acquisition
DCI - Dual coil ignition
EATS - Exhaust after-treatment system
ECU - Engine control unit
HLC - Homogeneous lean combustion
HP - High pressure
ICE - Internal combustion engine
NMEP - Net (indicated) mean effective pressure
KI - Knock intensity
KO - Knock onset
KT - Knock tendency
LNT - Lean NOx trap
LNV - Lowest normalized value
LP - Low pressure
MBT - Maximum brake torque
MFB - Mass fraction burned
MP - Medium power
P - Pressure
PMEP - Pump mean effective pressure

RON - Research octane number
SCR - Selective catalytic reduction
SI - Spark ignition
Std - Standard deviation
T - Temperature
TC - Turbocharger
TDC - Top dead center
THC - Total hydrocarbon
TWC - Three-way catalyst
V - Volume
VEA - Volvo engine architecture
VEP - Volvo engine petrol
WG - Wastegate
VNT - Variable nozzle turbine

ISSN 0148-7191

Paper II

2020-01-0959 Published 14 Apr 2020

Investigation of Homogeneous Lean SI Combustion in High Load Operating Conditions

Kristoffer H. Clasen and Lucien Koopmans Chalmers University of Technology

Citation: Clasen, K. and Koopmans, L., "Investigation of Homogeneous Lean SI Combustion in High Load Operating Conditions," SAE Technical Paper 2020-01-0959, 2020, doi:10.4271/2020-01-0959.

Abstract

Homogeneous lean combustion (HLC) can be utilized to substantially improve spark ignited (SI) internal combustion engine efficiency. Higher efficiency is vital to enable clean, efficient and affordable propulsion for the next generation light duty vehicles. More research is needed to ensure robustness, fuel efficiency/NO_x trade-off and utilization of HLC. Utilization can be improved by expanding the HLC operating window to higher engine torque domains which increases impact on real driving. The authors have earlier assessed boosted HLC operation in a downsized two-litre engine, but it was found that HLC operation could not be achieved above 15 bar NMEP due to instability and knocking combustion. The observation led to the conclusion that there exists a lean load limit. Therefore, further experiments have been conducted in a single cylinder research DISI engine to increase understanding of high load lean operation. HLC is known to suppress end-gas autoignition (knock) by decreasing reactivity and temperatures, but during the experiments knock was observed to be prominent and increasing in severity when engine load was increased despite operating ultra-lean close to lambda 2. Knock is normally mitigated by spark retardation which decreases peak cylinder pressure. However, to maintain stable combustion at lambda = 2 the combustion phasing had to be kept close to TC which resulted in high peak cylinder pressures. Therefore, the combustion event had to be balanced in a window where early combustion promoted knock and late resulted in instability and partial burns. A tumble flap was introduced to increase in-cylinder tumble which reduced knock and improved combustion stability. It could be observed that for most load-points assessed; increased tumble could suppress knock and increase the air-dilution limit which proved beneficial in decreasing the NO_x emissions. The highest engine load that could be achieved with highly diluted combustion was 16 bar NMEP.

Introduction

Seeking understanding of advanced combustion concepts is vital to find adequate means of improving engine efficiency to ensure availability of clean, efficient and affordable propulsion for future vehicles. Air diluted spark ignition combustion, or simply lean combustion/lean burn, is a well-known advanced combustion concept of such which has not yet reached market penetration since robustness and adequate fuel efficiency/NO_x trade-off have not been realized. Lean SI combustion can be incorporated by either introducing a stratified or homogeneous charge in the combustion chamber. Stratified lean combustion has previously been assessed and implemented on the market but with limited success due to difficulties in managing NO_x and soot emissions [1, 2]. In recent years more attention has been paid to homogeneous lean combustion. When a homogeneous charge is sufficiently leaned out the corresponding NO_x emissions from lean combustion can be decreased to very low levels. When leaned out, the charge also becomes more difficult to ignite and combust which limits the maximum applicable quantity of air-dilution. Modern exhaust aftertreatment and fast burning combustion systems allow for higher quantities of dilution compared to previous engine generations, which may result in NO_x levels and combustion instability sufficiently low which may render HLC feasible. In the context of ever-increasing demands on lowered CO_2 emissions from engines, it is therefore highly relevant to further investigate technologies such as HLC.

Lean combustion is known as a means of reducing pumping losses, increasing combustion efficiency and decreasing heat losses at partial load operation of SI-engines. Low torque levels of engine operation are the most dominant in the time domain during regular driving which is one reason why low torque performance is important to consider. Achieving high levels of dilution on low loads is however complicated due to undesired conditions in the combustion chamber such as low temperatures, density and turbulence. To obtain the lowest NO_x emissions possible the engine must be operated very lean, close to the combustion stability limit. This usually translates to a lambda of 1.6 or greater and therefore the engine will reach WOT at a lower load compared to stoichiometric operation. Without forced air induction, an engine is usually restricted to operating lean below approximately 7 bar NMEP, compared to 11-12 bar NMEP with stoichiometric combustion. This limits the share of time spent in lean combustion mode during engine

operation which in turn restricts the benefits from air-dilution that can be realized. The torque limit at which a mode switch from lean to stoichiometry must occur to reach higher loads than 7 bar NMEP, measured as absolute torque in Nm, will decrease with decreased engine displacement. Therefore, utilization of HLC will be more restricted in downsized engines compared to larger displacement, naturally aspirated engines, despite that they may deliver the same peak torque.

One may consider targeting HLC on higher engine loads to achieve a higher degree of lean combustion utilization which increases the impact on overall fuel efficiency and feasibility. Higher engine loads are equivalent to increased mean charge temperature and pressure. Increased mass flow through the engine increases turbulence in the combustion chamber. These are factors known to increase turbulent flame speed which is important to achieve efficient and stable air-diluted combustion. Therefore, it is logical to expect improved HLC performance at higher engine loads, possibly without the need for extraordinary technologies such as fuel stratification, intake heating or ultra-advanced ignition systems to aid the combustion. Less advanced technology would result in a lower production cost of a HLC engine. Utilizing HLC in high load also aligns with hybridized powertrain applications where the ICE is more frequently operated at higher load compared to non-hybrid powertrains. Examples of investigations of homogeneous lean combustion at specific engine loads above 12 bar NMEP is difficult to find in the literature, especially dedicated studies on high-load SI homogeneous lean combustion in reciprocating engines using liquid fuels. Lean combustion has historically foremost been considered at low load engine operating conditions of which there have been several studies conducted and published [3, 4, 5, 6, 7]. The benefits of using air-diluted mixtures to mitigate knock has been investigated at an intermediate engine load of 11 bar NMEP by Doornbos et al. [8]. It was shown that under the operating conditions investigated, knocking combustion was decreased by increased air-dilution above lambda = 1.4. Ratnak et al. investigated lean combustion at a high engine speed of 4000 rpm but did not exceed 11 bar NMEP in the experiments [9].

The authors of this paper have previously performed an experimental campaign of a two-litre four-cylinder downsized DISI engine producing 187kW/350Nm. The engine was equipped with a two-stage turbocharger. The turbocharger was designed to provide excess air of up to lambda 2 between 25% and 75% of the engine torque range and lambda 1.4 at peak power. A part of the study was to investigate the potential of boosted high load lean operation [10]. It was concluded that indeed the combination of boosting and lean combustion was advantageous. At an intermediate load of 11 bar NMEP, the engine could run up to lambda 1.9 with 1.5g/kWh NO_x and 12% BSFC improvement as a result. Due to the air dilution, the tendency of knocking combustion was reduced, and the combustion phasing could be substantially improved, confirming the conclusions made by Doornbos et al. that knock could be mitigated by air dilution. However, when the engine load was increased further, up to 15 bar NMEP, the air dilution tolerance (lean limit) was decreased to lambda 1.4. The combustion phasing could not be improved, and the restricted air-dilution resulted in NO_x emissions of approximately 6-8g/kWh.

The previous observation of poor lean combustion while operating at higher loads than 11 bar NMEP raised the hypothesis that there exists a lean load limit. With the study presented in this paper, the authors would like to clarify why air diluted combustion stability deteriorate at elevated loads, causing the apparent lean load limit. This has been done by conducting an experimental test campaign in a single cylinder research engine, equipped with a boosting system capable of sustaining lambda = 2 up to ca 25 bar NMEP and 3000 rpm. Various engine loads and speeds have been tested to characterize their effects on high load lean combustion. Additionally, the influence of increased in-cylinder tumble motion has been investigated to assess the possibility to utilize enhanced turbulence to improve high load lean operation. The conducted experiments provided resulted that could be used to conclude on how to characterize the lean load limit and high load lean combustion performance.

Experimental Methodology

Engine Properties

The experiments were conducted using a single cylinder research engine with a control system allowing full access to engine operating parameters. Details of the engine hardware is listed in Table 1 and a schematic overview of the engine and its auxiliaries is visualized in Figure 1. The engine was fitted with a pent roof cylinder head with a centrally mounded gasoline direct injector. The engine was provided with air through an

TABLE 1 Engine properties

Engine type	Single-cylinder research engine, AVL 5411
Number of cylinders	Four, in-line
Displaced volume	475 cc
Bore / Stroke	82 mm / 90 mm
Compression ratio	10:1
Combustion chamber	Pent roof
Tumble ratio	1.5/ 2.5 at open/ closed flap
Variable tumble	Tumble Flap, 0/50% blocked area
Valve train	DOHC, 4 valves
IVC	-141° ATC @ 1 mm lift
EVO	137° ATC @ 1 mm lift
Overlap	23° CA @ 0 mm lift
Ignition system	DCI, standard J-gap spark plugs
Fuel system / Injection pressure	DI / 200 bar
Fuel	Gasoline RON95 E10
Stoichiometric air/ fuel ratio	14.01:1
Start of injection	-310° ATC
Boosting system	2 bar gauge, external supply

FIGURE 1 Principal layout of the single cylinder research engine, auxiliaries and sampling points used in the experiments reported in this paper

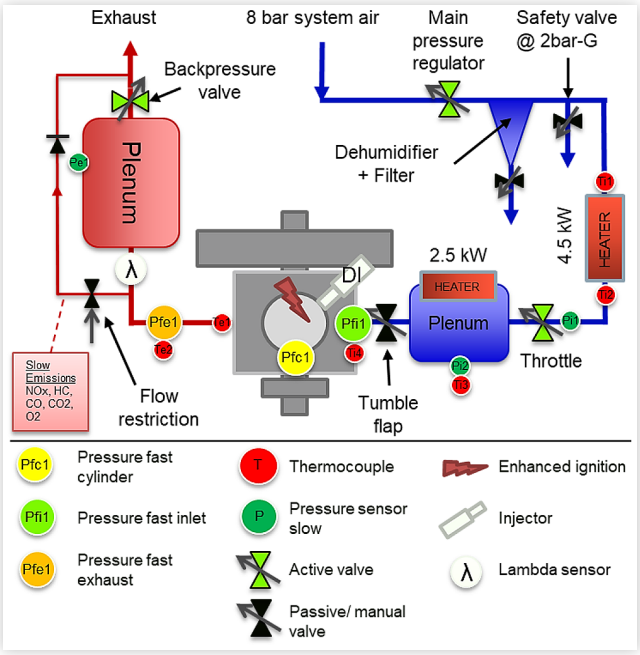

external boosting system. Air at 8 bar gauge pressure was supplied from a compressor and reduced to requested boost-pressure by a pressure regulator. The air temperature after the regulator was consistently at or below 20°C due to expansion. The air was passed through an electric heater which could be used to increase the intake air temperature up to 100°C. The final inlet air pressure of the inlet surge tank (plenum) was controlled by a throttle of butterfly-valve type that actively regulated pressure in the surge tank to a demanded value. Boost pressure regulated by the main pressure regulator was set so that 10-20kPa pressure drop would occur over the throttle valve.

The engine was equipped with a high energy ignition system to improve lean combustion performance. A dual coil ignition (DCI) system was utilized which could extend the spark duration up to 5000µs and deliver up to 800mJ energy to the secondary circuit. The DCI system incorporated a standard J-gap spark plug. Due to power limitations of the coils, the spark duration was reduced with increased engine speed from a maximum duration at 1000rpm of 5000µs to 2000rpm and 2500µs. The cylinder head air inlet port was fitted with a tumble flap. The tumble flap consisted of a disc which horizontally divided the intake port in two portions. With a throttle, the lower half of the intake port could be blocked which promoted increased gas velocity in the upper-portion of the inlet port and targeted the top-side of the intake valves which promoted a stronger tumble motion.

Data Acquisition

All measurement sensor positions are indicated in Figure 1. Cylinder pressure was measured using an AVL GH14DK (M5) piezoelectric pressure-transducer with a natural frequency of 170kHz. The transducer was flush mounted in the cylinder head pent-roof wall between the intake and exhaust valve and sampled at 0.1°CA resolution from -50°CA to +90°CA ATC and at 1° resolution during the rest of the cycle. Auxiliary or "slow" pressures were measured using Trafag 8862 pressure transmitters measuring gauge pressure and a Trafag 8863 transmitter measuring absolute pressure was used as reference to convert all pressures to absolute values. Temperatures were measured using type K thermocouples.

An emission sample was extracted from the exhaust runner, close to the exhaust port and before the exhaust surge tank, to minimize losses of hydrocarbons. The sample was extracted through a bleeding-line with a restriction valve. This device served to prevent pressure build-up in the sample line, potentially affecting measurement accuracy of the emission instruments, when operating with elevated exhaust pressures. From the bleed line, the emission sample was pumped through a heated hose maintained at 190°C, through a heated filter and heated pump and delivered to a standard emission measurement rack which measured total hydrocarbons (THC) wet with a flame ionization detector and nitrogen oxides (NO and NO_x) with a chemiluminescence detector wet. Carbon monoxide (CO) and carbon dioxide (CO_2) was measured dry using non-dispersive infrared radiation sensors and oxygen (O_2) measured dry with a paramagnetic susceptibility analyser. Emissions balance was calculated using the equations defined by Heywood using K = 3.8 [11]. The emission instruments were calibrated daily using calibration gases.

Air/fuel ratio was measured using a Horiba MEXA110 broadband lambda sensor (UHEGO). The sensor was mounted 500mm downstream of the cylinder head to ensure hot gases were measured. The lambda sensor signal was compensated by an empirical formula provided by Horiba to account for distortion due to high air/fuel ratios and exhaust pressures. For verification, lambda was also computed using the Brettschneider equation from the measured emission species. Fuel consumption was measured using a Coriolis mass flow meter.

Crank angle indicated signals were sampled using an AVL IndiModul with AVL Indicom 2.6 software. The indicated signals were sampled at 500 consecutive cycles for each measurement point. Time resolved signals were recorded using AVL Puma at, or higher than, 10Hz frequency. Puma was measured for a duration of 30 seconds simultaneously as the indicated signals, and the results were then averaged. All engine parameters were kept constant during the measurements.

Combustion Stability assessment

To assess combustion quality, the coefficient of variation (CoV) of NMEP can be implemented:

$$NMEP_{CoV} = \frac{NMEP_{std}}{NMEP_{mean}} \cdot 100 [\%] \quad (1)$$

It should be noted that CoV is normalized by the sample mean, which means that the higher the average NMEP is, the more dispersion (std) is tolerated with the same output (CoV). Therefore, it might be inappropriate to use CoV as a measurement for instability at high engine loads and one may consider

using only the standard deviation instead. Since CoV is well imprinted as the primary instability quantity for lean combustion studies, it was considered sufficient for this experimental campaign. An instability criterion of 2% CoV of NMEP was chosen which is in the lower end of common stability criterions used in various studies, normally in the range of 2-5% [12]. This was done to compensate for the high loads investigated thus reducing allowable standard deviation of NMEP.

Knock Characterization

At elevated engine loads, knocking combustion can be expected to a certain extent. The pressure traces obtained from sampling in-cylinder pressure were filtered using a finite impulse response (FIR) high-pass filter based on a Hanning window to assess knocking combustion properties. The FIR-filter introduces no phase shift to the pressure trace due to its symmetry. A high-pass threshold of 4.5kHz was utilized. A knock criterion of 0.5 bar pressure amplitude and maximum pressure rise of 10 bar / °CA of the high pass filtered signal was chosen. Each combustion cycle exceeding both two criterions was considered as a knocking cycle. Knock onset (KO), denoting the crank-angle of where knock was initiated, was determined at the zero-amplitude level before the first rising edge of a high pass pressure pulse exceeding the knock threshold. Knock intensity (KI) denoted the amplitude or strength of the knock. KI was calculated as the maximum positive half amplitude of the high pass pressure signal. Knock tendency (KT), denoting the occurrence frequency, was computed for each sample of 500 combustion cycles and was defined as the number of detected knocking cycles divided by the total number of cycles recorded.

A knock limit was implemented which defined the maximum allowable knock that the engine was considered to withstand during operation. The knock limit was used to compare different samples. A maximum of 10% knock tendency (KT) and a maximum knock intensity amplitude (KI) of 5bar was chosen. Due to increased instability of the combustion during lean operation, a few early combustion cycles tend to trigger strong knock while the average and late cycles display none. Therefore, when average knock intensity is computed the results is generally low and not representative of the few strong knocking cycles which is why the maximum amplitude criterion was implemented. Since the maximum amplitude is not reoccurring it is less harmful to the engine compared to low-amplitude continuous knocking, and therefore a rather high amplitude of 5 bar was considered safe for the engine in this study.

Heat Release

To assess combustion events the net heat release was calculated from the low-pass filtered in-cylinder pressure signals retrieved after removing potential knock-signals. The net heat release was computed using the first law of thermodynamics where heat loss and mass transfer through the system boundaries were omitted. The specific heat ratio was computed using the method develop by Ceviz and Kaymaz [13]. In-cylinder gas temperature was required to compute the specific heat ratio, and the gas temperature was computed by using the ideal gas law with reference conditions at inlet valve closing, Equation 2. The reference temperature at inlet valve closing (IVC) was estimated using the measured inlet port air temperature plus 40K as suggested by Grandin [14].

$$T_{cyl}(\theta) = T_{cyl,ivc} \frac{\left(P_{cyl}(\theta) \cdot V_{cyl}(\theta)\right)}{P_{cyl,ivc} V_{cyl,ivc}} \quad (2)$$

Operating Conditions

All primary operating parameters of the engine was set manually to fixed values during measurements. Injection quantity, inlet and exhaust pressure were held constant. Similarly, the ignition timing was set constant and no knock mitigation routine was utilized. Inlet air temperature was maintained constant at 40°C. An overview of the engine settings utilized together with threshold values are summarized in Table 2.

Three approaches of varying lambda may be considered. Constant load, constant fuel-mass flow and constant air-mass flow. At constant load, both the injection event and intake air mass flow must be adjusted to compensate for changes in efficiency when lambda is changed. Thus, both the injection and air motion will be affected directly. At constant fuel mass flow, only air mass flow must be changed to alter lambda. The injection event will remain during a lambda sweep but may be affected secondarily by the change in air motion and density in the combustion chamber. Constant air mass flow requires a change in fuel mass flow instead. Here, the air motion characteristics may be preserved during a lambda sweep but interaction from the changed injection spray may occur. During this measurement campaign, it was chosen to run at constant fuel mass flow because only the air mass must be adjusted to vary lambda. This reduces the potential for errors, since re-mapping of both fuel- and air-mass flow to achieve a certain torque output is obsolete and no oscillations from feedback controls are imposed. The main drawback of this method is that due to the changes in efficiency from altering lambda, the engine torque output varies significantly at different lambda. An advantage is that ignition timing can be adjusted freely at a certain lambda without remapping fuel and air, if the fuel mass flow is held constant.

An exhaust restriction valve was used to increase the exhaust pressure to simulate realistic pressure ratios between

TABLE 2 Overview of engine settings, limits and investigated operating conditions during the experimental campaign

Inlet air temperature	40°C
Coolant temperature	85°C
Engine speeds	1500-2000-2500 rpm
Engine loads	10 - 17 bar NMEP
Lambda	1-1.9
Tumble	Default/ Increased
Maximum CoV of NMEP	2%
Maximum Spark Timing	50° BTC
Maximum Knock Tendency	10%
Maximum Knock Intensity	5 bar amplitude

boost and exhaust pressure as would have been obtained utilizing a turbocharger. Without adapted exhaust pressure and elevated inlet-pressure, it is likely that scavenging will occur that scavenge residuals, decreases the in-cylinder air/fuel ratio and increases the positive pump work which then increases net efficiency. During the measurements, the exhaust pressure was kept the same as the intake pressure regardless of engine settings to mimic a turbocharger, i.e. a pressure ratio of inlet pressure versus exhaust pressure equal to unity. The intended pressures were measured in the inlet- and exhaust surge tanks respectively. The exhaust pressure was kept at atmospheric pressure if the inlet pressure was set to atmospheric or lower. Maintaining the pressure ratio at unity during boosted operation is a simplification, since the efficiency of a turbocharger at various operating points of the engine will change, which results in varying pressure ratio. A full imitation of turbocharger characteristics was out of the scope of this study and was therefore omitted.

Experimental Procedure

The experiments were executed accordingly: For each combination of engine configurations, a lambda sweep was performed to assess the effect in relation to air dilution. Additionally, for each lambda value, an ignition sweep was performed to account for effects from spark timing. The engine was first set to a certain load-point determined by engine speed and fuel injection quantity. The injection quantity was chosen as to achieve a certain engine load defined by NMEP at stoichiometric operation. Air-mass flow was adjusted accordingly to the injected fuel to achieve a desired lambda as have been previously discussed. The amount of injected fuel was kept constant throughout the lambda sweep, ignition sweep, and other engine configurations assessed at the same load-point. The ignition sweep was conducted first at stoichiometry, covering a window from a late combustion phasing, i.e. 50% MFB at ca 20° ATC, to the earliest permissible combustion phasing without producing harmful knock. Lambda was then incremented, and next ignition sweep was conducted. A minimum of three different ignition settings were targeted at each lambda to capture possible curvature in trends. Some load-points permitted the ignition timing to be adjusted freely and more timings could thus be included in the ignition sweeps, while at other load-points advancement was prevented by knock and retardation was prevented by poor combustion which limited available spark timings.

Results

The Effect of Combustion Phasing on Lean Combustion Quality

To understand the implication of lean combustion at high loads, it is vital to understand how air-diluted combustion is affected by spark timing and the corresponding phasing of heat release. The combustion phasing where highest efficiency is obtained, i.e. maximum brake torque (MBT) combustion phasing (CA50), is usually found around 8° ATC due to heat losses to cylinder walls, as opposed to ideal adiabatic constant volume combustion where MBT is found at 0° [15, 16]. An example of an ignition sweep illustrating the relation between 50% MFB (CA50) and NMEP at stoichiometric combustion can be seen in Figure 2. At each spark-timing setpoint, 500 consecutive combustion cycles were recorded. The grey cloud in the background are individual dots representing 500 cycles times 6 spark settings. As expected, the work output measured as NMEP varies depending on the spark timing and a maximum can be observed at 8° ATC. Standard deviation (thick coloured bars), and maximum/minimum values (thin/grey bars), of both CA50 and NMEP show little change in relation to the positions of average CA50. At stoichiometry, the engine can operate at CA50 = 20° ATC and sometimes even later without considerable loss of stability. As can be seen in the example in Figure 2, the instability measured as CoV of NMEP, stated in the figure legend for each ignition setting, is close to constant regardless of spark timing.

When air-dilution is introduced and increased beyond lambda = 1, the flame speed of the charge decreases due to the increased air/fuel ratio and due to lower in-cylinder temperatures because of the heat sink effect of the added air-mass. Lower flame speed in turn results in slower combustion which must be compensated for by advancing the spark timing in order to maintain the combustion phasing, and to avoid excessive burn during the expansion stroke. Additionally, when air dilution is admitted to the charge the dispersion of heat release increases compared to stoichiometric combustion. This reflects on an increase of dispersion of CA50 and an increase of dispersion of NMEP. An example of the relation between CA50 and NMEP during lean combustion is visualized in

FIGURE 2 NMEP vs CA50 of an ignition sweep at lambda = 1 and 1500rpm. Each marker represents 500 sample points at one ignition setting. Thick bars = standard deviation, thin bars = max/ min value of each sample.

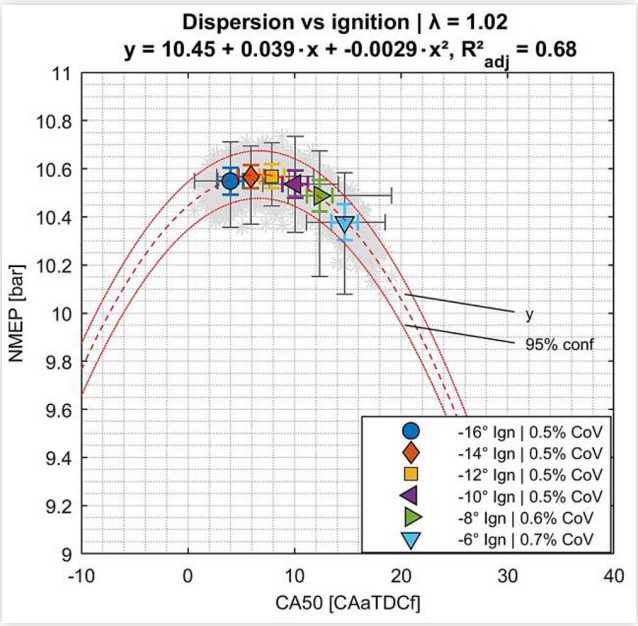

FIGURE 3 NMEP vs CA50 of an ignition sweep at lambda = 1.53 and 1500rpm. Each marker represents 500 sample points at one ignition setting. Thick bars = standard deviation, thin bars = max/ min value of each sample.

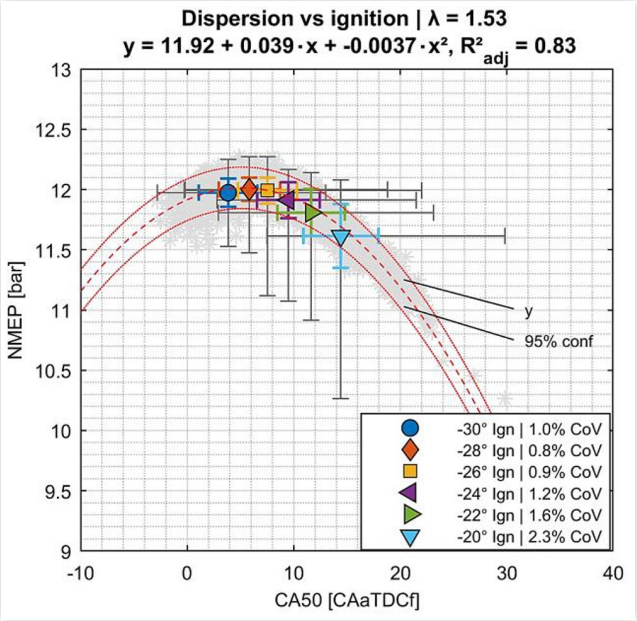

Figure 3. As can be seen, when the average CA50 occurs later in the cycle, the dispersion of NMEP tends to increase, both in terms of standard deviation (thick vertical bars) and in the total range (grey vertical bars). The standard deviation and range of CA50 (horizontal bars) do not change much in relation to different average CA50 positions.

One hypothesis is that the observed increase of dispersion of NMEP when combustion phasing is retarded, is caused by a correlation between dispersion of CA50 and dispersion of NMEP which increases later in the combustion cycle. This correlation can be described with the derivative (slope) of the fitted curve *y* which is included in Figure 3.

If it is assumed that the dispersion of CA50 is solely dependent on air-dilution and not affected directly by the combustion phasing or spark advance, a linear equation describing the nominal increase of standard deviation of CA50 in relation to lambda can be derived which describes the dispersion. Similarly, if it is assumed that there is a nominal dispersion of NMEP which increases proportional to lambda, a linear equation describing standard deviation of NMEP can be derived which describes the dispersion. By using the slope of the curve denoted *y*, which correlates instant CA50 and NMEP as seen in Figures 2 and 3, an approximating equation of the standard deviation of NMEP in relation to CA50 and lambda can be established (Equation 3).

$$NMEP_{std,nom}(\lambda) = -0.08 + 0.11\lambda$$

$$CA50_{std,nom}(\lambda) = -3.2 + 4.13\lambda$$

$$NMEP_{std}(CA50,\lambda) = NMEP_{std,nom}(\lambda) + |b + 2c \cdot CA50| \cdot CA50_{std,nom}(\lambda) \quad (3)$$

In Equation 3 the coefficients *b* and *c* are the first and second order polynomial coefficients from the fitted curve to the CA50 and NMEP relation. *b* and *c* changes slightly with lambda since the curve *y* tends to shift towards TC with increased lambda. The coefficients used to describe nominal NMEP and nominal CA50 versus lambda is derived from experimental data. Equation 3 is only valid for one engine configuration and load-point and should only serve as an example. A comparison of experimental data and results of Equation 3 is visualized in Figure 4. The experimental data shown in Figure 4 represents the same engine configuration and load-point as depicted in Figures 2 and 3 but with more increments of air-dilution included. As can be seen in Figure 4, there is a strong dependence of lambda and position of CA50 to the observed standard deviation of NMEP. With late combustion phasing as a result of late spark timing, the standard deviation of NMEP will be higher at lean combustion compared to MBT timing and stoichiometric combustion. The estimation of Equation 3 fails to predict the absolute values of the standard deviation of NMEP at lambda = 1.38 and 1.53, which can be expected due to the simplicity of the equation. The overall trends of the experimental curves is however predicted by the equation. This illustrates the influence of the slope of the efficiency-curve *y*, the dependence on CA50 position and lambda to the total standard deviation of NMEP. This offers some explanation to why the combustion phasing must be kept close to MBT while implementing lean combustion. Similar observations have been made for other engine configurations and load-points, using adapted coefficients.

Another factor that speaks on the behalf of advanced combustion phasing is the burn rate. If the combustion phasing is advanced, higher peak-pressure is obtained which

FIGURE 4 Correlation of standard deviation of NMEP versus position of CA50. Solid lines and filled markers denote measured points. Dashed lines and open markers denote model estimations

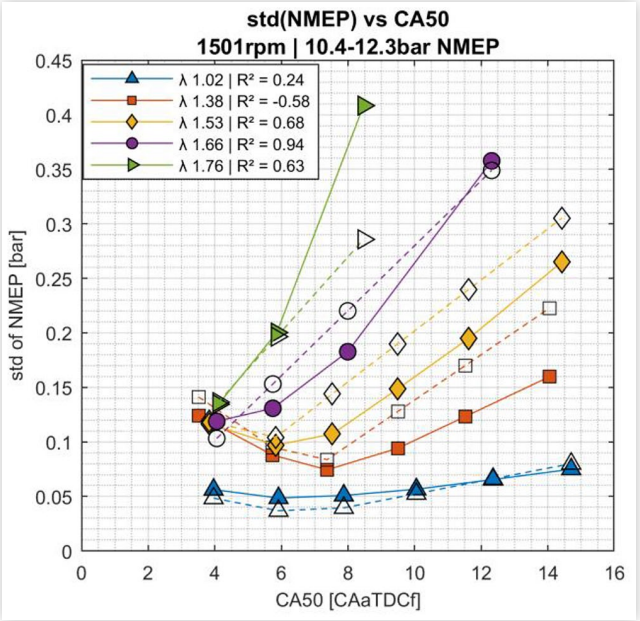

improves burn rate. This was demonstrated by Sjöberg and He [17]. It was shown that the burn duration, CA10-90 was highly dependent on the combustion phasing. Sjöberg and He obtained the highest efficiency at CA50 = 0° ATC, where mixed mode combustion could be induced. Mixed mode combustion occurs when end-gas autoignition is initiated without causing harmful or noisy pressure oscillations. The study was conducted at a low engine load of 3.5 bar NMEP.

The Effect of Knock on High Load Lean Combustion Boundaries

Due to knocking combustion prominent at high-torque low-speed engine operation, the spark advance and corresponding combustion phasing cannot be adjusted freely. At stoichiometric operation, the spark timing can be retarded to decrease peak pressure to avoid end-gas auto-ignition without considerable sacrifice of combustion stability, as was demonstrated in the previous section of this paper. Due to the inherent increase of dispersion of heat release under diluted conditions, the spark timing cannot be retarded without sacrificing stability. This results in a conflict of interests; combustion stability requires advanced spark timing while knocking combustion requires retarded spark timing. Whether or not these meets determines if successful combustion can be established. If the knock threshold occurs at an earlier spark advance compared to the stability threshold, a stability window exists wherein the spark timing can be positioned.

An example of how a stability window is defined will be described in this section. In Figure 5, the CoV of NMEP as a function of lambda is visualized, using the same load-point which have been depicted through Figures 2 to 4. In Figure 5, the black circle-markers denotes measured points, and black dashed lines are linear interpolation in between the measured points. The vertical distribution of the data points at each increment of lambda is caused by different spark timings. If the combustion stability criterion at a maximum of 2% CoV of NMEP is imposed, a line can be drawn through the interpolated data. This line (red, down-facing triangle markers) is denoted the stability boundary and represents the latest permissible spark-timing that do not exceed the stability limit. As can be seen in Figure 5, at lambda = 1 and 1.38, there is no experimental data that exceeds the stability boundary. This is because the engine could not be triggered to produce such instability with reasonable spark timings. Therefore, at lambda = 1 and lambda = 1.38, the stability boundary is determined by available data and not the threshold. When lambda is increased beyond lambda = 1.5, the stability criterion restricts the stability boundary and limits available spark timings.

In the same manner as with the stability boundary, the knock limit can be imposed and used to produce a second line. This line (blue, up-facing triangle markers) denotes the earliest possible spark timing that can be utilized without exceeding the knock threshold. This line is denoted as the knock boundary and is represented in Figure 5. The knock boundary is equivalent to the earliest permissible spark timing which is normally the most beneficial for combustion stability, which is why it can be observed that the knock boundary corresponds well to the lowest numbers of CoV of NMEP, as can be seen in Figure 5.

Additionally, the corresponding knock tendency of the same lambda sweep as in Figure 5 is visualized in Figure 6 and the corresponding maximum knock intensity in Figure 7. The threshold value is indicated with a horizontal red dashed line in both figures. In Figure 7, it can be observed that the knock boundary aligns with its threshold value of 5 bar at lambda = 1.38, 1.52 and 1.66 and is thus restricting the stability

FIGURE 5 CoV of NMEP versus Lambda for a range of different ignition settings at 1500 rpm and intermediate load. The grey area denotes the stability window. The CoV limit of 2% is indicated in the figure by a red dashed line.

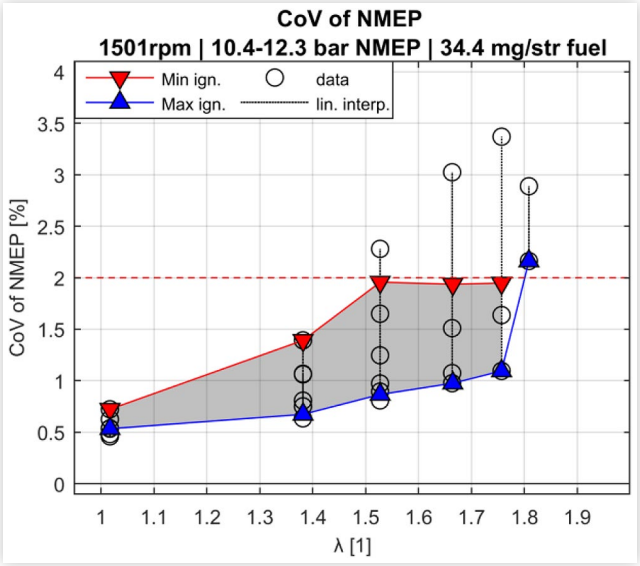

FIGURE 6 Knock tendency versus Lambda for a range of ignition settings at 1500 rpm and intermediate load. The grey area denotes the stability window. The KT limit of 10% is indicated in the figure by a red dashed line.

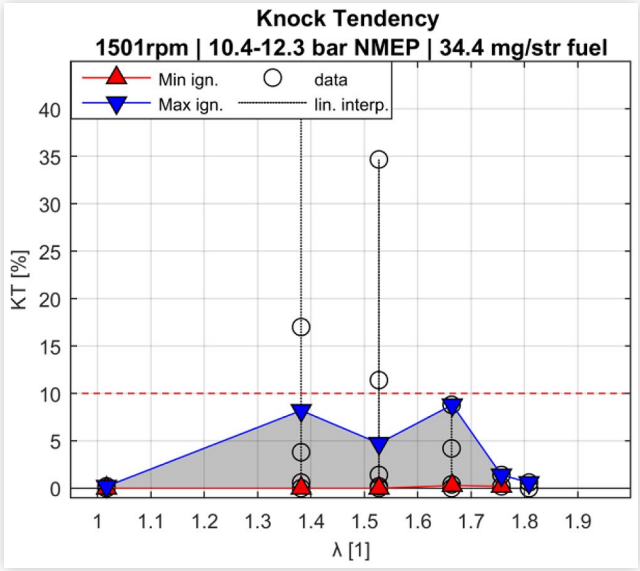

FIGURE 7 Maximum detected knock intensity (KI) versus Lambda for a range of ignition settings at 1500 rpm and intermediate load. The grey area denotes the stability window. The KI maximum limit of 5 bar is indicated in the figure by a red dashed line.

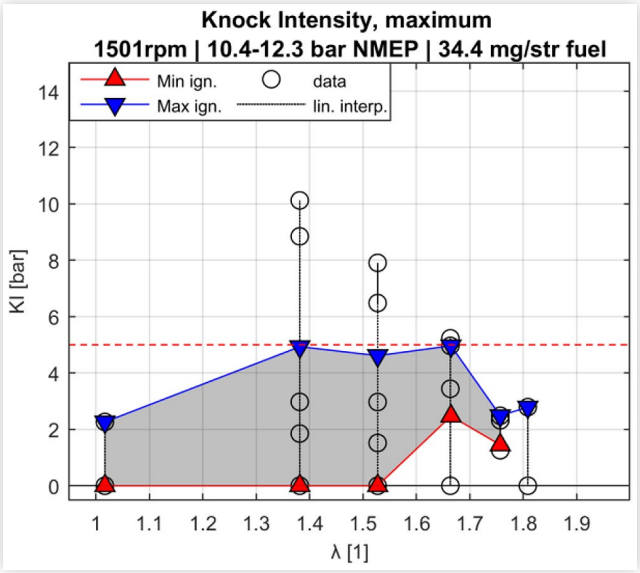

window. In Figure 6, the knock tendency criterion which is indicated by a horizontal red dashed line is not reached by the knock boundary line since the knock intensity criterion is attained first.

Figures 5 to 7 serves to demonstrate how the stability window is enclosed by either limited data, stability or knock criterions. The corresponding stability window as available CA50 positions is visualized in Figure 8. The CA50 window is preferably used to display the stability region rather than any of the criterion entities themselves since CA50 represents available setpoints.

As can be observed in Figure 8, the latest available CA50 position with sustained stable combustion defined by the stability boundary, shifts towards TC with increased lambda. This observation is analogous to what was seen in Figure 4. After lambda 1.76, the spark timing became excessive (more than -50°ATC) which prevented further increase of lambda without exceeding the stability limit. At intermediate lambda of 1.38 and 1.52, the earliest permissible combustion phasing was retarded due to the knock boundary, but it could be recovered closer to lambda 1.66. This is a typical behaviour where the tendency of knocking increase at low degree of air dilution, but at higher rates the cooling effect and decrease in reactivity of the end gas due to dilution mitigates the knock. As a result, the stability window, displayed as the grey shaded area, is quite wide at stoichiometry but narrows down when lambda is increased. In the example in Figure 8, the stability boundary and knock boundary do not converge. Instead, combustion stability is exceeded due to limitations of the combustion system to sustain stable combustion after lambda = 1.76.

The properties displayed in Figures 5 to 8 represents an intermediate load-point close to the stoichiometric naturally aspirated limit. At this load-point, knock is not prominent,

FIGURE 8 CA50 versus Lambda for a range of ignition settings at 1500 rpm and intermediate load. The grey area denotes the stability window.

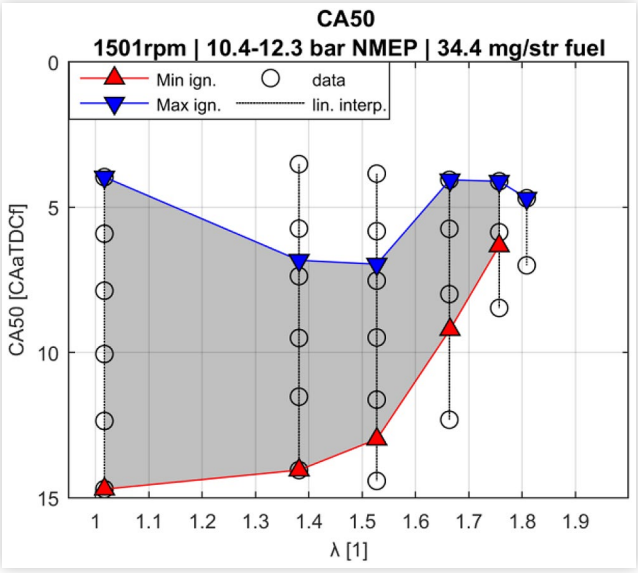

and air-dilution is sufficient to suppress auto-ignition to allow for sufficient spark advance to sustain stable combustion up to lambda 1.76. When the load was further increased, to 13 bar NMEP and higher, it was observed that the knock mitigation capability of air dilution decreased.

The resulting combustion phasing (CA50) of increased engine load is visualized in Figure 9. Starting at stoichiometry, a combustion phasing at 10° ATC could be achieved without exceeding the knock threshold. When lambda was increased, the allowable combustion phasing was substantially retarded

FIGURE 9 CA50 versus Lambda for a range of ignition settings at 1500 rpm and increased load. The grey area denotes the stability window.

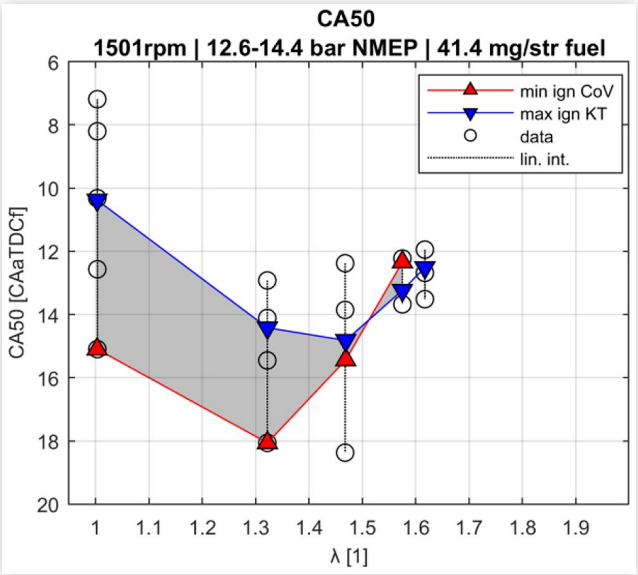

due to the knock limit and the combustion phasing could not be recovered by increased lambda. Therefore, the boundary of stability and knock converged slightly above lambda 1.5, as seen in Figure 9. At the location where the stability and knock boundary converges, the lean load limit is reached.

The demonstrated results showed in this section corresponds to the combustion behaviour experienced during the previous study conducted by the authors [10]. It is possible to operate the engine within the demonstrated boundaries, but when the amount of air-dilution is substantially restricted as in the case shown in Figure 9, the engine will produce high levels of NO_x. If neither knock mitigation nor lower levels of NO_x can be realised, the benefits of operating with HLC above 11-12 bar NMEP can be questioned.

The Effect of Speed and Tumble on the High Load Lean Boundaries

To further investigate high load HLC operation, more engine load-points in terms of speed and torque were examined. The autoignition-delay of the end-gas is time dependent, and increased engine speed increases the autoignition-delay in the crank angle domain. Therefore, increased engine speed was expected to improve knock-suppression and was of interest to investigate further. A potential drawback of increased engine speed in combination with air-dilution is that the combustion duration, defined in the crank-angle domain, may become excessive. The increase of turbulence due to increased engine speed in relation to the decrease of the cycle duration in the time domain may be insufficient to increase burn rate accordingly. This may be disclosed by obtaining extremely early spark timings at a lower air-dilution rate compared to lower engine speeds.

Another factor to consider when assessing knock during lean combustion is the slower burn rate experienced with air dilution. When the burn rate decreases, the end-gas is exposed to the pressure build up and the corresponding temperature gradient under a longer period. If the autoignition-delay of the end-gas is insufficient, knock may occur. When considering the potential drawbacks of air-dilution on burn rate and knock at higher engine load and speed, it is highly relevant to assess the influence of turbulence. Increased turbulence can be induced by improving the tumble motion inside the combustion chamber. The benefits of increased turbulence is known to effectively improve diluted combustion speed, as summarized by Hayashi et al. [18]. Studies covering high load air-diluted combustion with enhanced turbulence is however scarce. Increased air-motion in the combustion chamber may, in addition to improving the combustion speed, also reduce formation of local hot-spots. Hot-spots can cause exothermal centres to form of which auto-ignition originates [19].

In the graphs that will follow, the results are represented as single lines instead of the complete stability window as were shown in the previous section. This is to simplify comparison between different configurations. The graphs represent the best results obtained at each level of air-dilution, i.e. the highest efficiency of each ignition sweep, while not exceeding the knock boundary. If the stability criterion of 2% CoV of NMEP could not be satisfied, the graphs are coloured grey and provided with open markers. Results showing the CoV of NMEP for three different engine speeds are presented in Figure 10. Throughout this section, dashed lines represent standard engine configuration while solid lines represent closed tumble-flap.

In Figure 10, the results obtained with open tumble flap (default engine) can be compared. Figure 10 shows that the highest dilution could be achieved at 2500 rpm with default tumble. At 2500 rpm, equilibrium between combustion stability and knock could be achieved up to lambda = 1.7. The results visualized for 1500 rpm with open tumble-flap corresponds to the same load-point that was presented in Figure 9. At this condition, it can be observed that the stability limit was exceeded after lambda = 1.45.

At 2000 rpm, the stability limit was exceeded already at lambda 1.3. Reaching the lean limit already at lambda = 1.3 was unexpected whereby a repetition was included (pentagon marker) to verify the deviant behaviour. As the results in Figure 10 demonstrates, the repetition corresponds well to the original experiment at 2000 rpm. The decline in air-dilution tolerance at 2000 rpm may be explained by a discrepancy in gas exchange behaviour. No adjustments were made to the camshaft's timings with respect to engine speed which meant that the frequencies of the intake and exhaust runners were left free to dictate the gas-exchange pulses. It was therefore possible that a disadvantageous pressure pulse trapped increased amounts of residuals and restricted admittance of fresh charge to the cylinder at 2000 rpm. This theory was supported by the fact that the boost pressure had to

FIGURE 10 CoV of NMEP of three different engine speed, with closed tumble-flap (indicated as TF in the legend) and open tumble-flap, versus Lambda at constant fuel injection quantity. A repetition is included with pentagon markers. Dashed lines denote standard engine configuration. Solid lines denote closed tumble-flap (TF).

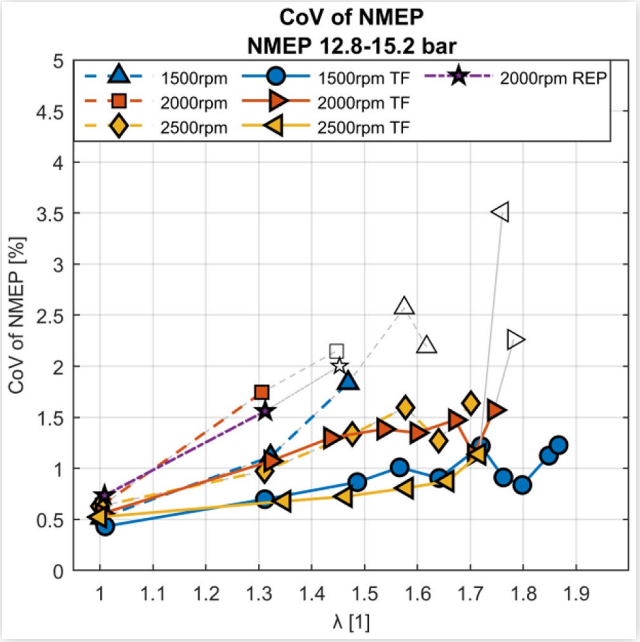

be increased approximately 10 kPa at 2000 rpm, both with open and closed tumble-flap, to achieve the same air/fuel ratios as the two other engine speeds included. It was also observed from the crank-angle resolved cylinder pressure diagrams that at TC of gas-exchange, a pressure pulse peak occurred in the cylinder (higher pressure than the intake) at 2000 rpm, which was likely to force some residuals into the intake port at IVO before sufficient suction was created by the piston to admit fresh charge to the cylinder. In addition to potentially causing increased quantities of trapped residuals, the deviation in the gas-exchange event may also affect the charge-motion in the cylinder to a less favourable composition. More trapped residuals add to the total in-cylinder charge dilution which causes higher combustion instability. Increased quantity of hot residuals are also known to promote end-gas auto-ignition [20].

In Figure 10, it can be clearly seen that the instability (CoV of NMEP) decreased for all engine speeds when the tumble flap was closed, compared to default tumble. This enabled that higher rates of air-dilution could be achieved. With closed tumble flap, i.e. higher tumble ratio, the engine could be operated with air-dilution above lambda = 1.7 at all three engine speeds. However, at 2500 rpm, closing the tumble-flap did not offer any improvement to the maximum air-dilution, despite that the combustion stability was improved by 0.5% units. At 2000 rpm, closed tumble-flap improved the maximum air-dilution from lambda = 1.3 to lambda = 1.75. At 1500 rpm, closed tumble flap increased maximum air-dilution from lambda = 1.45 to lambda = 1.85. To conclude, increased tumble generally improved both combustion stability and maximum air-dilution. With default tumble ratio, higher air-dilution was possible at higher engine speed. On the contrary, increased tumble ratio favoured maximum air-dilution at lower engine speed.

The corresponding combustion phasing (CA50) of the same load-points and engine configurations as demonstrated in Figure 10 is visualized in Figure 11. The resulting combustion phasing offers some explanation to the deviation between the different engine speeds and configurations in terms of stability.

The results visualized in Figure 11 confirm that increased engine speed decreases the tendency of knocking in general, which can be concluded from more advanced combustion phasing at the highest engine speed. The combustion phasing of 2500 rpm and open tumble-flap experiences approximately a 4° CA advancement compared to the two lower engine speeds ranging from stoichiometry to the highest air-dilution. Additionally, all engine speeds experienced advancement of the combustion phasing with closed tumble flap, compared to default tumble. Similar to Figure 10, Figure 11 shows deviating results for the 2000 rpm case. At 2000 rpm and open tumble-flap the most retracted combustion phasing could be observed. The combustion phasing of 2000 rpm both with open and closed tumble-flap demonstrates retardation of the combustion phasing compared to the two other engine speeds, which contradicts the expectation that increased engine speed strictly reduces knock. This deviation may once again be explained by higher quantities of residuals at 2000 rpm which was likely to increase the tendency of knock.

FIGURE 11 CA50 of three different engine speeds, with closed tumble-flap (indicated as TF in the legend) and open tumble-flap, versus Lambda at constant fuel injection quantity. A repetition is included with pentagon markers. Dashed lines denote standard engine configuration. Solid lines denote closed tumble-flap (TF).

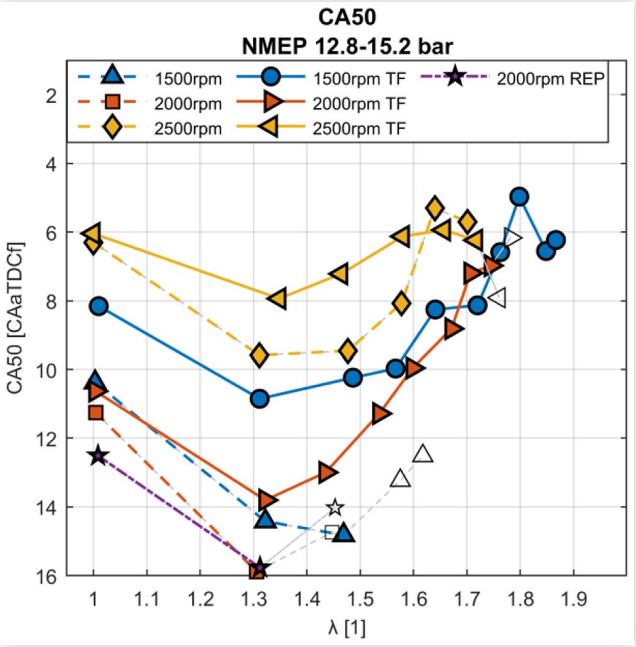

As could be observed for all six cases in Figure 11, the graphs showed a curvature. All curves experienced a retardation of CA50 when lambda was increased from unity due to increased tendency of knock. The largest retardation was found approximately at lambda = 1.3 for most of the engine speeds and tumble-levels. At higher lambdas, for the load-points and tumble-levels of which stability were sustained, the combustion phasing was successively recovered when increasing lambda towards the ultimate lean limit. At 1500 and 2000 rpm with closed tumble flap, it could be observed that the combustion phasing was improved at the highest levels of lambda compared to stoichiometry.

One reason why the tendency of knocking initially increased when lambda was increased above unity, demonstrated as the retardation of CA50 in Figure 11, is that the cylinder pressure increased. More air was admitted to obtain a higher lambda. Since the injection quantity was held constant the efficiency improvement of air-dilution increased the energy release from combustion, resulting in higher peak cylinder pressures. In other words, the engine load increased when lambda was increased and was therefore by default more prone of producing knocking combustion. However, it is not clear to the authors what is causing the prominent non-linear trends visible in Figure 11, where knock tendency initially increases with increased lambda and later decreases when lambda exceeds lambda = 1.3-1.4. Doornbos et al. proposed the explanation that NO_x in the retained residuals affects the tendency of knocking [8]. The NO_x concentration is often seen to reach maximum values with respect to lambda in the lean region of lambda = 1.1-1.3. The concentrations of NO have

been observed to increase tendency of knocking in experimental studies which points to that this explanation has relevance [21]. Other explanations in the literature have not been found and the knock behaviour in relation to air-dilution may therefore be subject to further investigations to fully understand the mechanisms.

As was observed from the results in Figure 11, the addition of increased tumble saw no benefits in increasing maximum lambda at the highest engine speed of 2500 rpm. It is the authors experience that when reaching high levels of air-dilution, using a standard spark plug, the spark timing generally becomes excessive. When the spark occurs at an early timing, both the temperature of the charge and the intensity of the turbulence is lower compared to a timing closer to TC. Therefore, onset combustion (CA0-10) may become excessive. The corresponding onset combustion is visualized in Figure 12. The results obtained from closing the tumble-flap demonstrated in Figure 12 shows an overall advantage compared to the default tumble case in terms of onset combustion duration. Despite that the onset combustion of 2500 rpm and closed tumble-flap was substantially reduced compared to default tumble at very lean conditions, the air-dilution tolerance was hardly increased at all.

The implemented spark timings at this point were in the range of 35-40° BTC. At the load-point investigated and demonstrated in Figures 5 to 8 with default tumble, the spark timing reached 50° BTC with sustained stability, which indicates that the spark timing used at 2500 rpm and closed tumble flap should produce stable combustion. It is possible that the location of the sparkplug experiences high mean flow velocity with insufficient small-scale turbulence. This may lead to flame quenching or prevention of turbulent flame propagation when the spark timing exceeds approximately 35° BTC. Therefore, increased spark advance may not be utilized to its full extension to stabilize combustion with increased tumble, as compared to lower tumble when stable combustion can be sustained with earlier spark timings around 50° BTC.

Corresponding main combustion duration (CA10-90) is visualized in Figure 13, and the resulting NMEP of the various engine speeds and tumble levels is presented in Figure 14. Since constant fuel injection was implemented, any changes in efficiency with respect to tumble level and lambda can be directly observed from changes of NMEP. As is demonstrated in Figure 13, the increased tumble offers substantial increase of combustion rate compared to the default tumble level. The difference was most pronounced in the very-lean region at lambda = 1.7. The increased combustion rate was expected to enable a higher degree of useful energy-release to the combustion chamber. Excessive burning duration results in heat release during expansion which cannot be utilized, highlighted by Sjöberg and He [17]. Once more, it can be observed in Figure 13 that the results from 2000 rpm deviated. At 2000 rpm, the combustion duration was evidently longer compared to the other two engine speeds. This was believed to be a result from the later combustion phasing of 2000 rpm due to knock. When the combustion is phased later, the peak pressure decreases which slows down the combustion. It is also possible that higher quantities of residuals might increase the combustion duration, since residuals contributes to the total dilution factor which in turn decreases the flame speed. Similarly, if the charge motion is changed to a less

FIGURE 12 Onset combustion duration (CA00-CA10) of three different engine speeds and versus Lambda at constant fuel injection quantity. A repetition is included with pentagon markers. Dashed lines denote standard engine configuration. Solid lines denote closed tumble-flap (TF).

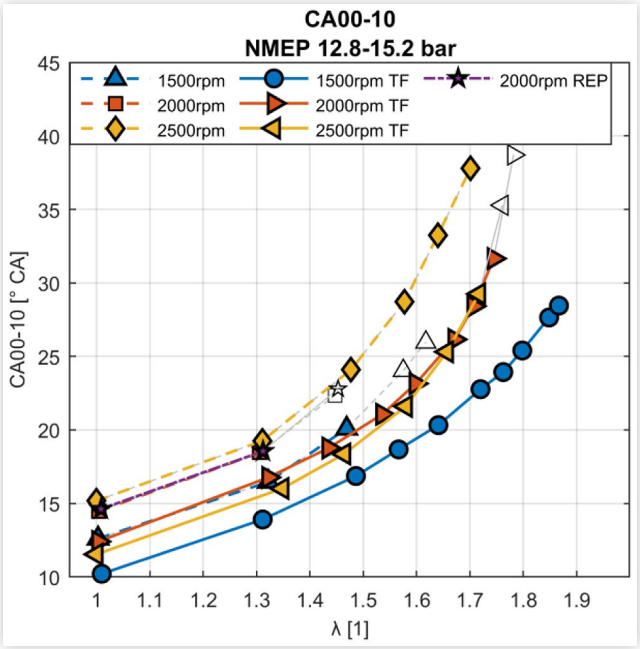

FIGURE 13 Main combustion duration (CA10-CA90) of three different engine speeds versus lambda at constant fuel injection quantity. A repetition is included with pentagon markers. Dashed lines denote standard engine configuration. Solid lines denote closed tumble-flap (TF).

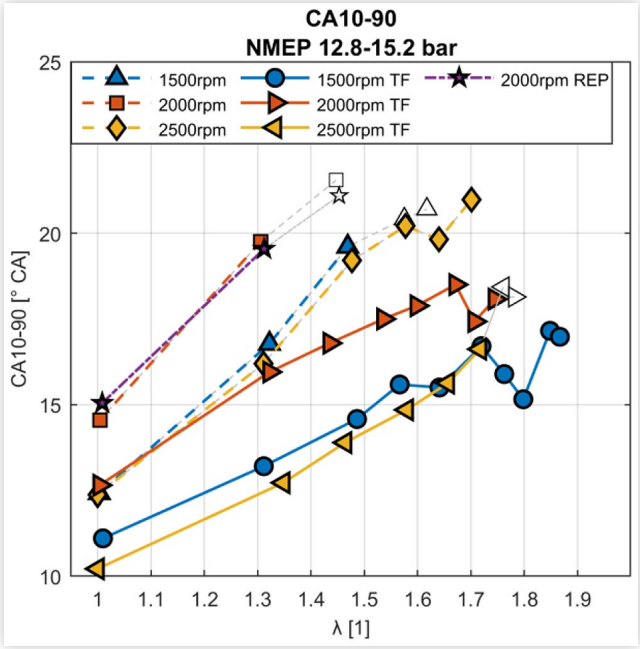

FIGURE 14 NMEP of three different engine speeds versus lambda at constant fuel injection quantity. A repetition is included with pentagon markers. Dashed lines denote standard engine configuration. Solid lines denote closed tumble-flap (TF).

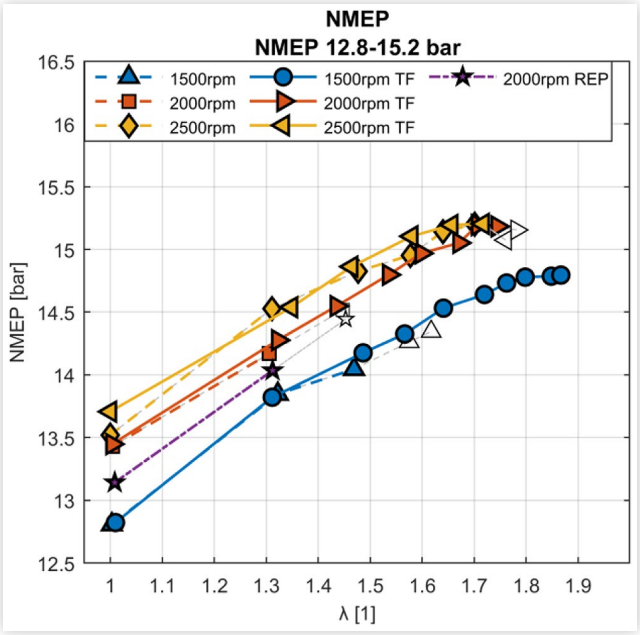

FIGURE 15 Relative pumping losses of three different engine speeds versus lambda at constant fuel injection quantity. A repetition is included with pentagon markers. Dashed lines denote standard engine configuration. Solid lines denote closed tumble-flap (TF).

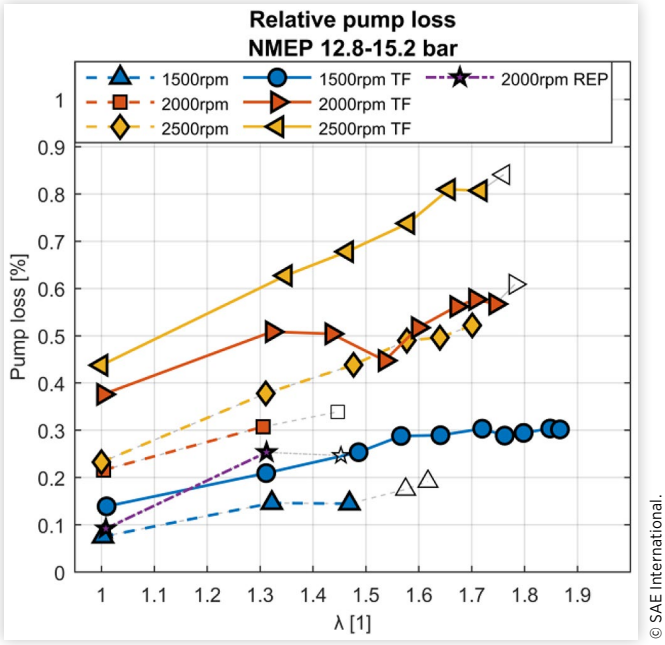

favourable composition due to the deviating gas-exchange, it might also extend the combustion duration.

Potential drawbacks of introducing increased tumble by a tumble-flap is that the pressure drop in the inlet port may increase, and heat losses to the cylinder walls may increase due to increased heat flux [16]. As could be observed in Figure 14, the addition of increased tumble offered little or no benefit to the output of indicated network at each increment of lambda. Pumping losses were computed as the pump mean effective pressure (PMEP) and an energy balance, using the method described by Berntsson et al., was used to estimate the in-cylinder heat losses [22]. Relative pumping losses, scaled by the total available energy of the fuel, is visualized in Figure 15, and the computed heat losses scaled by fuel energy is presented in Figure 16.

Figure 15 shows that closing the tumble-flap at all speeds increases the pumping losses which counteracts some of the expected benefits from increased tumble. Since combustion duration was decreased, combustion stability was improved and combustion phasing advanced by increased tumble, it was expected to result in significant efficiency improvements. The repeated test case at 2000 rpm indicates an in-consistency in the data which questions the significance of the result, but since all other comparisons between low and high tumble have shown clear consistency it was concluded that increased tumble has a negative effect on pumping losses at the investigated conditions. The repetition experienced slightly more knock, which results in later ignition timing. Later ignition timing delays the pressure rise thus producing less negative work during compression, explaining why the repetition deviates slightly.

The graphs in Figure 15 demonstrates increases in pumping losses in relation to lambda. The total pump losses are all below 1% of the fuel energy and has therefore little impact on the total engine efficiency. It can be concluded that increased air-dilution offers no reduction, but an increase, of pumping losses in boosted operation compared to low load lean operation where de-throttling is often referred to as an important factor of efficiency improvement.

Figure 16 demonstrates the reduction of heat losses in relation to increased lambda. Heat losses answers for a substantial part of the efficiency improvements obtained when increasing air-dilution. If the heat losses are compared between default tumble and enhanced tumble the results are inconclusive. At 1500 rpm, the graphs indicate that the heat losses were slightly increased by increased tumble, an increase of approximately 1% unit. 2000 rpm also experienced an increase of heat losses, but smaller in magnitude than the 1500 rpm case. The change was also less than the observed deviation between the original test case at 2000 rpm and the repetition. In the same manner as with the pumping losses, it was believed that a small retardation of spark advance due to increased knock was responsible for the deviation between the first test and the repetition at 2000 rpm. At 2500 rpm, the effect of increased tumble was slightly positive, showing a decrease in heat loss. The results visualized in Figure 16 thus indicates that the effect of tumble on heat-losses is dependent on the engine speed since the change of losses appear to decrease with increased speed. However, it could not be confirmed that the computed in-cylinder heat losses were overall negatively impacted by increased tumble, which contradicted the expectation. Similarly, it could not be concluded that in-cylinder heat-losses were a main contributor in cancelling any expected efficiency gains from the improved combustion by increasing the tumble.

FIGURE 16 Relative in-cylinder heat losses of three different engine speeds versus lambda at constant fuel injection quantity. A repetition is included with pentagon markers. Dashed lines denote standard engine configuration. Solid lines denote closed tumble-flap (TF).

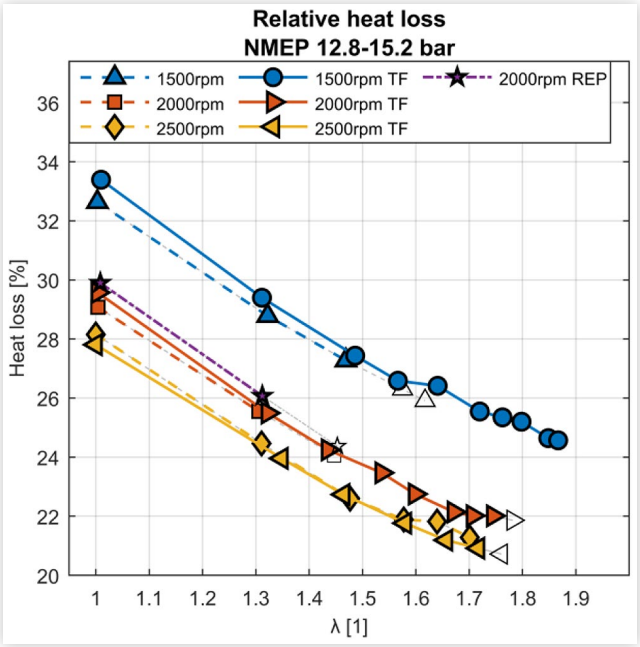

FIGURE 17 NMEP of four different fuel injection quantities versus lambda at constant engine speed. Dashed lines denote standard engine configuration. Solid lines denote closed tumble-flap (TF).

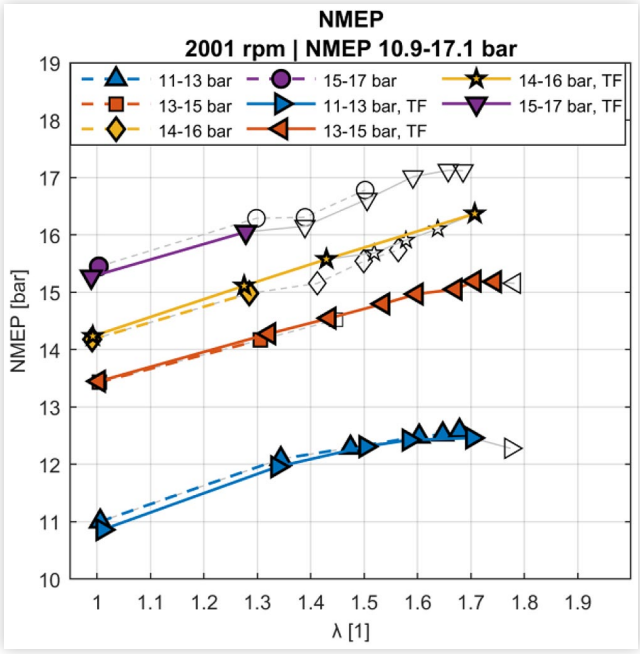

FIGURE 18 CA50 of four different fuel injection quantities versus lambda at constant engine speedy. Dashed lines denote standard engine configuration. Solid lines denote closed tumble-flap (TF).

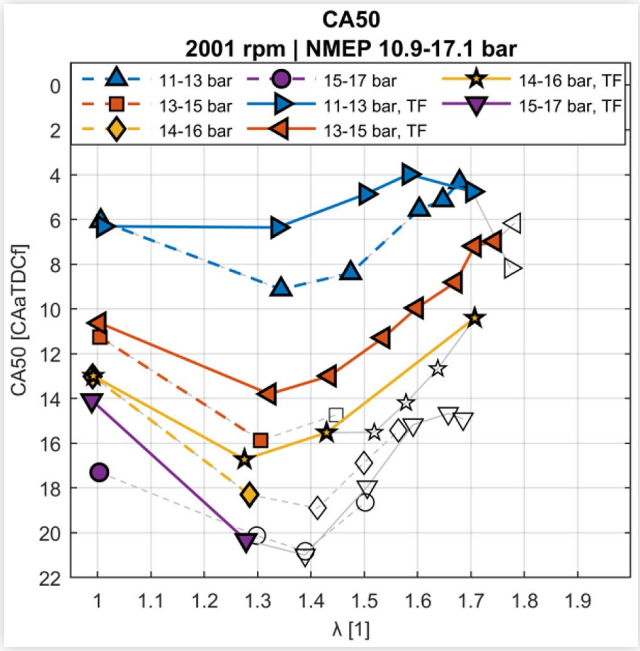

The investigation of three engine speeds and two levels of tumble revealed that increased tumble could offer improvements in combustion stability, knock mitigation and rate of combustion at high load lean operation. Increased tumble had highest positive impact on the air-dilution limit at lower engine speeds, while the effect was comparatively small at the highest engine speed investigated. This despite that increased tumble resulted in substantial combustion stability improvements. No significant, direct benefit in efficiency was observed by increased tumble. Increased tumble did however increase the air-dilution limit which in turn resulted in improved efficiency since the engine could be operated at higher lambda values. Improved knock mitigation and higher stability by enhanced tumble increased the width of the stability window which made the combustion less sensitive to the ignition timing which is beneficial for robustness.

The Effect of Load and Tumble on the High Load Lean Boundaries

In addition to the investigated engine speeds, lean combustion was assessed at further increased loads up to 17 bar NMEP. Four different engine loads determined by different fuel injection quantities were examined at a constant engine speed of 2000 rpm, all represented with and without increased tumble. The resulting work output from the combustion as NMEP is visualized in Figure 17. The corresponding combustion phasing attained from investigating the four different loads is presented in Figure 18. The results shown in Figure 17 denoted as 13-15 bar is the same load-point that was included as 2000 rpm when comparing 1500, 2000 and 2500 rpm in the previous section of this paper. Figure 17 reveals the overall highest achieved engine load in HLC mode during the

experimental campaign of this paper. The highest attempted load-point, starting from 15.5 bar NMEP, failed to satisfy the stability and knock criterions at the first lean lambda increment with default tumble. With enhanced tumble, the criterions could be met at lambda = 1.3 but failed thereafter. At both cases, severe knock occurred which necessitated a combustion phasing at 20° ATC when introducing air-dilution, as can be seen in Figure 18. At the second highest attempted load-point, starting slightly above 14 bar NMEP, a lambda of 1.7 could be obtained with enhanced tumble (pentagon markers). As can be seen in Figure 17, this lambda sweep failed to comply with the stability criterion between lambda = 1.5 to lambda = 1.65 (indicated by grey open markers), but due to recovery of the combustion phasing from knock mitigation, stability could be obtained at the last increment of lambda by advancing the combustion phasing. Figure 18 shows the implication of engine load on the available combustion phasing CA50. The higher the load, the more pronounced is the occurrence of knock which shifts the combustion phasing later in the cycle. The curved shape moving from stoichiometry to lean, discussed earlier in this paper, becomes more pronounced with higher load. At the lowest load included, ranging from 11 to 12.5 bar NMEP, the combustion phasing saw only little compromise due to knock in the intermediate air-dilution range, both with and without tumble. At the highest load included, ranging from 15.5 to 17 bar NMEP, the combustion phasing had to be retarded 6° CA due to knock when increasing dilution from stoichiometry to lambda = 1.3 with enhanced tumble.

As was demonstrated with different engine speeds, the results obtained with increased tumble by closing the tumble-flap outperformed the default tumble case with respect to achieving lambda at or above 1.7 and in terms of combustion phasing. Similar to the comparison of various engine speeds, it could also be observed from Figure 17 that enhanced tumble did not exhibit significant improvements in terms of total work output compared to default tumble. Once again, pumping losses proved to be the most consistent factor counteracting any efficiency improvements from enhanced tumble, while heat losses showed to be inconclusive as explanation. Whereas the case of default tumble could only reach very-lean condition at the lowest load-point included (11-12.5 bar NMEP), enhanced tumble increased the engine load at which very-lean air-dilution could be obtained to 16 bar NMEP.

The corresponding specific NO_x emissions from the different engine loads investigated is presented in Figure 19. The air-dilution rates obtained by implementing enhanced tumble proved sufficient to reach sub 2 g/kWh NO_x emissions. The testcases with default tumble failed to exceed lambda = 1.3 for all load-points except for the lowest load. This meant that the corresponding NO_x peak at lambda = 1.3 could not be overcome for most of the default tumble cases at higher loads. Despite that there were no distinguishable efficiency benefits from increased tumble, it proved to have large impact on the NO_x emissions due to the increase of maximum air-dilution rates. It could be observed, that in order to obtain sub 2 g/kWh NO_x, it was sufficient to reach approximately lambda = 1.7. This amount of air-dilution is similar to the air-dilution rates usually achieved at lower engine loads below 10 bar NMEP, regarding conventional sparkplug-based

FIGURE 19 Indicated specific NOx mass flow of four different fuel injection quantities versus lambda at constant engine speedy. Dashed lines denote standard engine configuration. Solid lines denote closed tumble-flap (TF).

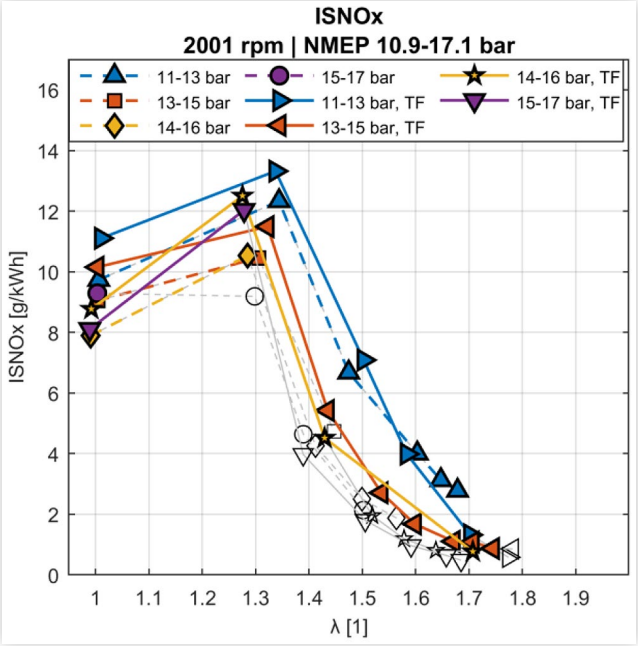

technology and homogeneous charge. Thus, high loads do not necessitate that lambda must be increased further compared to low loads, in order to obtain low NO_x-emissions.

Conclusions

In this paper, high load HLC has been assessed at three different engine speeds and specific engine loads ranging from 11 to 17 bar NMEP. It could be concluded that air-dilution solely was in-sufficient to prevent end-gas autoignition at higher engine loads in several of the cases investigated. This behaviour is most likely to change for different fuels and combustion systems which affect the combustion characteristics and knock-sensitivity. It could be concluded from the experiments that there exist a lean load limit and it was identified as the convergence of the stability boundary and knock boundary. These two boundaries enclose the stability window and when the two convergence, valid options of spark advance and combustion phasing is eliminated, making successful engine operation impossible. At stoichiometric operation, the combustion instability is negligible and therefore there exists no stability boundary. This means that only the knock boundary must be respected, and spark advance will not be limited to a stability window. With lean combustion, the stability boundary appears due to dispersion of heat-release and work-output. The dispersion is inherent to lean combustion, negatively affected by the retarded spark timing. If the dispersion of heat release can be decreased, the stability boundary can be retarded and the stability window enlarged to accommodate later combustion phasing and knock

mitigation if necessary, making lean combustion available at higher engine loads.

No improvement to heat release dispersion and the corresponding CoV of NMEP could be observed with respect to increased engine load. This contradicts the suggestion that higher engine load conditions alone, i.e. increased charge temperature, density and turbulence, should improve lean combustion. The dispersion of heat release remains similar in relation to lambda, irrespective of engine load. The dispersion could however be decreased by introducing enhanced tumble. With increased tumble, tendency of knocking combustion could be decreased and simultaneously combustion stability improved. This allowed for increased air-dilution rates at operating conditions which was not achievable with default tumble. Due to high dilution rates, NO_x emissions could be reduced to reasonable levels of sub 2 g/kWh even at high load lean combustion operation at 16 bar NMEP.

Increased tumble by closed tumble-flap did not offer a distinguishable improvement to the efficiency of the engine, compared to default tumble, despite improvements in combustion quality. It did however enable a substantial increase of the lean limit at lower engine speed which in turn provided higher engine efficiency. Higher boost pressure was required to deliver the same air-mass to the combustion chamber compared to open tumble-flap as was expected. This imposes increased demands on boosting systems if the high-tumble approach should be implemented in a production engine. Another aspect to consider is the very high cylinder pressures obtained during high load lean combustion. The peak cylinder pressures occasionally exceeded 120 bar during the experiments conducted to produce this paper. The tumble-flap utilized in this study did not necessarily present the best trade-off between pressure-drop and desired charge-air motion. By optimization of the tumble-flap, it is possible that further improvements to the stability and lean limit can be achieved in future work.

As mentioned earlier in this paper, the lean load limit denotes the highest load at which converging air-dilution can be implemented. Converging air-dilution refers to that the air-dilution can be sufficiently increased beyond lambda = 1.6 to obtain low NO_x emissions in the 0-2 g/kWh range. There will remain a possibility to further increase the load while operating lean but at more restricted air-dilution quantities which will result in elevated NO_x emissions. In such case, the combustion phasing will likely not improve compared to stoichiometric combustion, which has been demonstrated in this paper. Slightly improved combustion efficiency and decreased in-cylinder heat losses can be achieved from such engine operation, but the benefits are arguably not outweighing the cost of the high amount of NO_x that will be produced.

References

1. Kiyota, Y., Akishino, K., and Ando, H., "Concept of Lean Combustion by Barrel-Stratification," SAE Technical Paper 920678, 1992, doi:https://doi.org/10.4271/920678.
2. Johansson, A.N., Hemdal, S., and Dahlander, P., "Experimental Investigation of Soot in a Spray-Guided Single Cylinder GDI Engine Operating in a Stratified Mode," SAE Technical Paper 2013-24-0052, 2013, doi:https://doi.org/10.4271/2013-24-0052.
3. Sjöberg, M. and Zeng, W., "Combined Effects of Fuel and Dilution Type on Efficiency Gains of Lean Well-Mixed DISI Engine Operation with Enhanced Ignition and Intake Heating for Enabling Mixed-Mode Combustion," *SAE Int. J. Engines* 9(2):750-767, 2016, doi:https://doi.org/10.4271/2016-01-0689.
4. Sjöberg, M., Zeng, W., Singleton, D., Sanders, J.M. et al., "Combined Effects of Multi-Pulse Transient Plasma Ignition and Intake Heating on Lean Limits of Well-Mixed E85 DISI Engine Operation," *SAE Int. J. Engines* 7(4):1781-1801, 2014, doi:https://doi.org/10.4271/2014-01-2615.
5. Doornbos, G., Hemdal, S., and Dahl, D., "Reduction of Fuel Consumption and Engine-Out NOx Emissions in a Lean Homogeneous GDI Combustion System, Utilizing Valve Timing and an Advanced Ignition System," SAE Technical Paper 2015-01-0776, 2015, doi:https://doi.org/10.4271/2015-01-0776.
6. Hanabusa, H., Kondo, T., Hashimoto, K., and Furutani, M., "Study on Cyclic Variations of Laminar Flame Speed in Homogeneous Lean charge Spark Ignition Combustion," SAE Technical Paper 2016-01-2173, 2016, doi:https://doi.org/10.4271/2016-01-2173.
7. Hanabusa, H., Kondo, T., Hashimoto, K., Sono, H. et al., "Study on Homogeneous Lean Charge Spark Ignition Combustion," SAE Technical Paper 2013-01-2562, 2013, doi:https://doi.org/10.4271/2013-01-2562.
8. Doornbos, G., Hemdal, S., Denbratt, I., and Dahl, D., "Knock Phenomena under Very Lean Conditions in Gasoline Powered SI-Engines," *SAE Int. J. Engines* 11(1):39-54, 2018, doi:https://doi.org/10.4271/03-11-01-0003.
9. Ratnak, S., Kusaka, J., Daisho, Y., Yoshimura, K. et al., "Experiments and Simulations of a Lean-Boost Spark Ignition Engine for Thermal Efficiency Improvement," *SAE Int. J. Engines* 9(1):379-396, 2016, doi:https://doi.org/10.4271/2015-32-0711.
10. Clasén, K., Koopmans, L., and Dahl, D., "Homogeneous Lean Combustion in a 2lt Gasoline Direct Injected Engine with an Enhanced Turbo Charging System," SAE Technical Paper 2018-01-1670, 2018, doi:https://doi.org/10.4271/2018-01-1670.
11. Heywood, J.B., *Internal Combustion Engine Fundamentals* (McGraw-Hill Inc., 1988).
12. Matthias, N., Wallner, T., and Scarcelli, R., "Analysis of Cyclic Variability and the Effect of Dilute Combustion in a Gasoline Direct Injection Engine," *SAE Int. J. Engines* 7(2):633-641, 2014, doi:https://doi.org/10.4271/2014-01-1238.
13. Ceviz, M.A. and Kaymaz, I., "Temperature and Air-Fuel Ratio Dependent Specific Heat Ratio Functions for Lean Burned and Unburned Mixture," *Energy Conversion and Management* 46(15-16), 2004, doi:10.1016/j.enconman.2004.12.009.
14. Grandin, B., "Knock in Gasoline Engines," Ph.D., Department of Thermo and Fluid Dynamics, Chalmers University of Technology, Göteborg, 2001.
15. Lavoie, G.A., Ortiz-Soto, E., Babajimopoulos, A., Martz, J.B. et al., "Thermodynamic Sweet Spot for High-Efficiency, Dilute, Boosted Gasoline Engines," *Int. J. Engine Research* 14(3), 2012, doi:10.1177/1468087412455372.
16. Ogink, R. and Babajimopoulos, A., "Investigating the Limits of Charge Motion and Combustion Duration in a High-Tumble

Spark-Ignited Direct-Injection Engine," *SAE Int. J. Engines* 9(4):2129-2141, 2016, doi:https://doi.org/10.4271/2016-01-2245.

17. Sjöberg, M. and He, X., "Combined Effects of Intake Flow and Spark-Plug Location on Flame Development, Combustion Stability and End-Gas Autoignition for Lean Spark-Ignition Engine Operation Using E30 Fuel," *Int. J. Engine Research* 19(1), 2018, doi:10.1177/1468087417740290.
18. Hayashi, N., Sugiura, A., Abe, Y., and Suzuki, K., "Development of Ignition Technology for Dilute Combustion Engines," *SAE Int. J. Engines* 10(3):984-995, 2017, doi:https://doi.org/10.4271/2017-01-0676.
19. Grandin, B., Denbratt, I., Bood, J., Brackmann, C. et al., "A Study of the Influence of exhaust Gas Recirculation and Stoichiometry on the Heat Release in the End-Gas Prior to Knock Using Rotational Coherent Anti-Stokes±Raman Spectroscopy Thermometry," *Int. J. Engine Research* 3(4), 2002, doi:10.1243/146808702762230914.
20. Grandin, B.,Ångström, H.-E., Stålhammar, P., and Olofsson, E., "Knock Suppression in a Turbocharged SI Engine by Using Cooled EGR," SAE Technical Paper 982476, 1998, doi:https://doi.org/10.4271/982476.
21. Stenlåås, O., Einewall, P., Egnell, R., and Johansson, B., "Measurement of Knock and Ion Current in a Spark Ignition Engine with and without NO Addition to the Intake Air," SAE Technical Paper 2003-01-0639, 2003, doi:https://doi.org/10.4271/2003-01-0639.
22. Berntsson, A.W., Josefsson, G., Ekdahl, R., Ogink, R. et al., "The Effect of Tumble Flow on Efficiency for a Direct Injected Turbocharged Downsized Gasoline Engine," *SAE Int. J. Engines* 4(2):2298-2311, 2011, doi:https://doi.org/10.4271/2011-24-0054.

Contact Information

Lucien Koopmans
+4631 - 772 14 19
koopmans@chalmers.se

Acknowledgement

The work performed to create this paper was conducted within a project called UPGRADE - "High efficient Particulate free Gasoline Engines". This project has received funding from the European Union's Horizon 2020 Research and Innovation program under grant agreement 724036

The authors would like to acknowledge Joop Somhorst for his assistance in establishing the filtering of pressure signals to assess knock.

Abbreviations

ATC - After top centre
BSFC - Brake specific fuel consumption
BTC - Before top centre
CA - Crank angle (degrees)
CA00 - 0% mass fraction burned = spark timing
CA10 - 10% mass fraction burned
CA50 - 50% mass fraction burned
CA90 - 90% mass fraction burned
CAaTDCf - Crank angle (degrees) after top dead centre firing
CoV - Coefficient of variation
Cyl - Cylinder
DCI - Dual coil ignition
DISI - Direct injection spark ignition
DOHC - Double over-head camshafts
E10 - 10% Ethanol
EVC - Exhaust valve closing
EVO - Exhaust valve opening
HLC - Homogeneous lean combustion
ICE - Internal combustion engine
IVC - Inlet valve closing
IVO - Inlet valve opening
KI - Knock intensity
KO - Knock onset
KT - Knock tendency
MBT - Maximum brake torque
MFB - Mass fraction burned
NMEP - Net (indicated) mean effective pressure
P - Pressure
RON - Research octane number
SI - Spark ignition
Std - Standard deviation
T - Temperature
TC - Top centre
V - Volume
ATC - After top centre
BSFC - Brake specific fuel consumption
BTC - Before top centre

ISSN 0148-7191